

Particle identification and photon detection

Peter Križan

University of Ljubljana and J. Stefan Institute

UNIVERZA V LJUBLJANI

Particle identification and photon detection

Particle identification: why and what?

Ring Imaging CHerenkov detectors

Time-Of-Flight and Time-Of-Propagation detectors

dE/dx and dN/dx

Photosensors: why?

Vacuum-based photodetectors

Solid state low light level photosensors

Summary and outlook

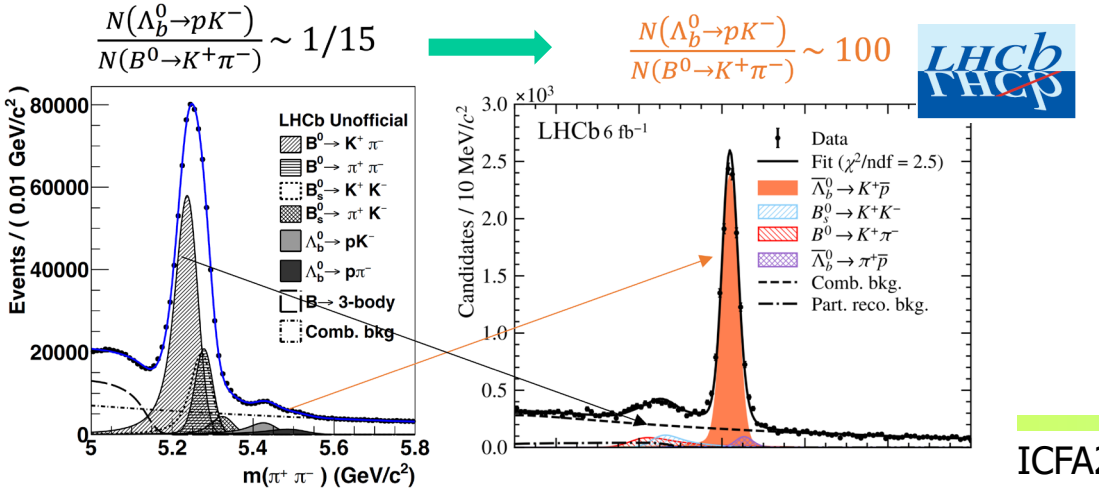
Why particle identification?

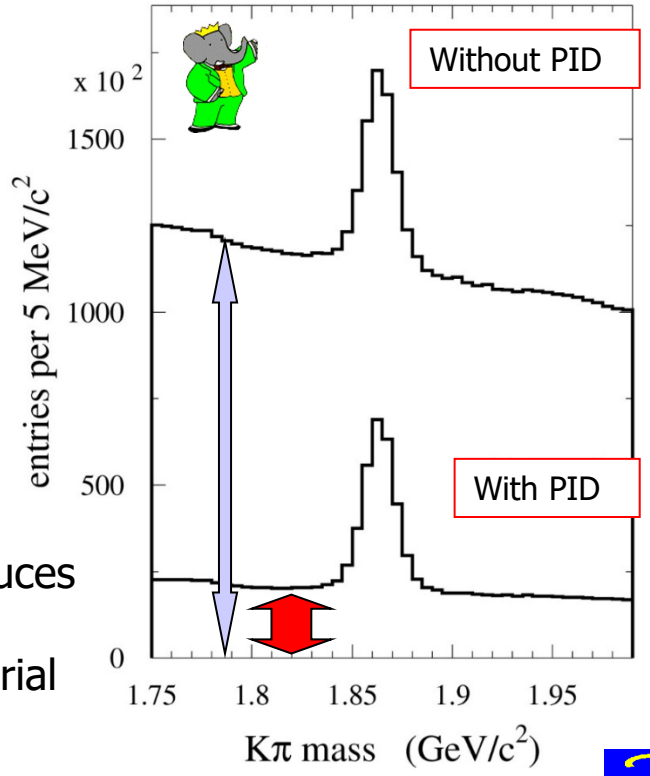
PID is often what turns a topology into a physics signal.

Flavour physics: suppress wrong K/π combinations and tag flavour.

Spectroscopy: reveal narrow hadronic states above combinatorial background.

Future colliders: flavour tagging and precision measurements demand robust hadron ID.

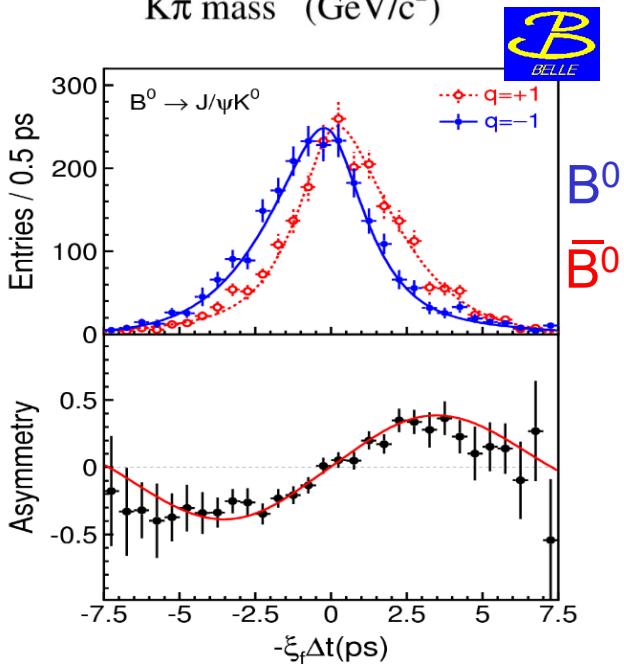




B factories:

Particle identification reduces the fraction of wrong Kπ combinations (combinatorial background) by ~5x

PID was essential for the observation of CP violation in the B meson system.



Why particle identification?

PID is often what turns a topology into a physics signal.

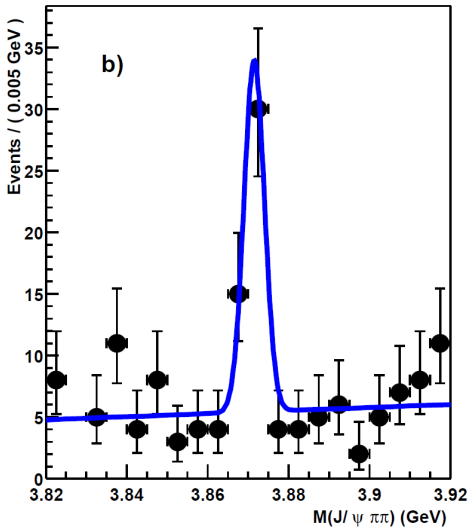
Flavour physics: suppress wrong K/π combinations and tag flavour.

Spectroscopy: reveal narrow hadronic states above combinatorial background.

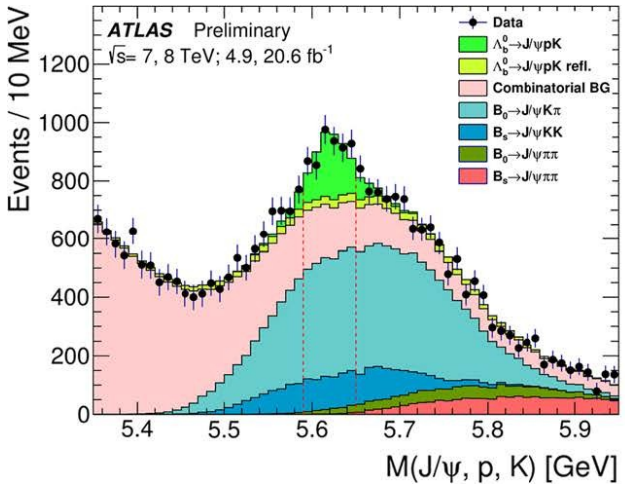
Future colliders: flavour tagging and precision measurements demand robust hadron ID.

The observation that in 2003 started the avalanche of discoveries of heavy-quark states: X(3872) by Belle

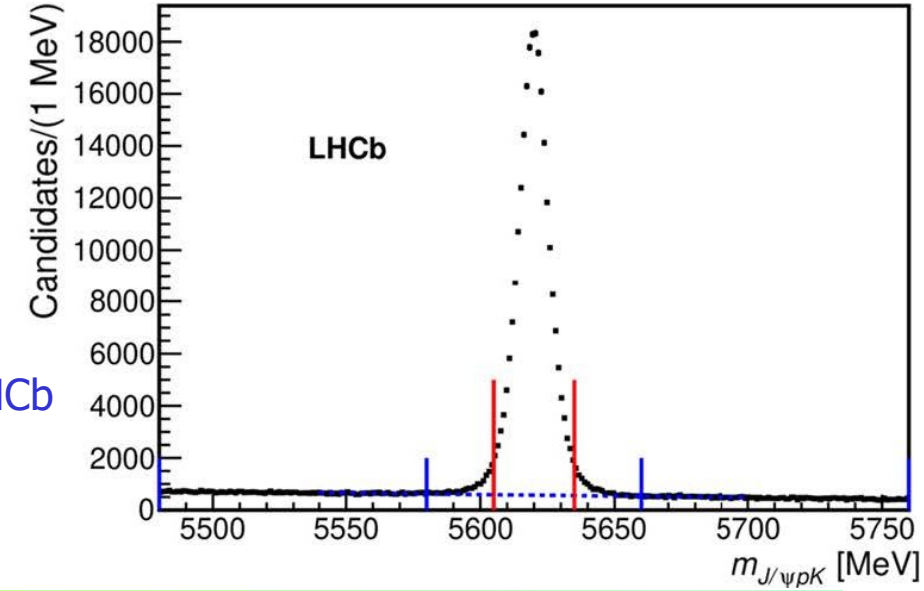
PRL91 (2003) 262001



Pentaquark at ATLAS



Pentaquark with LHCb



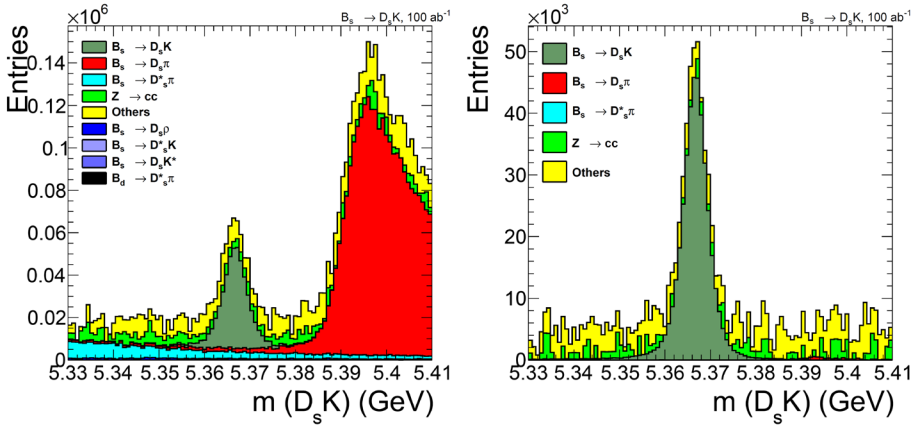
Why particle identification?

PID is often what turns a topology into a physics signal.

Flavour physics: suppress wrong K/π combinations and tag flavour.

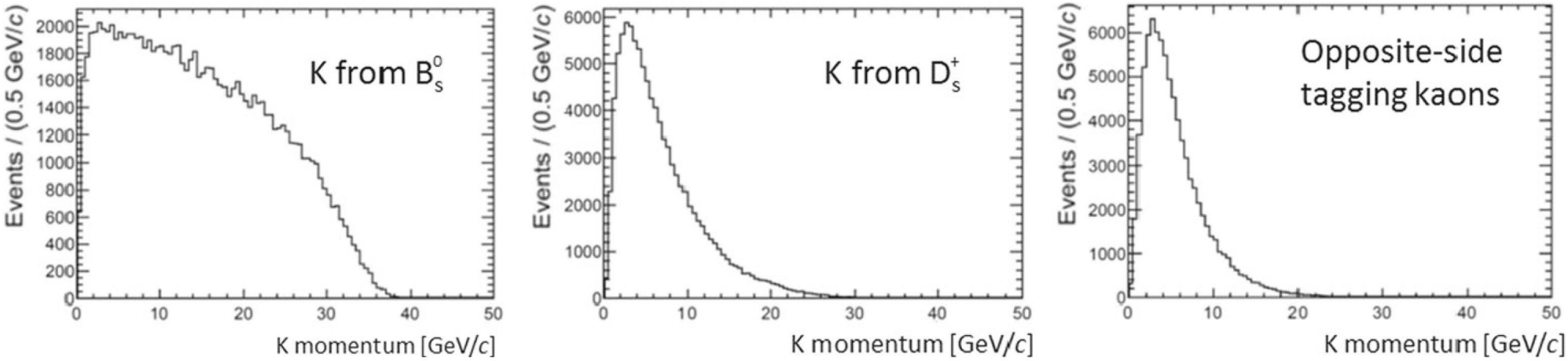
Spectroscopy: reveal narrow hadronic states above combinatorial background.

Future colliders: flavour tagging and precision measurements demand robust hadron ID.



$B_s \rightarrow D_sK \rightarrow \varphi(KK)\pi K$ decay channel, prior to any PID cut and after PID of the fast K.

FCC-ee: momentum spectra for the $B_s^0 \rightarrow D_s^+ K^-$ decay at Z^0



Why particle identification?

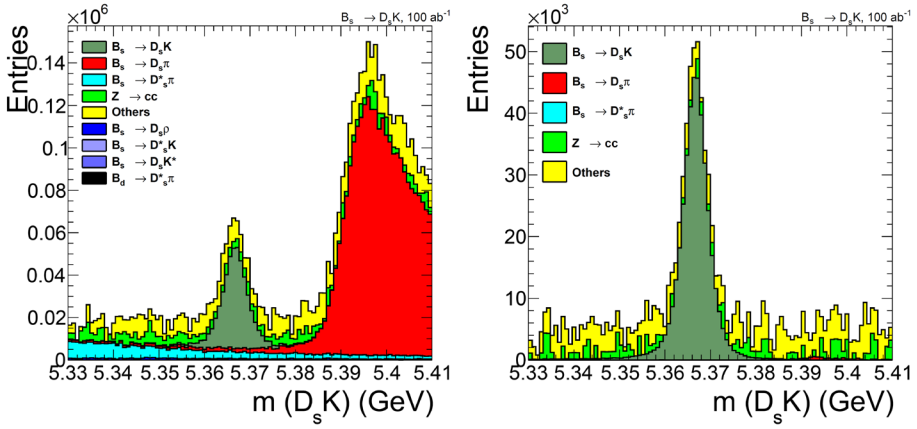
PID is often what turns a topology into a physics signal.

Flavour physics: suppress wrong K/π combinations and tag flavour.

Spectroscopy: reveal narrow hadronic states above combinatorial background.

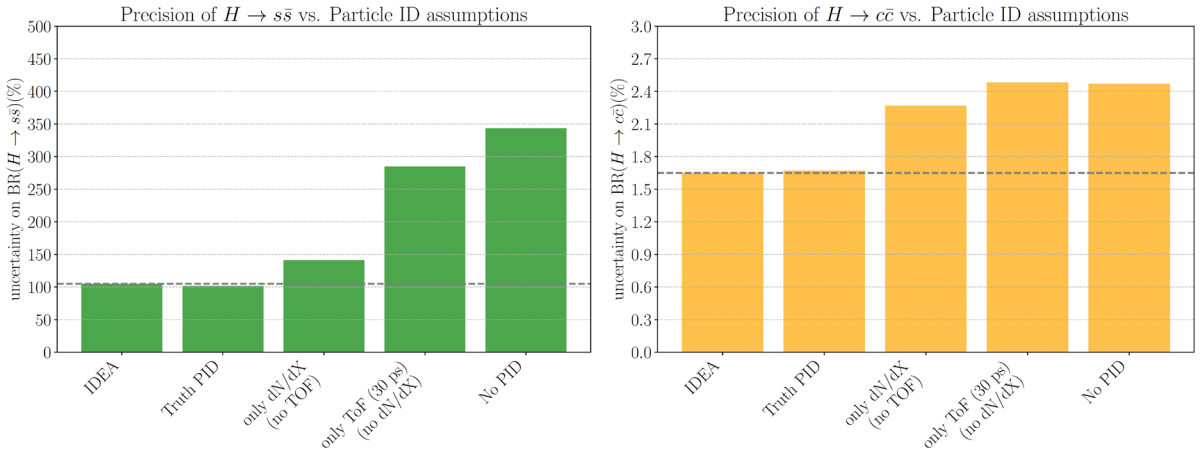
Future colliders: flavour tagging and precision measurements demand robust hadron ID.

Future colliders: PID required also for Higgs physics, e.g., BR measurement of the H → $s\bar{s}$ and $c\bar{c}$ decays



$B_s \rightarrow D_sK \rightarrow \varphi(KK)\pi K$ decay channel, prior to any PID cut and after PID of the fast K.

FCC-ee: impact of PID assumptions on precision of BR for H → $s\bar{s}$ and $c\bar{c}$ decays



FCC Feasibility Study Report, Volume 1

Identification of charged particles: measure mass — or exploit interaction signatures

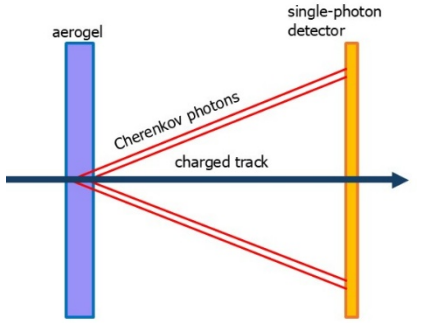
Particles (e, μ, π, K, p) in the final state are identified by their mass or by the way they interact.

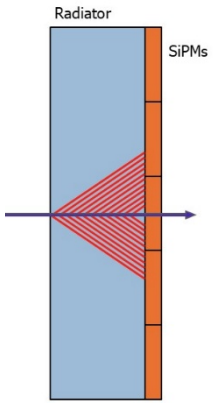
Determination of mass: from the relation between momentum and velocity, $p=\gamma mv$ (p is known - radius of curvature in the magnetic field)

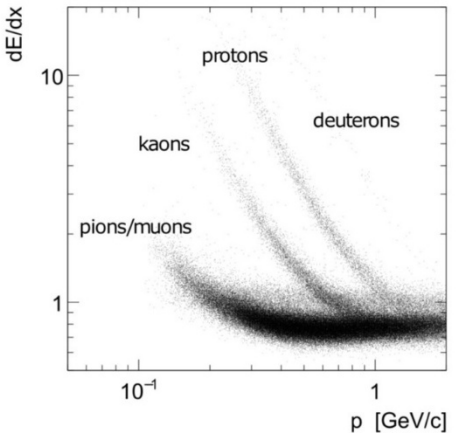
→Measure velocity by:

- Cherenkov photon angle
- ionisation losses dE/dx, dN/dx
- time of flight
- transition radiation

Mainly used for the identification of hadrons.





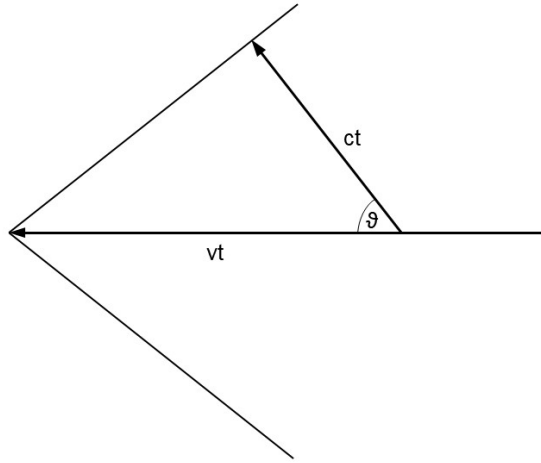


Identification through interaction: electrons and muons

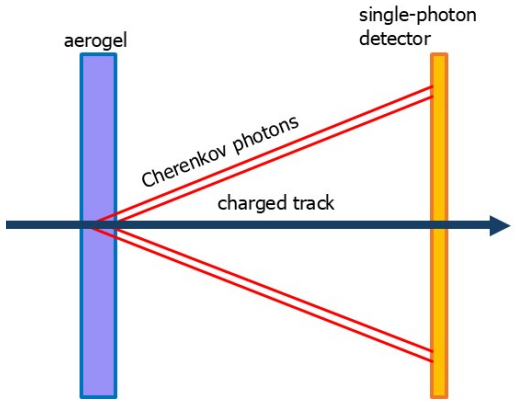
- muon systems
- electromagnetic calorimeters

No single technique covers all particles and momenta → combine complementary observables.

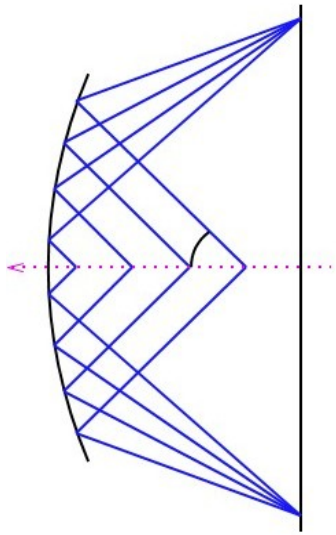
Cherenkov imaging: turn velocity into geometry



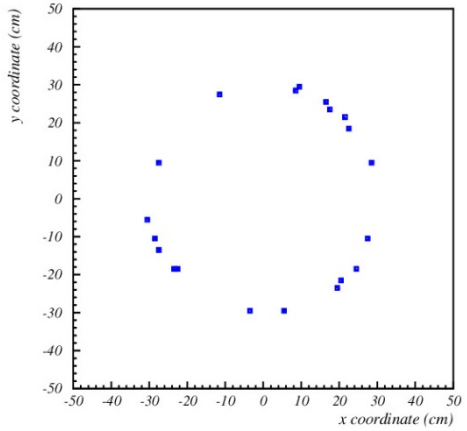
cosθ = c/nv = 1/βn → measure θ



Proximity focusing RICH



RICH with a focusing mirror

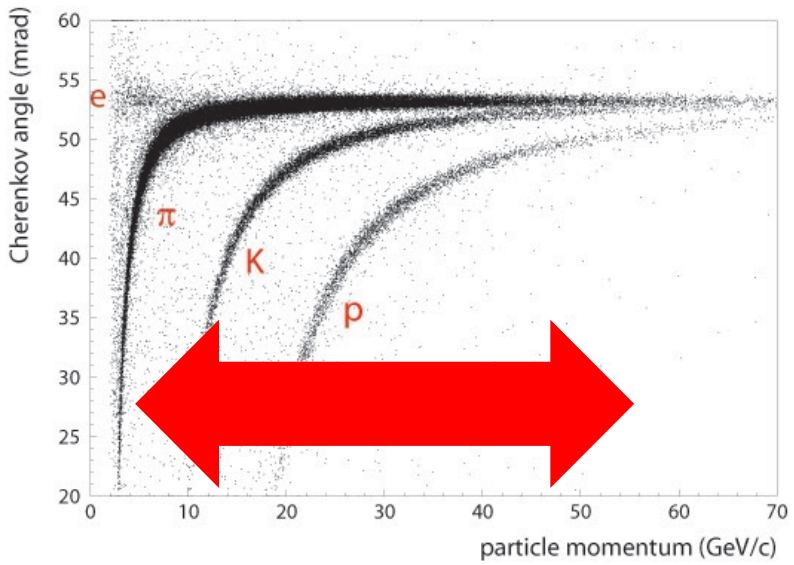


Idea: transform the direction into a coordinate → ring on the detection plane

→ Ring Imaging Cherenkov (RICH) detector

Few detected photons → photosensor is the critical element

Kinematic range of a RICH counter



Example: kinematic range for kaon/pion separation

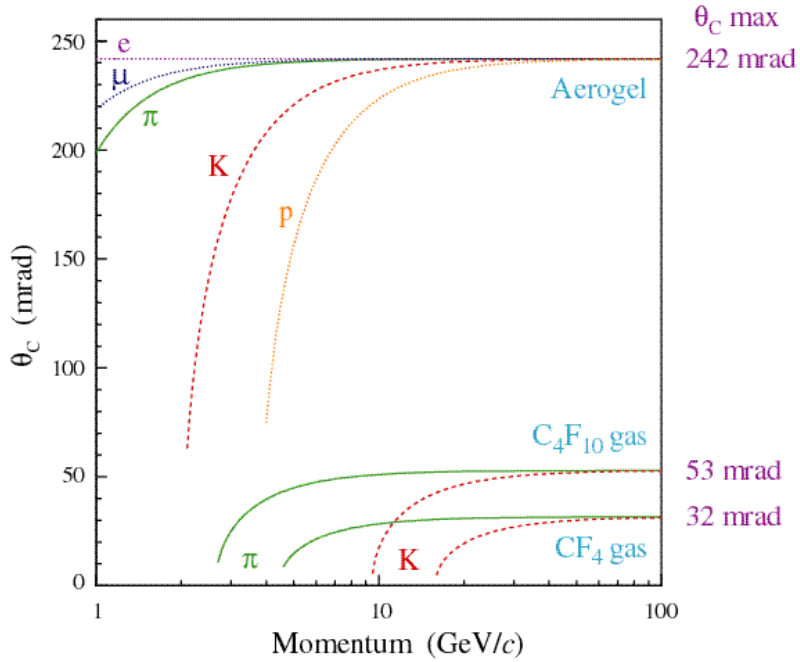
Kinematic range for separation of two particle types:

- Lower limit p_{min}: sufficiently above lighter particle threshold
- Upper limit p_{max}: given by Cherenkov angle resolution – overlap of the two bands

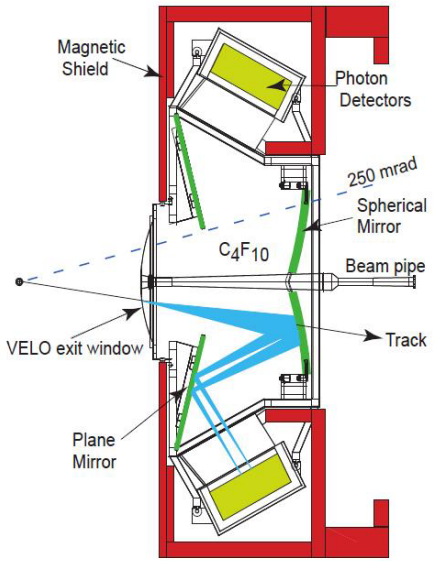
Rule of thumb: $p_{max} / p_{min} < 10$

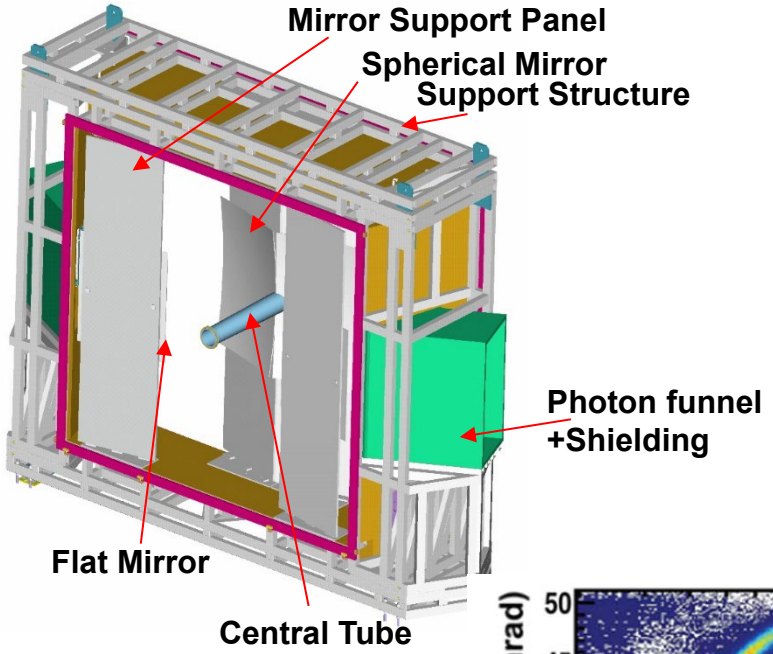
Larger kinematic range: need more than one radiator

LHCb RICHes: original scheme with three radiators, aerogel, C_4F_{10} gas, CF_4 gas



LHCb RICH detectors

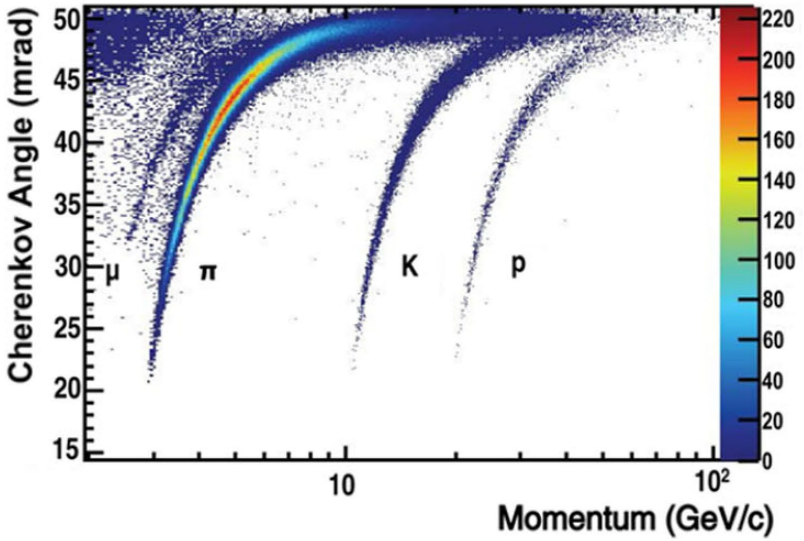


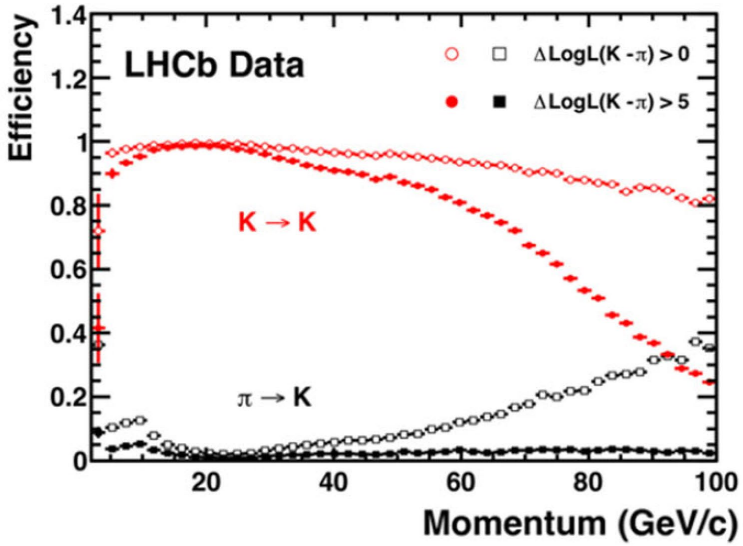


Excellent performance, one of the main components in the successful flavour and spectroscopy program of the experiment.

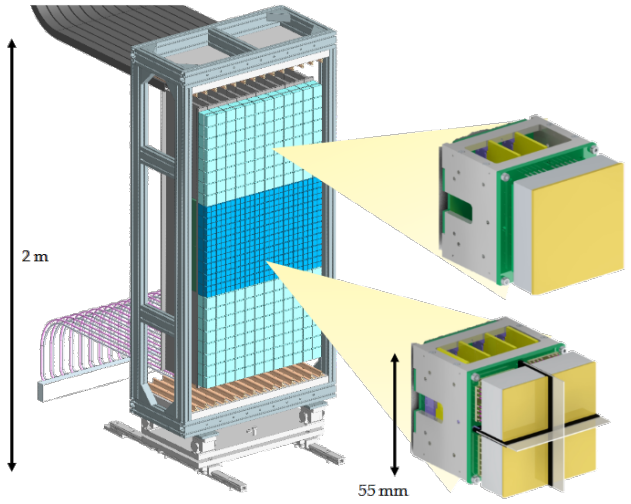
Large kinematic range: two RICH detectors

- RICH1 with C_4F_{10} gas (before the magnet)
- RICH2 with CF_4 gas

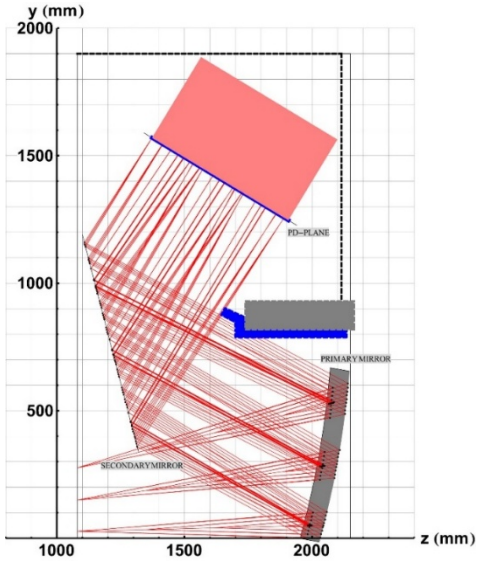


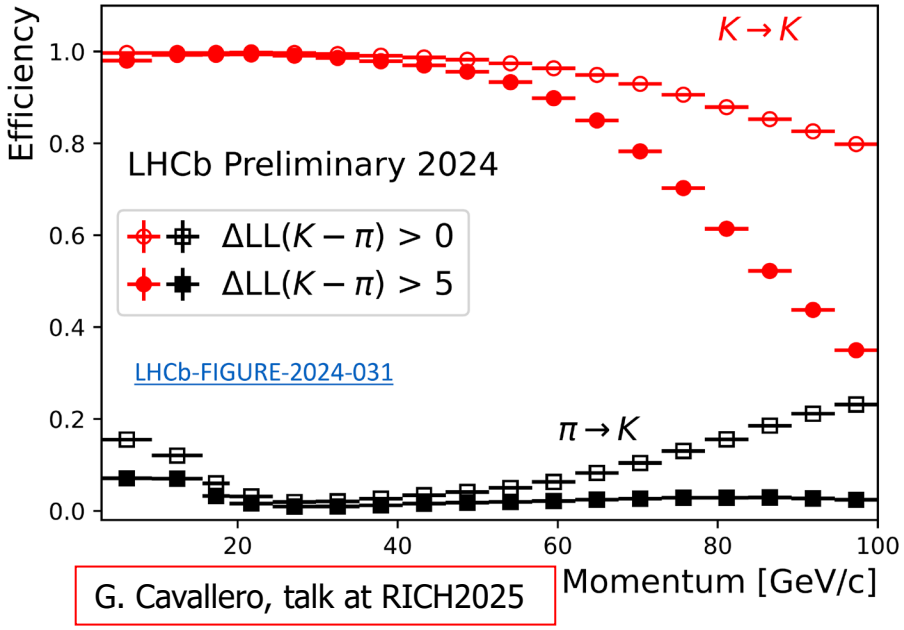


LHCb: upgraded RICH detectors



- New photon detectors: MaPMTs Hamamatsu R13743 (H12700) and R13742 (R11265)
- New electronics working at 40 MHz readout rate
- New optics layout for RICH 1





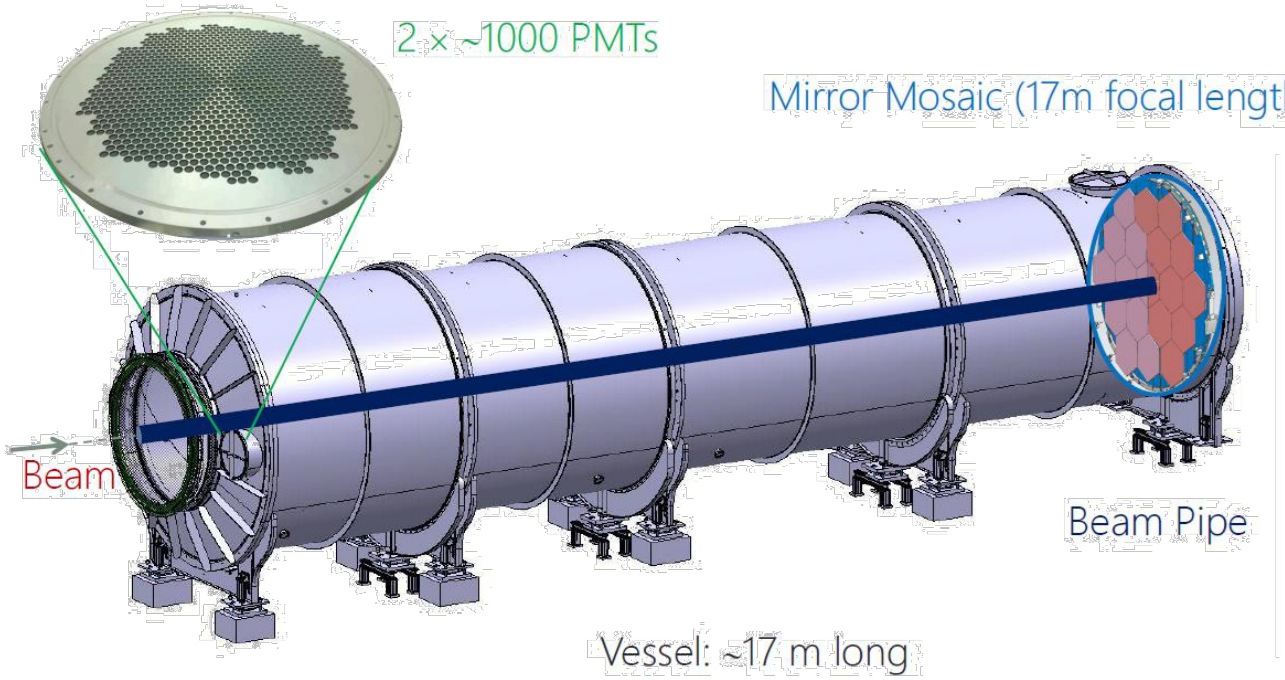
G. Cavallero, talk at RICH2025

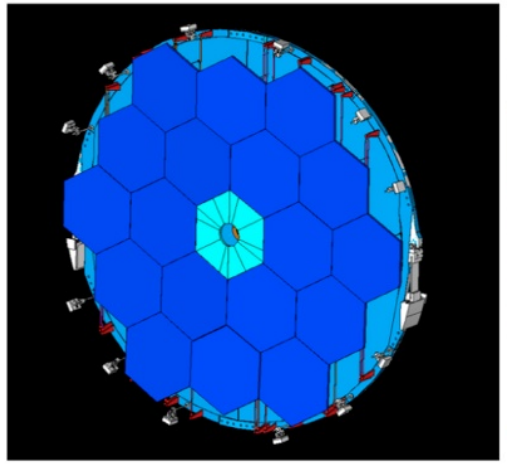
Further upgrade planned (Upgrade 2) to maintain the same (or better) PID performance of Run 3 with a 5x - 7.5x higher luminosity, details under study

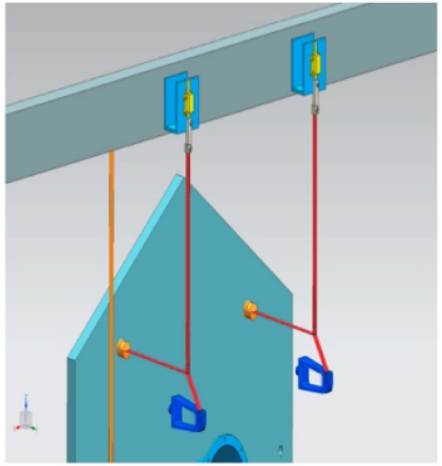
- New photosensors with finer granularity (most likely SiPMs) and excellent timing (~100ps)
- Modified optics (smaller mirror tilt for lower aberration, longer focal length)

NA62 RICH

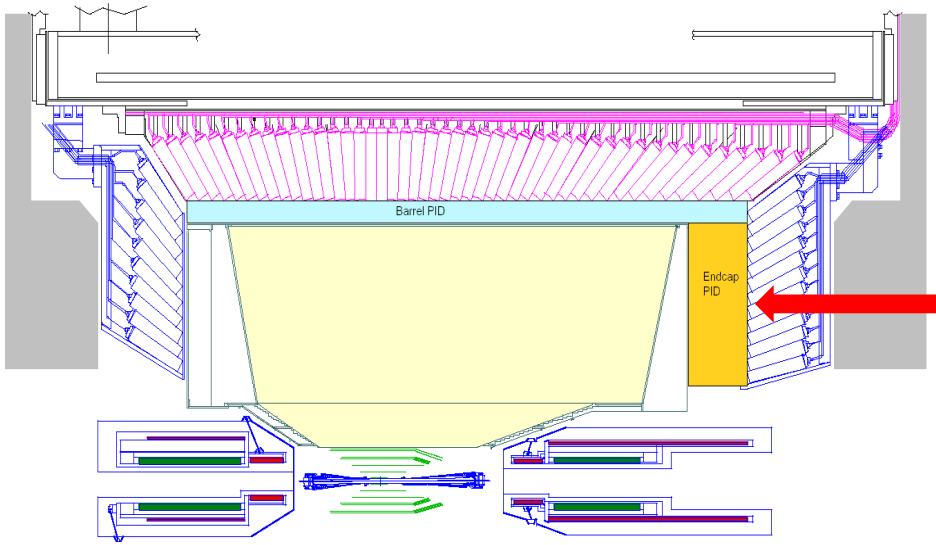
- Momentum range 15-35 GeV/c
- 17m long, 200m^3 cylindrical vacuum proof tank with Neon radiator
- Photon detectors: 2000 PMTs (16mm, 8mm active, with Winstone cone light guides)
- Mirror alignment ~30 μrad
- Single photon resolution: ~140 μrad
- Operational since 2014

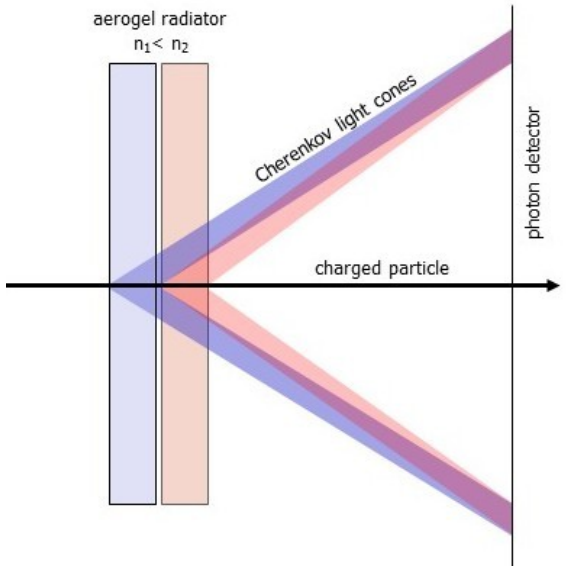


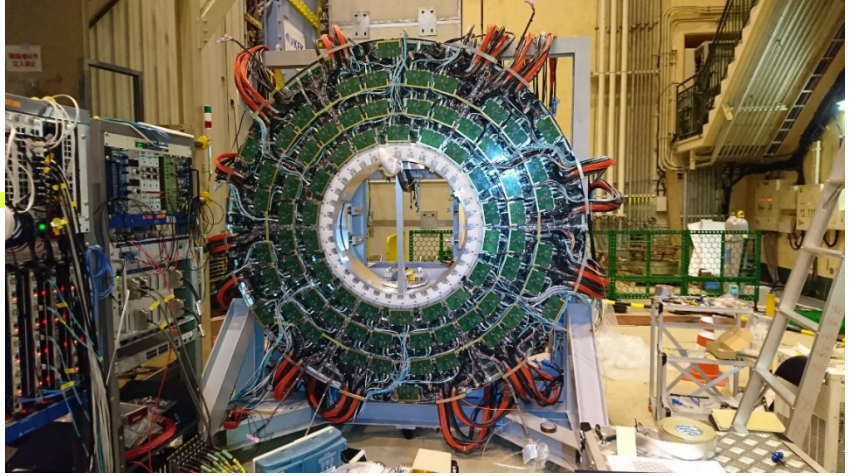


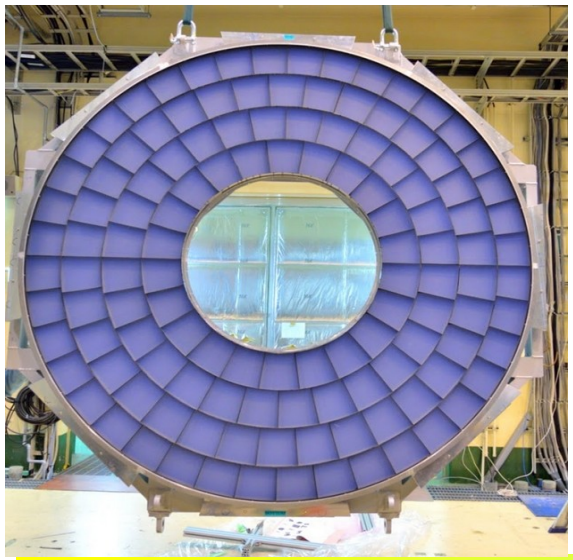


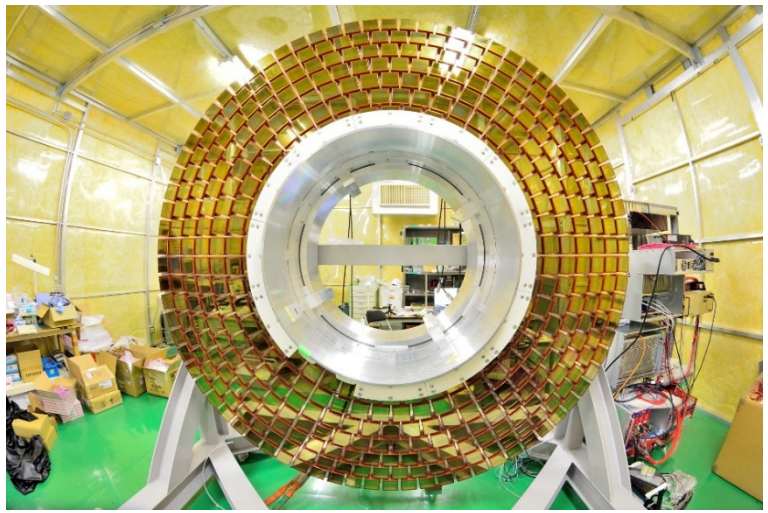
Aerogel RICH (ARICH) – forward endcap of Belle II

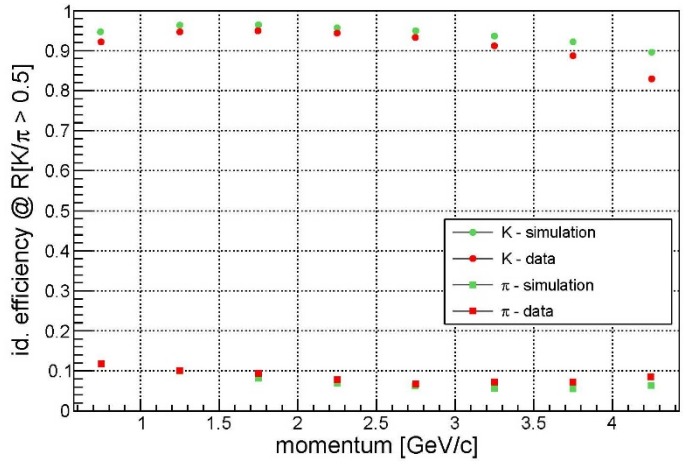


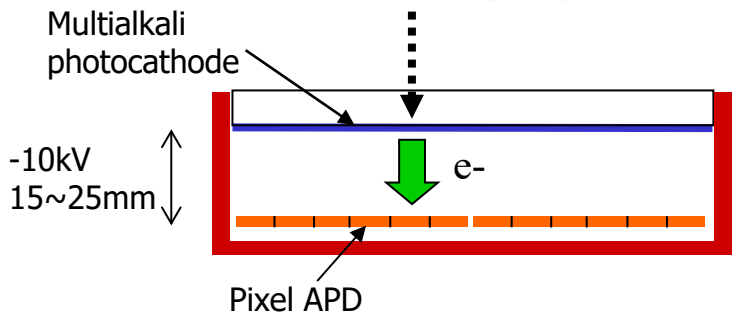












Sensor: Hybrid APD - HAPD

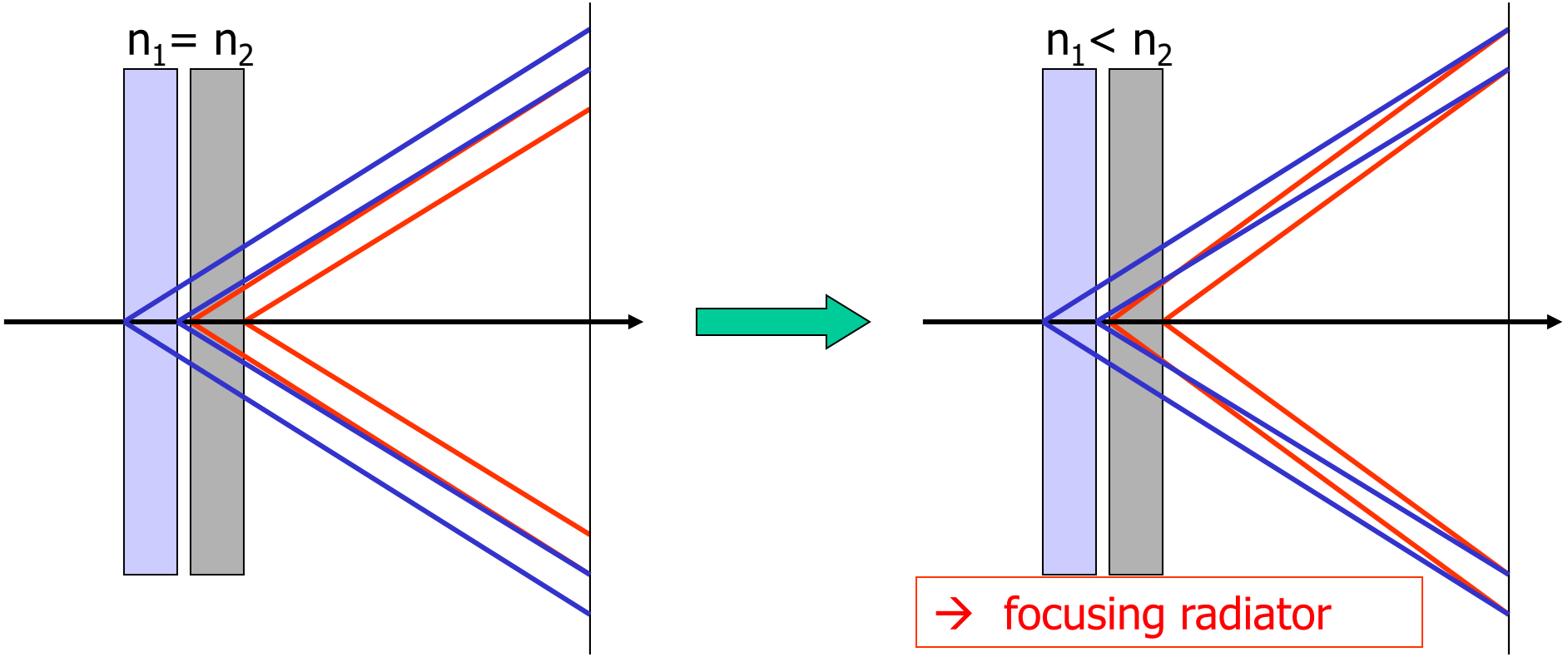
I. Adachi et al, NIMA 1089 (2026) 171592

Radiator with multiple refractive indices

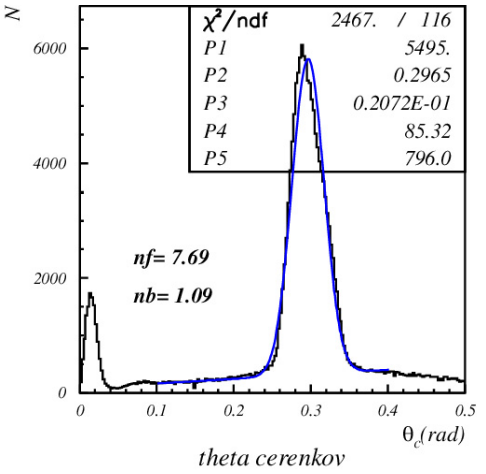
Small number of photons from aerogel → need a thick layer of aerogel → would degrade resolution

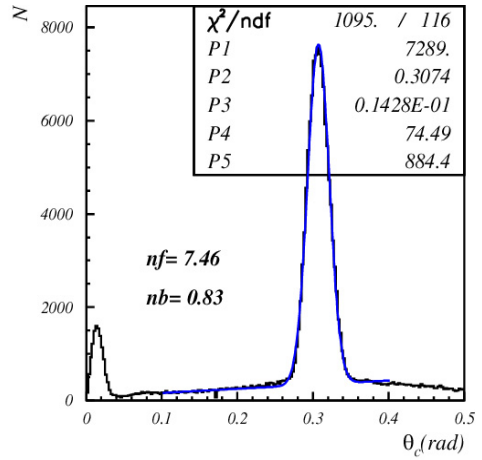
How to keep the resolution by increasing the number of photons?

→ stack two tiles with different refractive indices: "focusing" configuration



→ focusing radiator





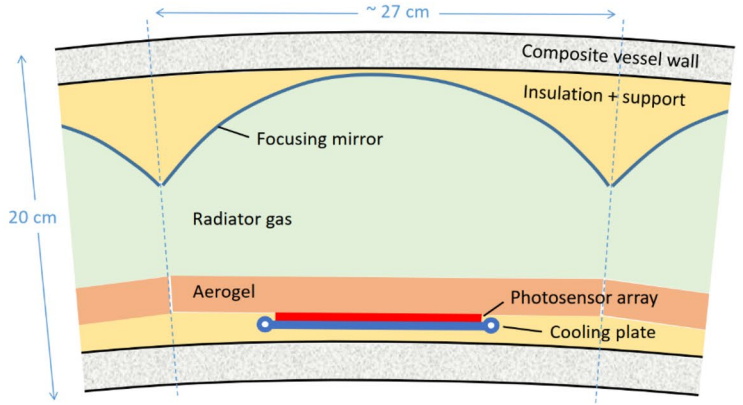
T. Iijima, S. Korpar et al NIMA 548 (2005) 383, NIMA 565 (2006) 457

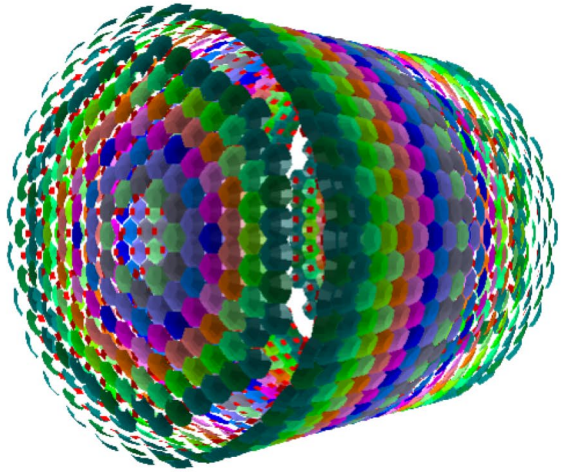
ARC: Array of RICH Cells for FCC-ee

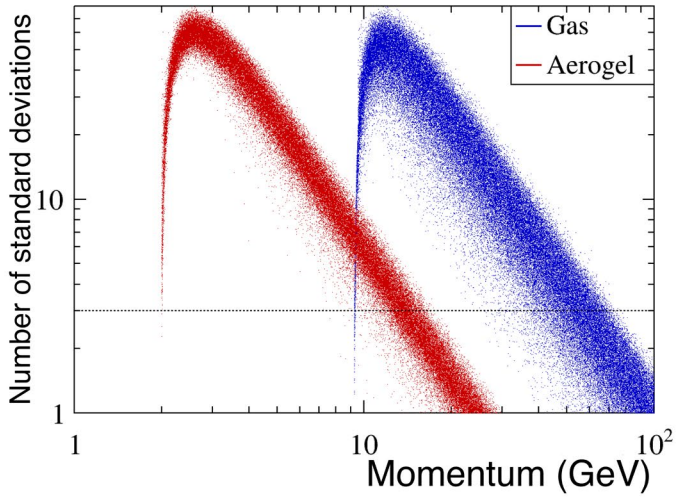
compact cell
silica aerogel
+ gas radiator
+ spherical mirror
+ SiPM plane

modular barrel
many similar cells
compact radial envelope
shared sensor technology

physics reach
charged-hadron PID
~1–40 GeV/c
K/π separation





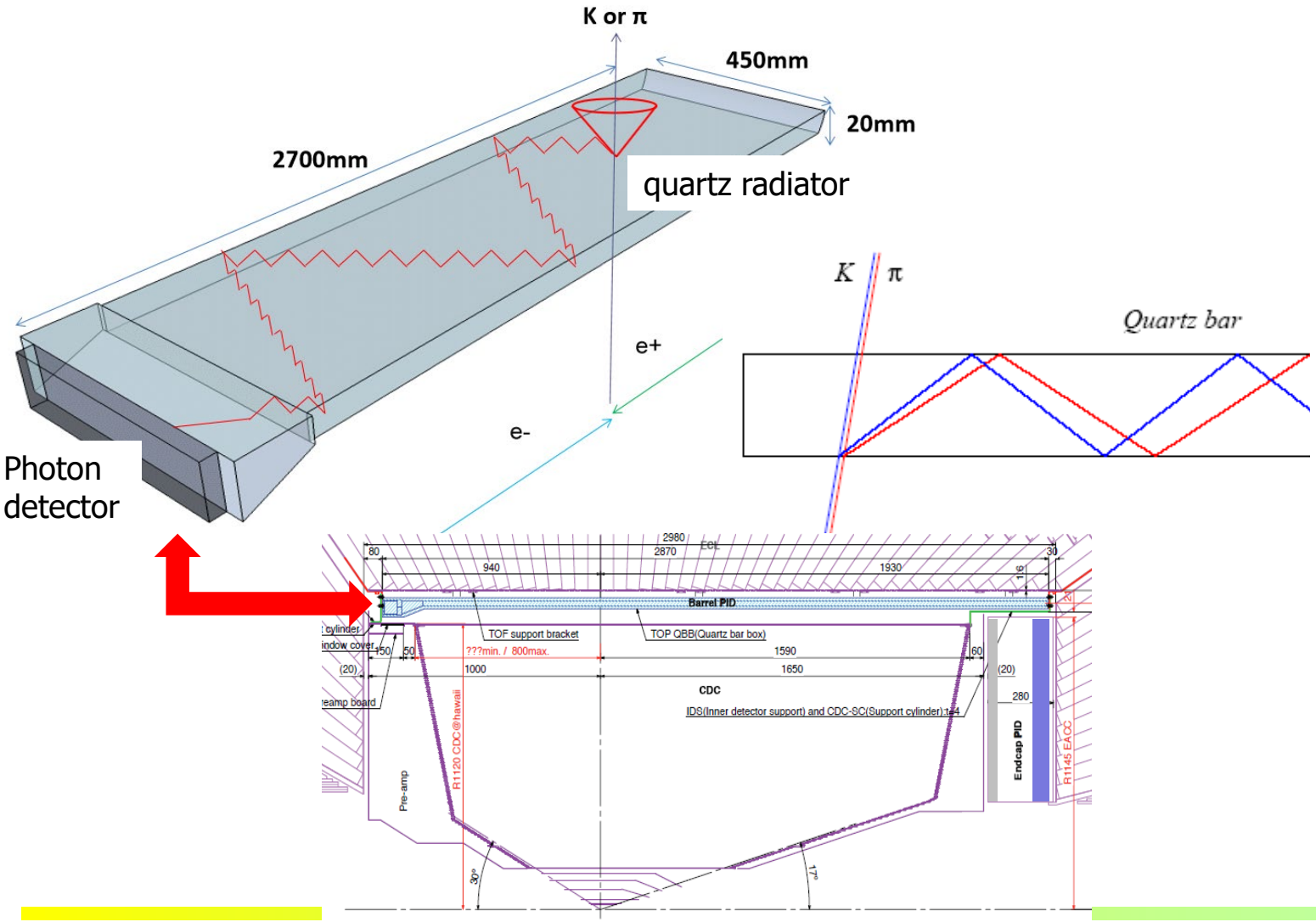


ARC is a direct example of future PID requirements driving low-light sensor R&D.

S. Pezzulo et al., NIMA 1086 (2026) 171327; FCC-ee detector review (2025).

Belle II Barrel PID: Time of propagation (TOP) counter

Similar to the DIRC, Cherenkov ring imaging with precise time measurement.

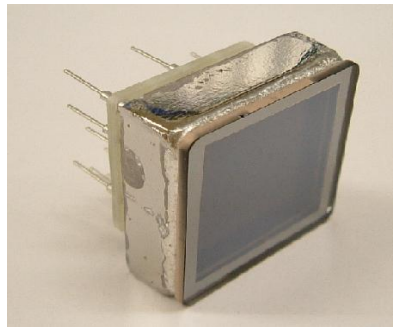


Reconstruct Cherenkov angle from two hit coordinates and the time of propagation of the photon

-Quartz radiator (2cm thick)

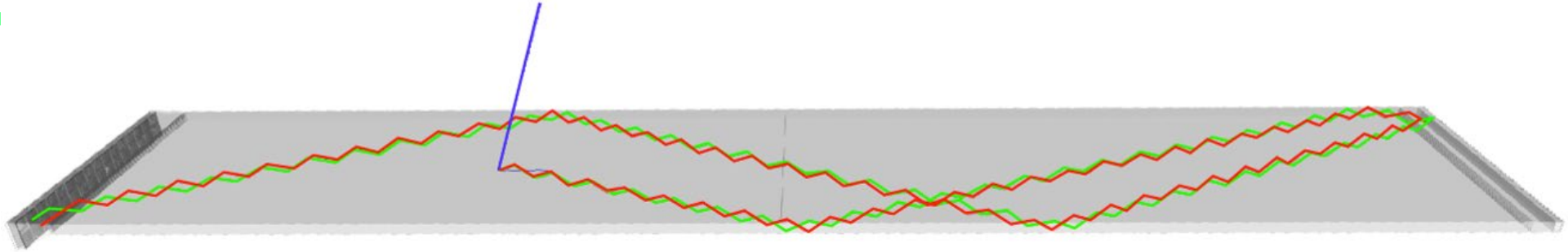
-Photon detector (MCP-PMT)

- Excellent time resolution ~ 40 ps
- Single photon sensitivity at 1.5 T

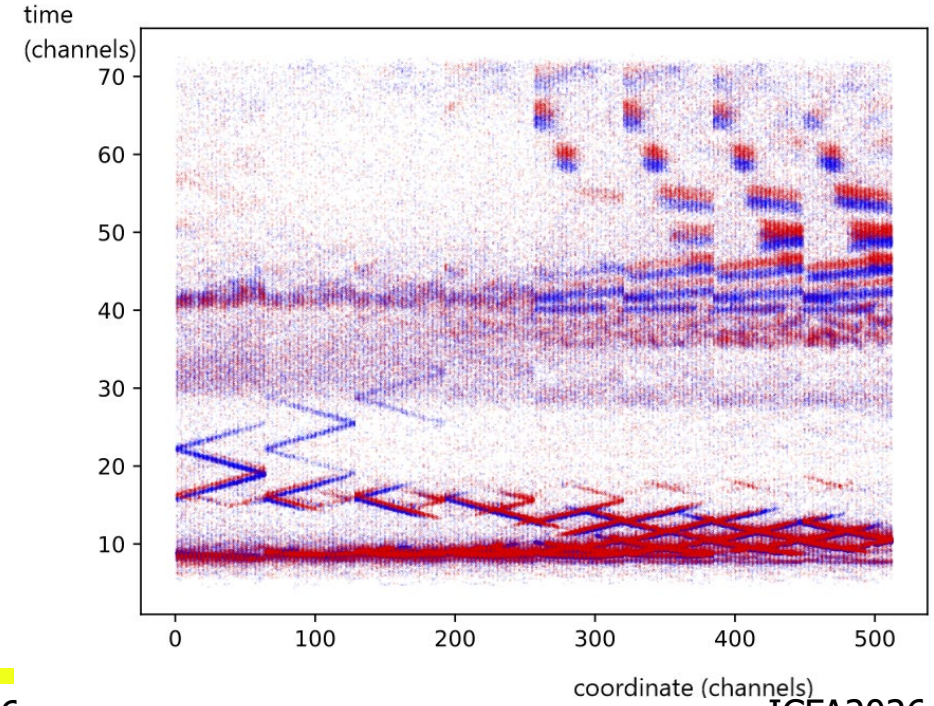


Hamamatsu SL10, 1" MCP-PMT

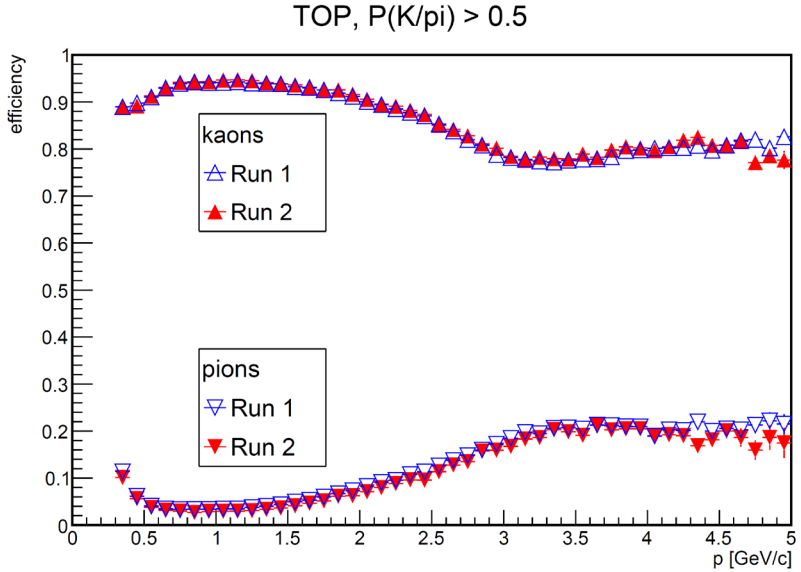
Separation of kaons and pions



Pions vs kaons in TOP:
different patterns in the time vs PMT impact point coordinate



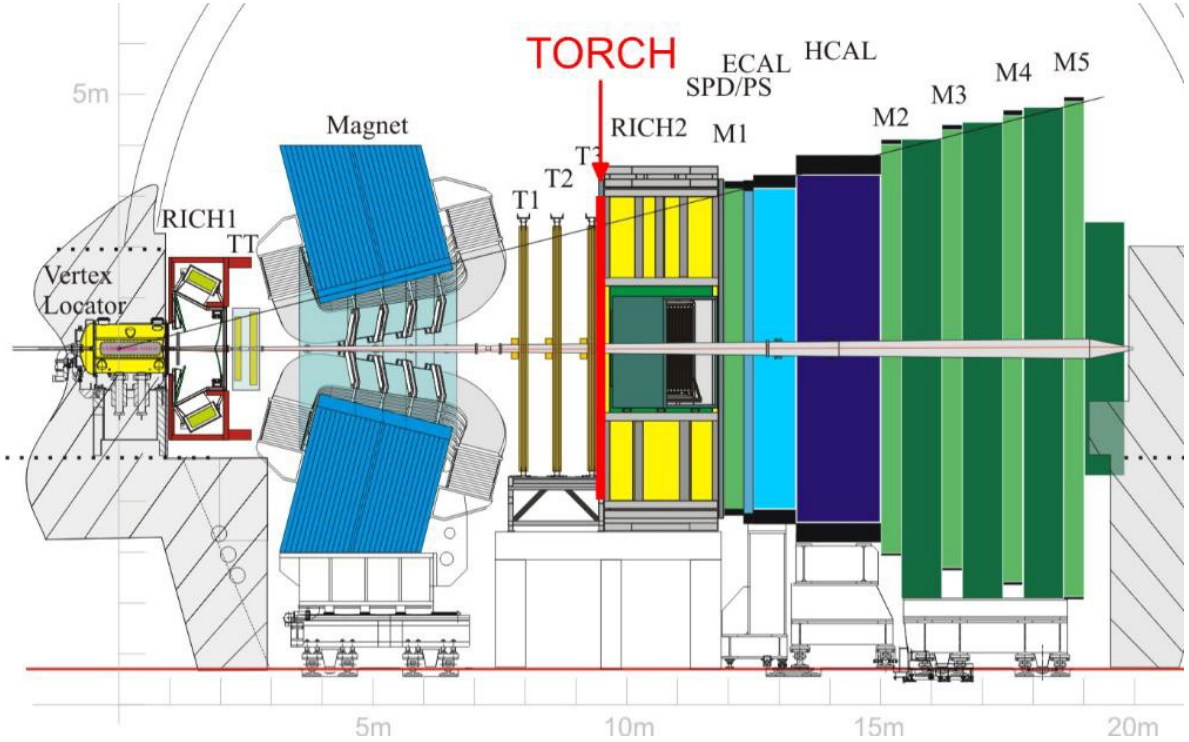
Pions vs kaons:
PID efficiency and misidentification probability.

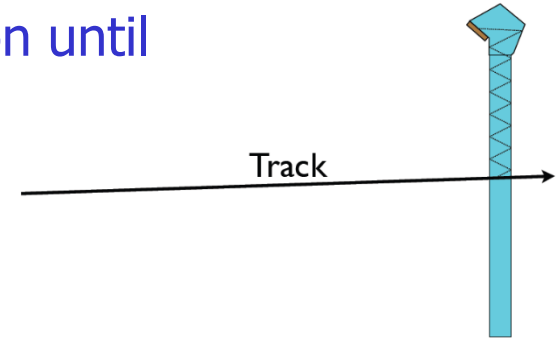


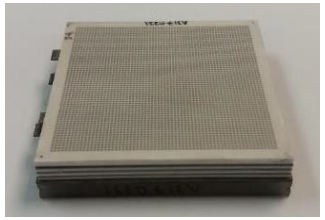
H. Atmacan et al, NIMA 1080 (2025) 170627

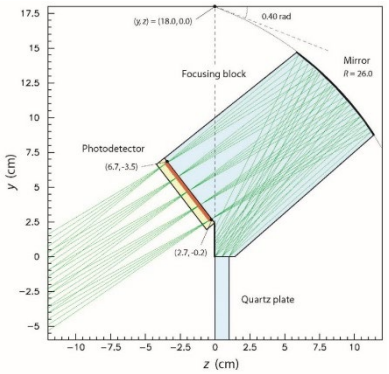
TORCH: A special type of Time-of-Propagation counter

Possible LHCb upgrade to cover pion/kaon separation until ~10 GeV/c – was considered for Upgrade 2



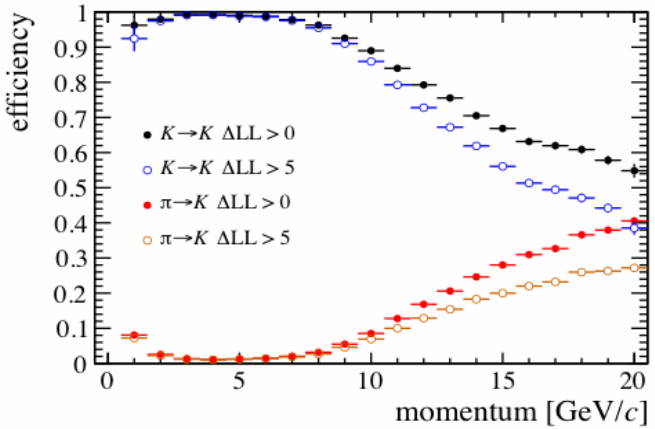






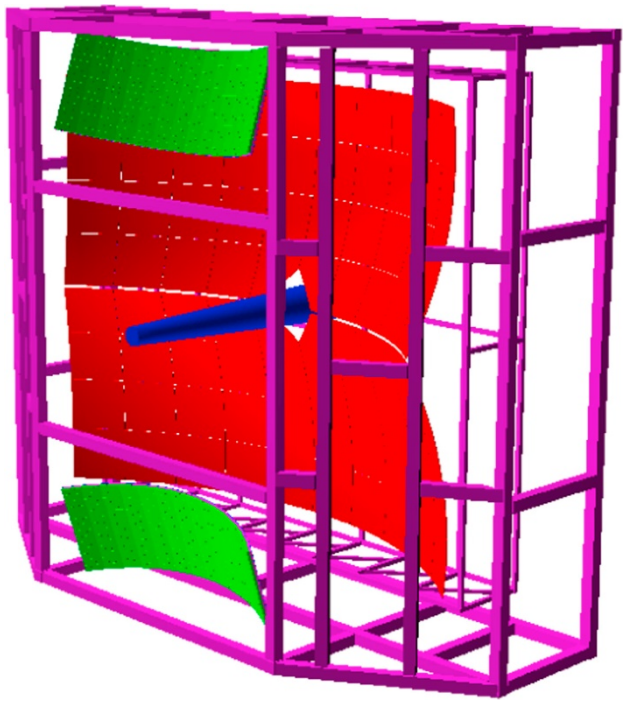
Focusing block with light sensors (MCP PMTs from Photek)

Expected performance

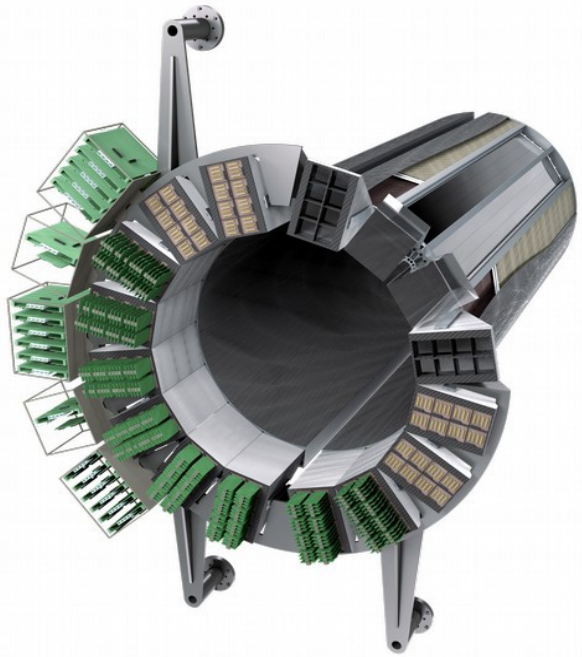


- TORCH area 5 x 6 m^2
- 18 module system
- 11 MCPs per module

FAIR: CBM RICH and PANDA Barrel DIRC



- RICH with CO_2 radiator
- MaPMTs: Hamamatsu H12700
- Cylindrical photon detection surface
- Momentum up to 8 GeV/c
- Expected pion suppression factor ~5000 (including TRD)



Design: based on BABAR DIRC and SuperB FDIRC with key improvements

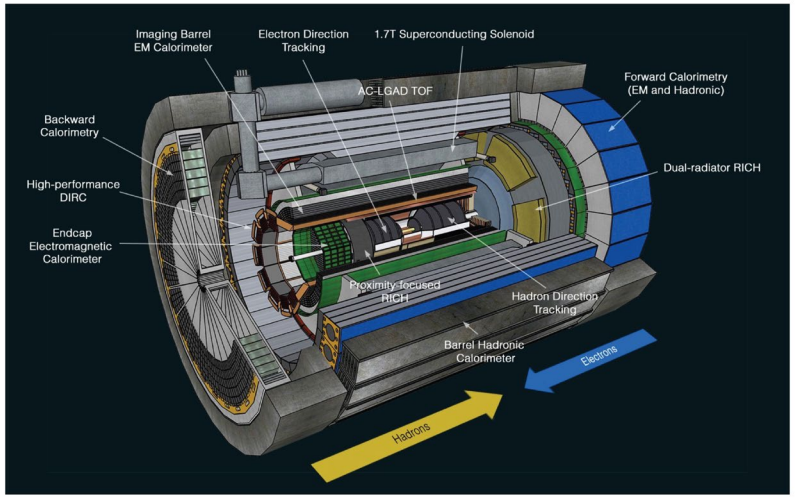
Barrel radius ~48 cm; expansion volume depth: 30 cm.
48 narrow radiator bars, synthetic fused silica,
17 mm x 53 mm x 2400 mm

Compact photon detector:
30 cm fused silica expansion volume
8192 channels of MCP-PMTs in ~1T B field

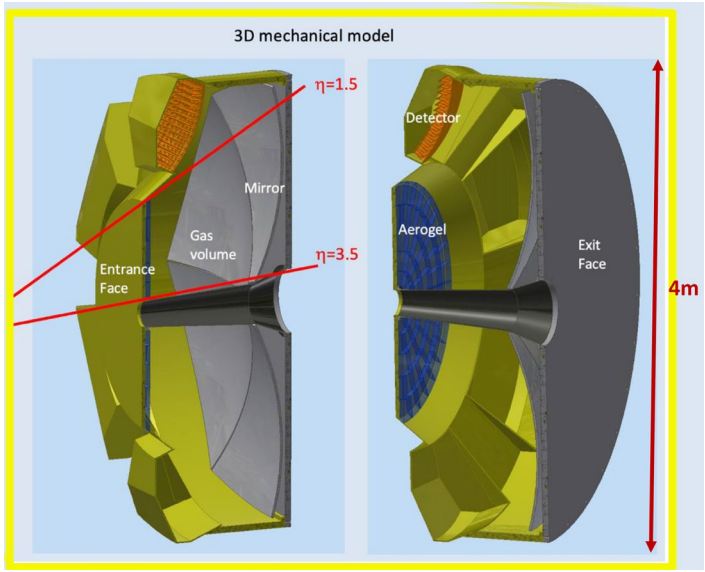
Focusing optics: spherical lens system

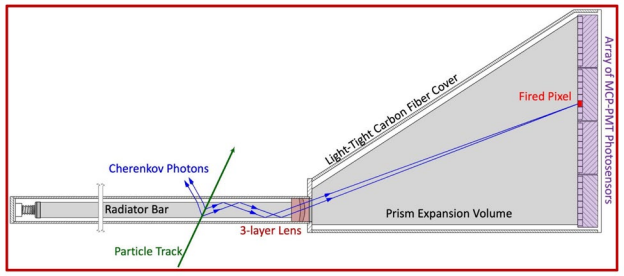
Fast photon detection: fast TDC plus TOT electronics,
→ 100-200 ps timing

EPIC at EIC: three RICH detectors

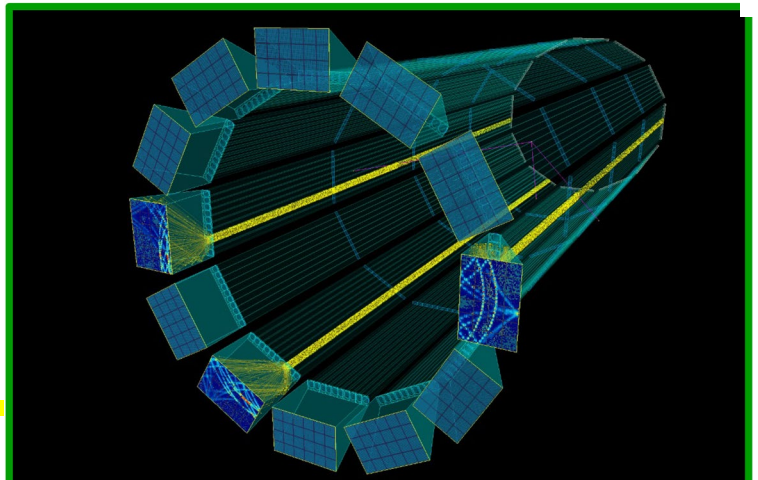


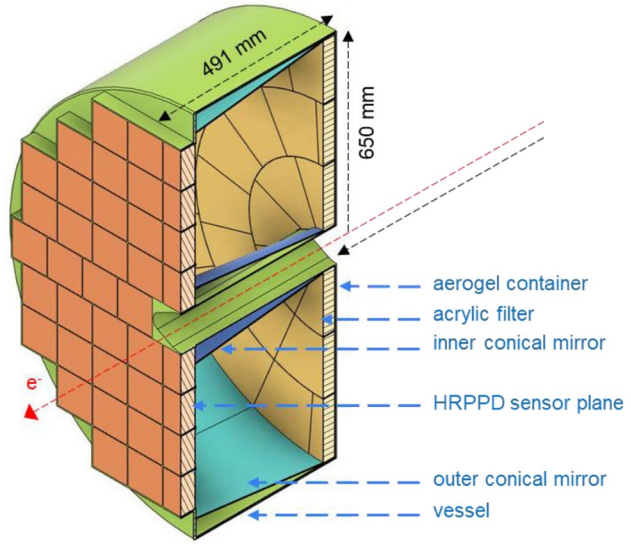
dRICH: Dual radiator RICH (aerogel+gas) with SiPM readout





hpDIRC – high performance DIRC





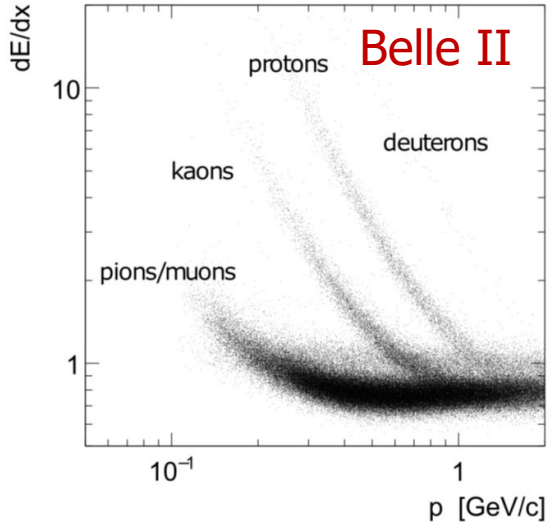
pfRICH: proximity focusing RICH with aerogel radiator and MCP-PMTs (half-size LAPPD – HRPPD)

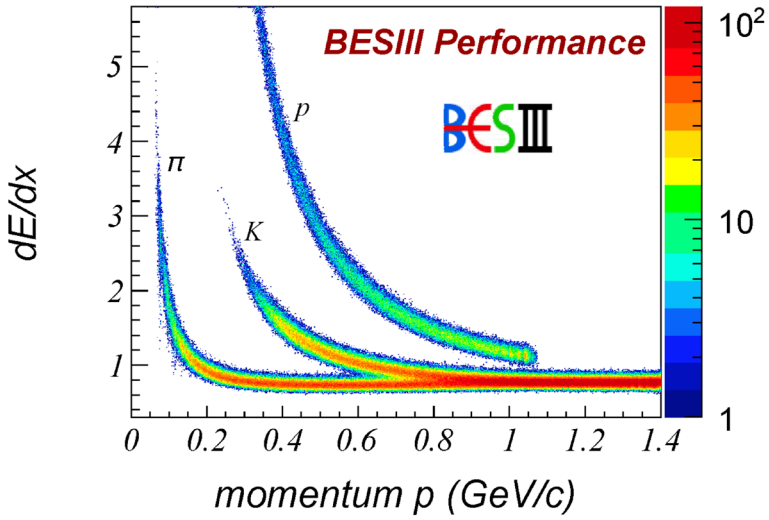
dE/dx and dN/dx

Belle II Central Drift Chamber (CDC)

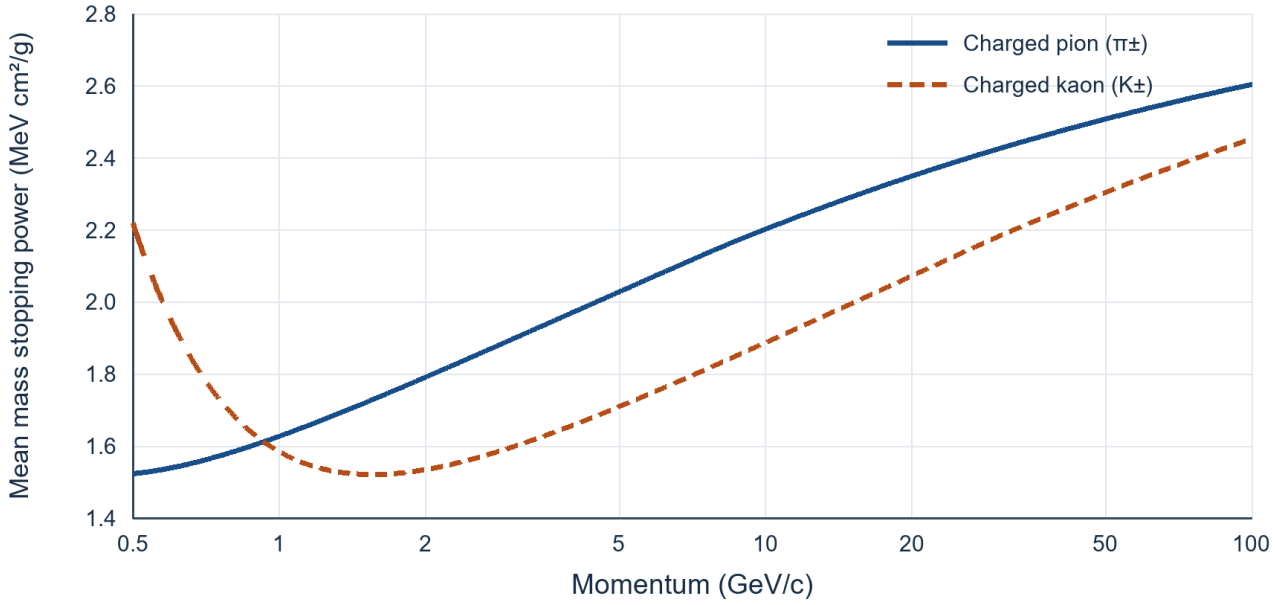
- Typical resolution in the experiment σ(dE/dx)~7% (He/ethane 50/50 mixture)
- Covers a considerable fraction of the kinematic range of the experiment (complemented at higher momenta by ARICH + TOP)

Similar: main drift chamber of BESIII





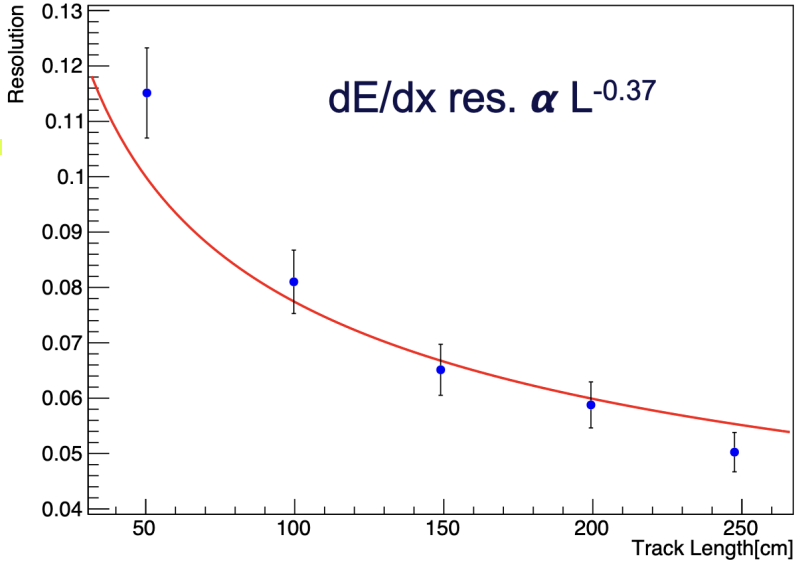
To extend the PID performance into several tens of GeV, as required for the FCC-ee, need better resolution → a larger drift chamber or TPC with a different gas, and possibly using a different method

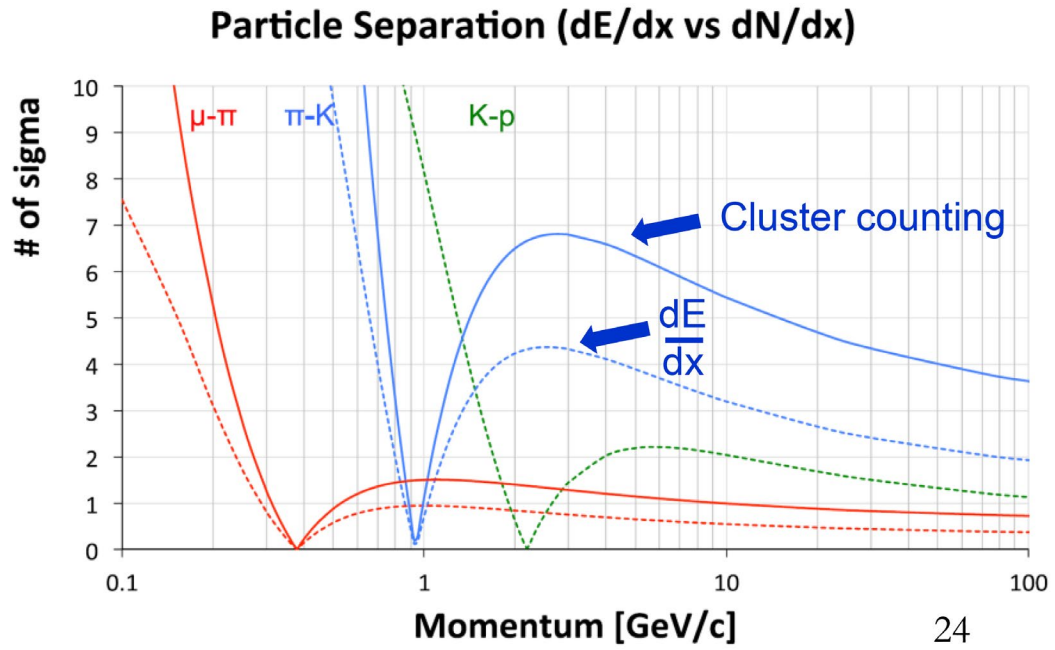


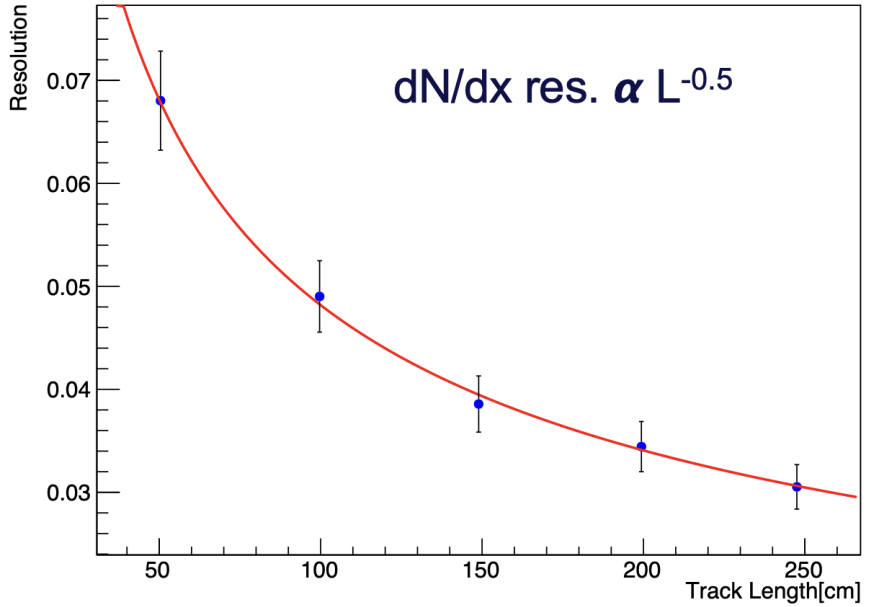
dE/dx, dN/dx

Resolution as a function of track length (L) for the energy loss (dE/dx) and cluster counting (dN/dx) methods (He/isobutane 90/10 mixture).

The red curves superimposed on the plots show the fits of $L^{-0.37}$ for dE/dx and $L^{-0.5}$ for dN/dx.





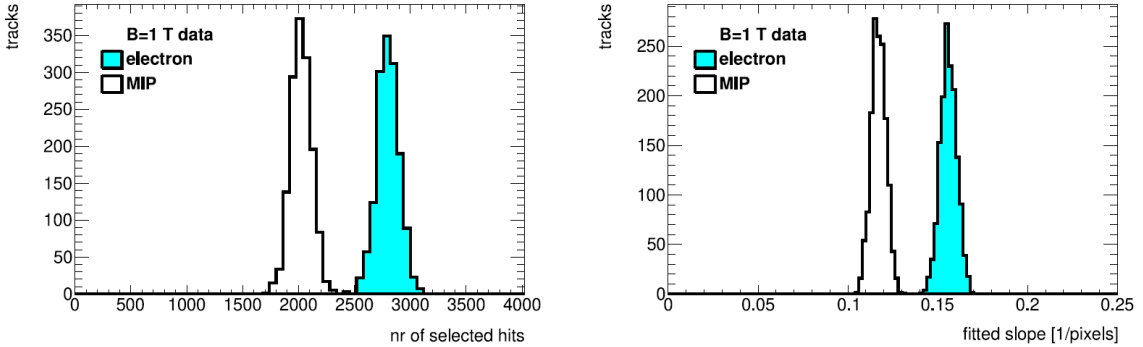


W. Elmetenawee et al, PoS (ICHEP2024) 1067

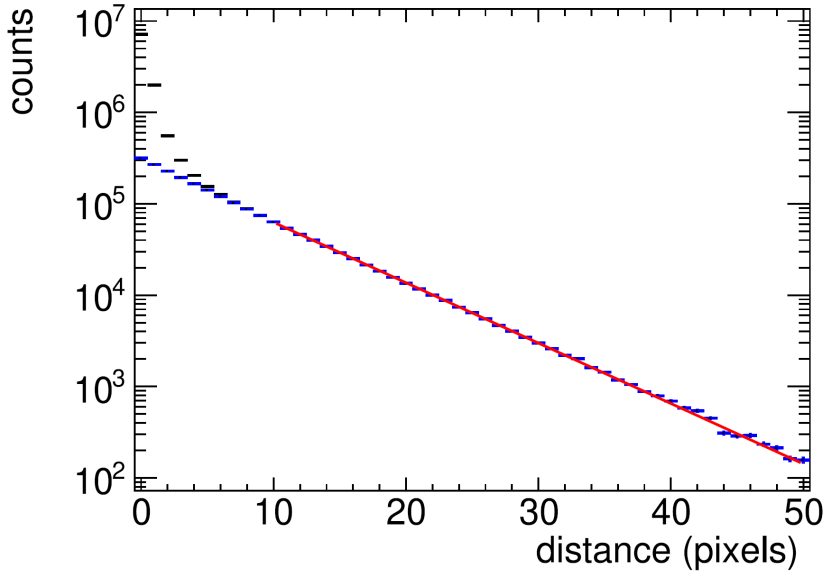
dE/dx, dN/dx

Results of a beam test in 1 T field of a TPC (Ar/CF_4/isobutane 95/3/2 mixture) with GridPix read-out.

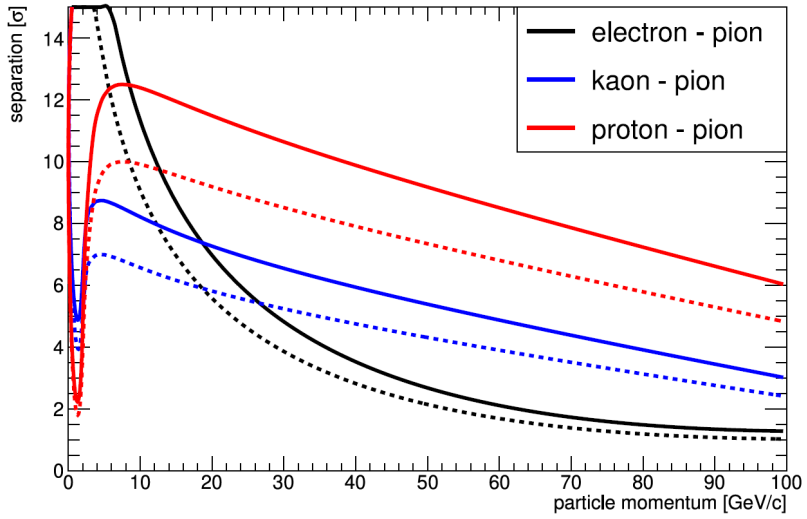
Use the hit-to-hit distance along the track as the discriminating variable. → 2.4% resolution for 144cm long track.



Distribution of the number of selected hits per track for the dE/dx truncation method (left) and the fitted slope for the template fit method (right) for an electron (light blue shaded) and for a MIP, using 1 m long tracks with 60% coverage, for the B = 1 T data.



Distribution of the number of selected hits as a function of the distance in pixel units (55μm x 55μm) for the B = 1 T data is shown in black. The exponential fit result is shown with a red line.



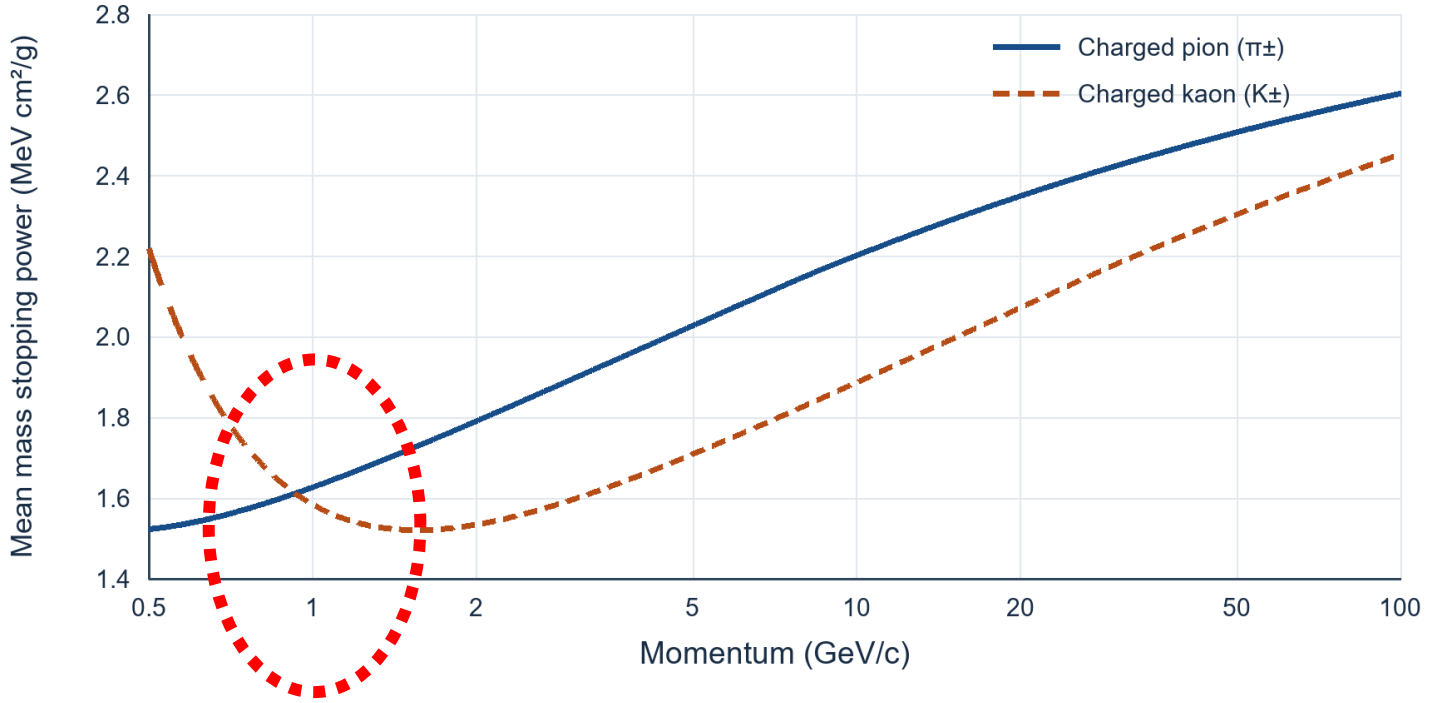
The projected PID separation for a GridPix TPC in ILD for electrons, kaons and protons w.r.t. pions at cos θ = 0. Full curves correspond to electron PID resolution of 2.4%, dashed 3%.

M. Van Beuzekom et al, NIMA 1081 (2026) 170849

Time-of-flight at FCC-ee: closing the low-momentum PID gap

Precision timing provides complementary PID at low momentum

- dE/dx and dN/dx: “blind region” around 1 GeV/c for pion vs kaons



Time-of-flight at FCC-ee: closing the low-momentum PID gap

Precision timing provides complementary PID at low momentum

- dE/dx and dN/dx: "blind region" around 1 GeV/c
- TOF naturally fills this gap
- 30 ps / track: π/K separation to ~3 GeV/c
- 10 ps / track: extends π/K separation to ~5 GeV/c

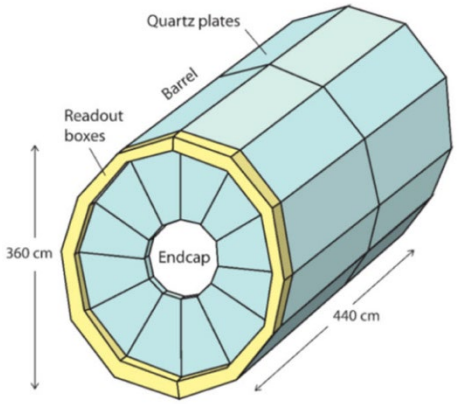
HL-LHC timing developments: ~30 ps/track is realistic (ATLAS HGTD and CMS MTD)

Towards O(10 ps): Cherenkov TOF

- TORCH: ~70 ps / photon

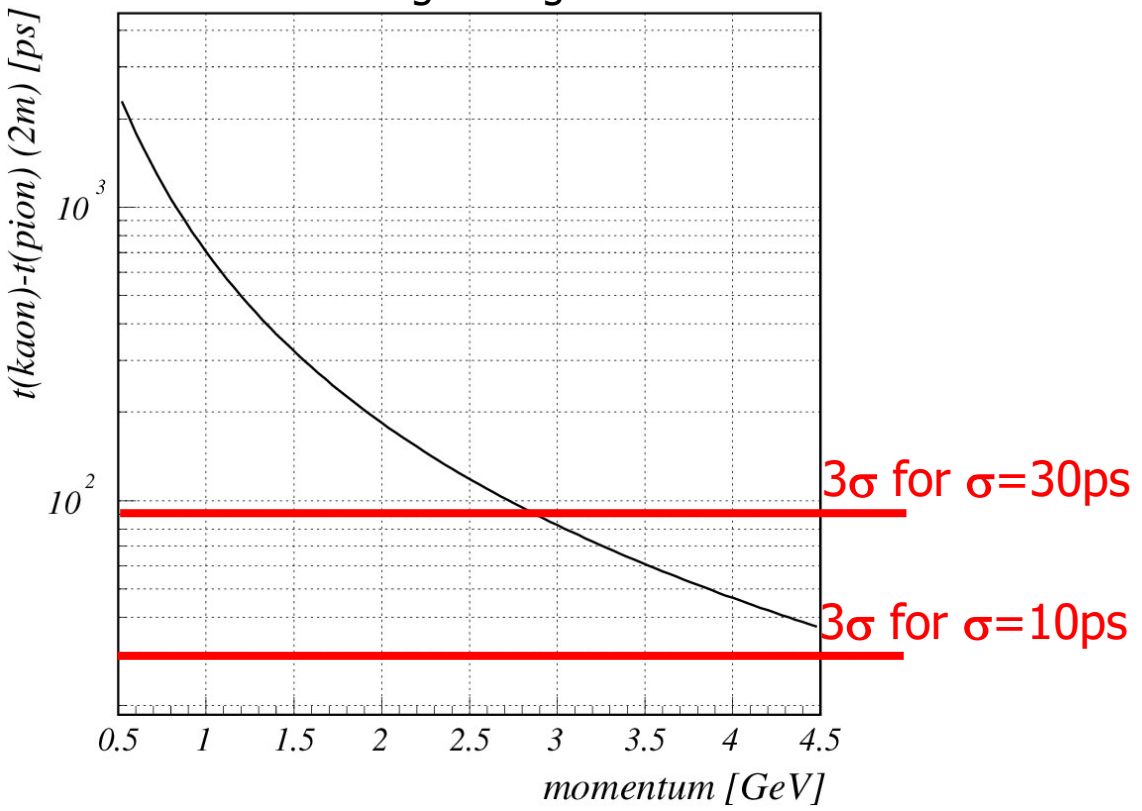
→ 10–15 ps / track

(similar to Belle II TOP)



Time difference between π and K:

2m flight length



Time-of-flight at FCC-ee: closing the low-momentum PID gap

Precision timing provides complementary PID at low momentum

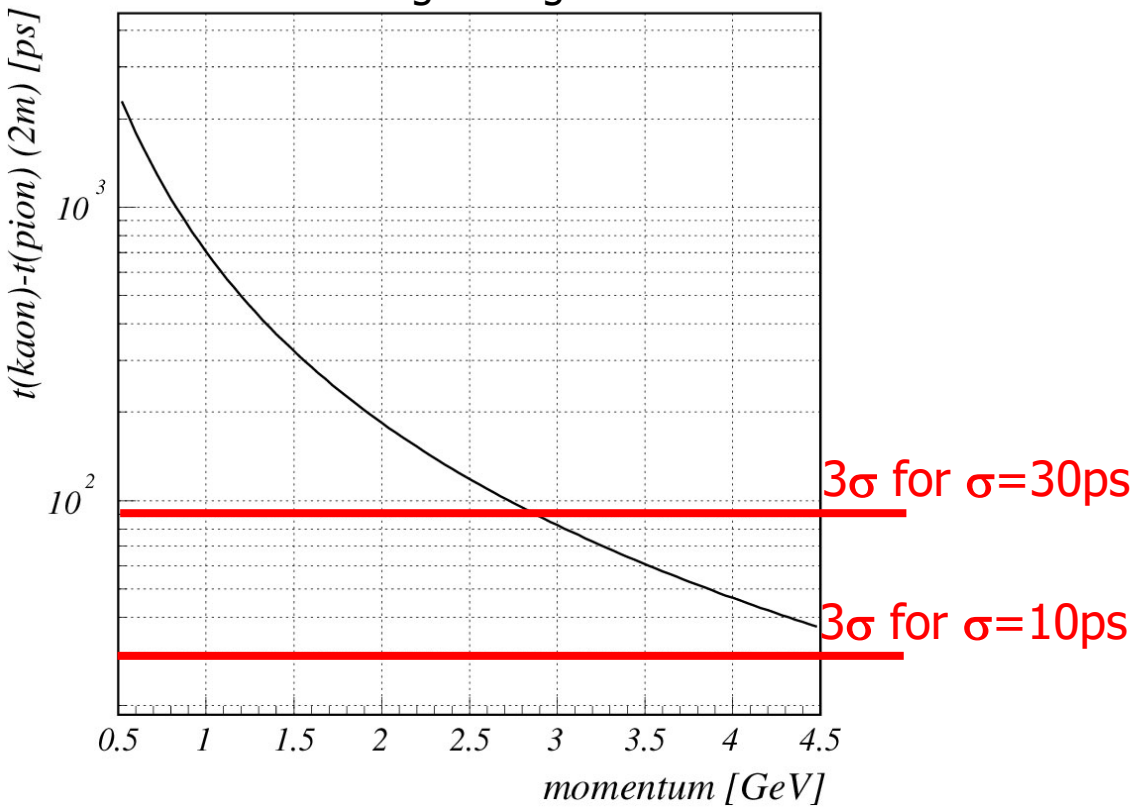
- dE/dx and dN/dx: "blind region" around 1 GeV/c
- TOF naturally fills this gap
- 30 ps / track: π/K separation to ~3 GeV/c
- 10 ps / track: extends π/K separation to ~5 GeV/c

HL-LHC timing developments: ~30 ps/track is realistic (ATLAS HGTD and CMS MTD)

Towards O(10 ps): Cherenkov TOF

- TORCH: ~70 ps / photon → 10–15 ps / track
- Dedicated Cherenkov TOF with 10-20 ps /track

Time difference between π and K:
2m flight length



TOF + dN/dx → complementary PID over a broad momentum range

TOF with Cherenkov light

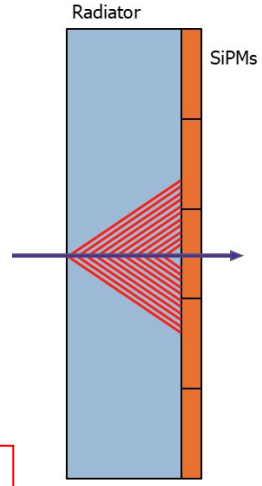
Idea: detect Cherenkov light (prompt) with a very fast photon detector

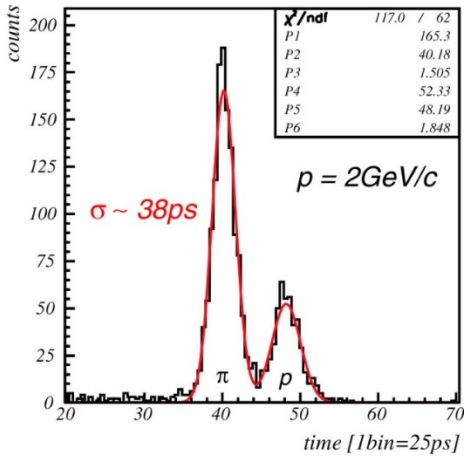
Cherenkov light is produced in a radiator (e.g., quartz plate) in front of the photosensor and in the PMT window.

→resolution ~5ps with quartz+MCP-PMT

K. Inami et al NIMA 560 (2006) 303

J. Va'vra et al NIMA 595 (2008) 270





Proof of principle: beam test with MCP-PMT, pions and protons at 2 GeV/c. Cherenkov photons from MCP-PMT window only.

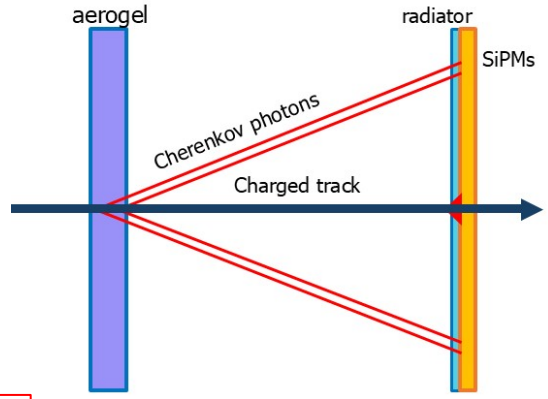
S. Korpar et al., NIMA 572 (2007) 432

DRD4 WP4: developing the

- detector concept +
- read-out electronics +
- lightweight support for large detector areas

Potential use: FCC-ee and ALICE3

N. Mazziotta et al NIMA 1090 (2026) 171648

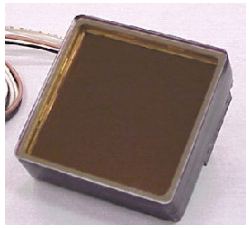


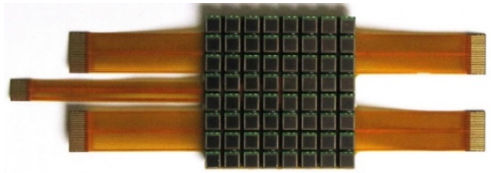
RICH+TOF: combine aerogel RICH to identify particle above Cherenkov threshold in aerogel with TOP: positive identification of particles below Cherenkov threshold in aerogel

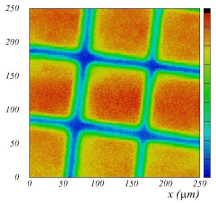
P. Križan, NIMA 581 (2007) 57

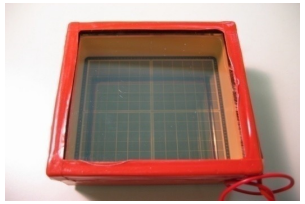
Photon detection

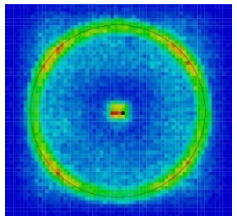




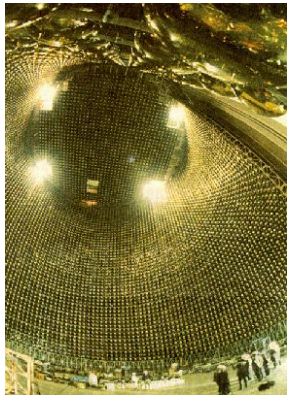


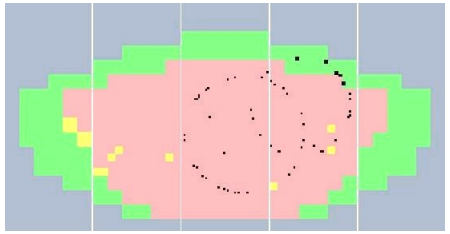


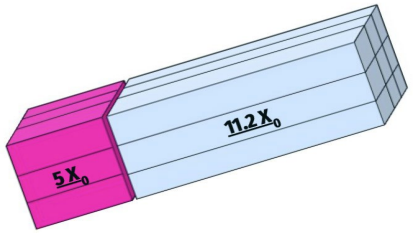


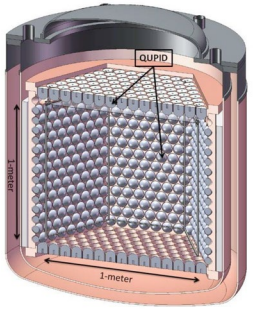


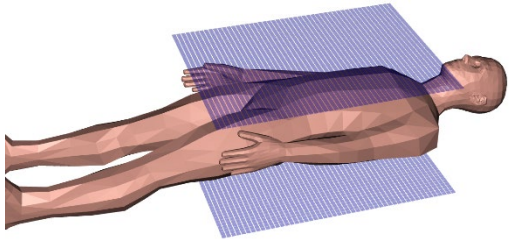
Low-light-level detection: why?











Photon detectors are at the heart of most experiments in particle and nuclear physics. Moreover, they are also finding applications in other scientific fields (chemistry, biology, medical imaging) and are ubiquitous in society in general.

New environments where we need to detect light (in particular low light levels) → need advances in existing technology and transformative, novel ideas to meet the demanding requirements.

Two main lines of R&D to be pursued, identified by the ECFA Detector R&D Roadmap:

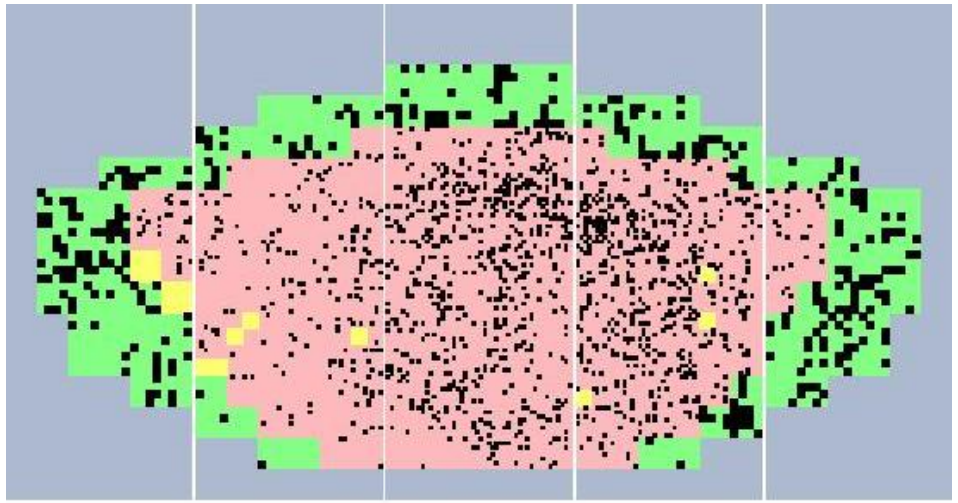
- Enhance timing resolution and spectral range of photon detectors.
- Develop photosensors for extreme environments.

Cherenkov counters in LHC-like environments

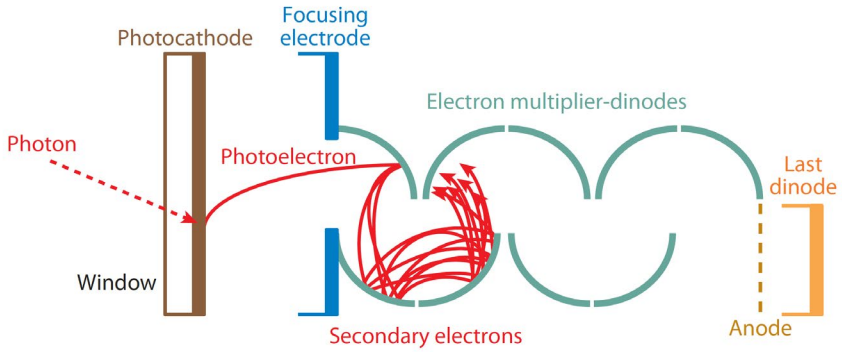
Operation at high rates (~1 MHz/cm^2) over extended running periods (years)

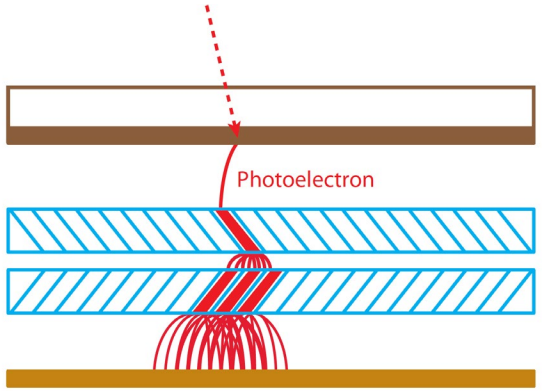
Good spacial resolution (pads with ~5 mm size or smaller) over a large detector area

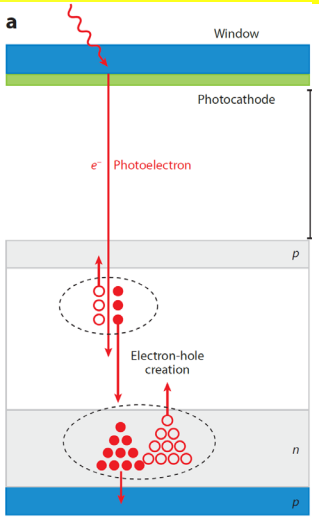
In mid-1990s the solution was vacuum-based multichannel photodetectors,
multianode PMTs (MaPMTs) and hybrid photodetectors (HPDs).



Vacuum-based photodetectors

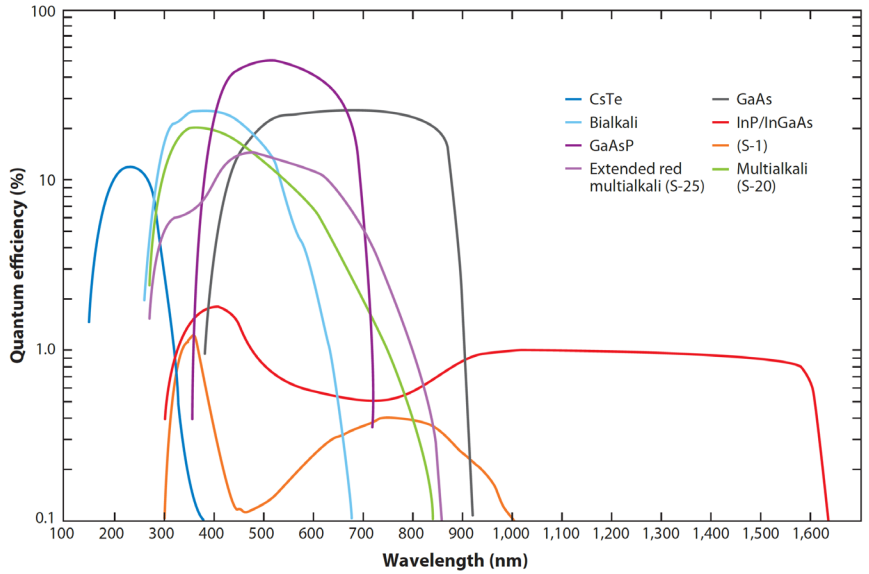




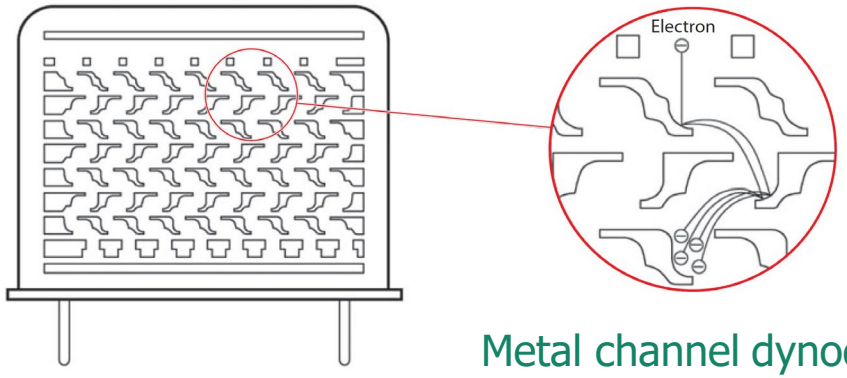


Generic steps:

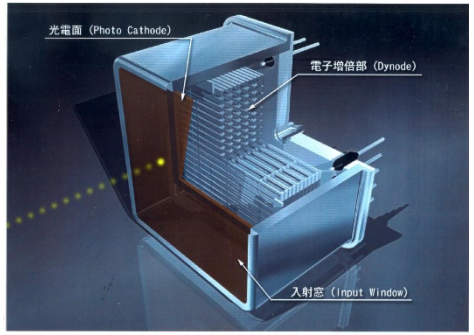
- Photon → photoelectron conversion
- Photoelectron collection in the multiplication system
- Mutiplication (dynodes, microchannel plates, high E field + Si)
- Signal collection



Multianode photomultiplier tubes (PMTs)

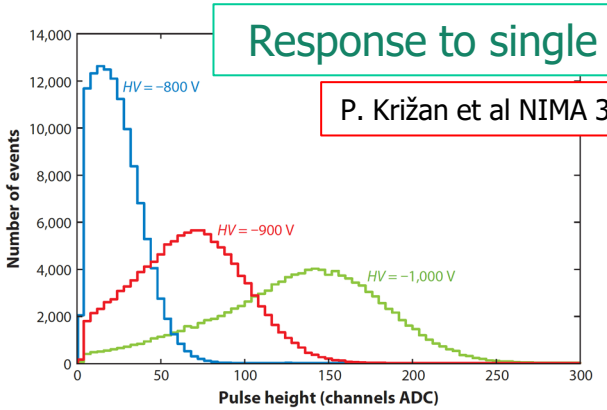


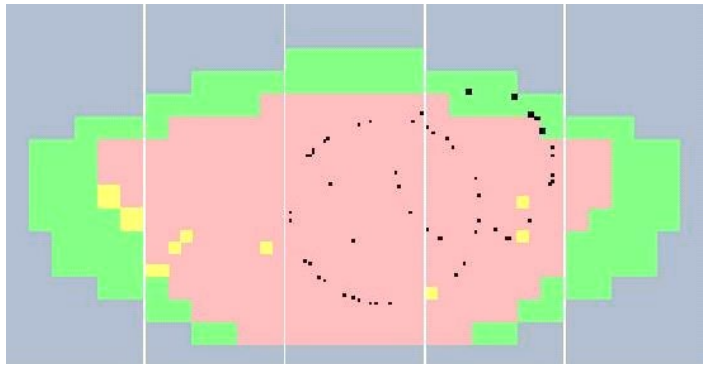
Metal channel dynodes



Response to single photons

P. Križan et al NIMA 394 (1997) 27





Pioneered in the HERA-B RICH, later used in RICH detectors of COMPASS, CLASS12 and GlueX

Recent use in the upgraded LHCb RICH detectors;
in construction: CBM RICH

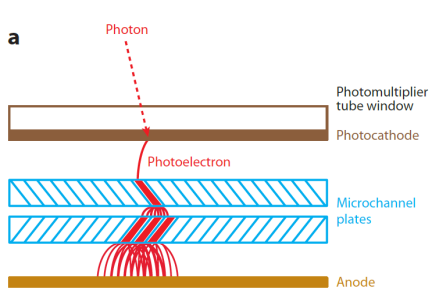
Excellent performance (excellent single photon detection efficiency, very low noise, low cross-talk), game changer in mid-1990s for RICH detectors, still the best choice for large areas with no B field

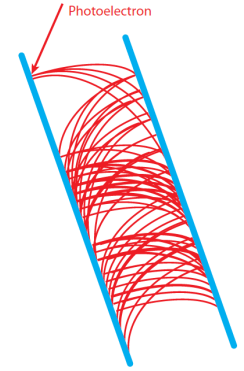
Micro Channel Plate PMT (MCP-PMT)

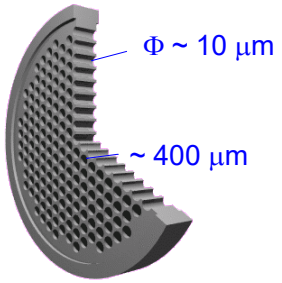
Similar to ordinary PMT – the dynode structure is replaced by MCPs.

Basic characteristics:

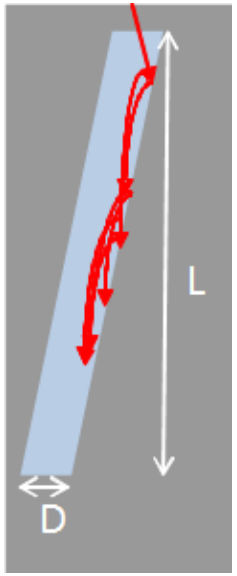
- Gain ~ 10^6 → single photon
- Collection efficiency ~ 60%
- Small thickness, high field → very fast
- Works in magnetic field
- Segmented anode
  → position sensitive



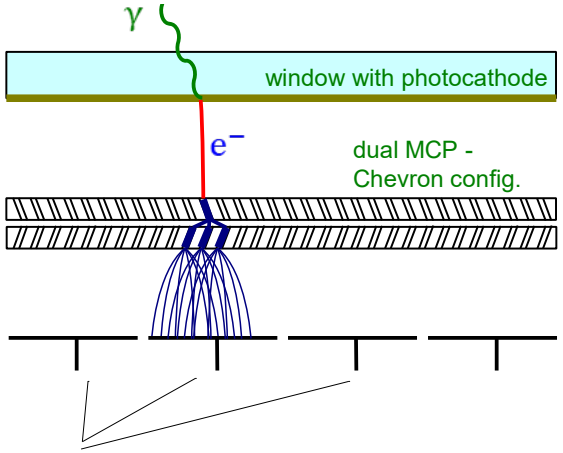




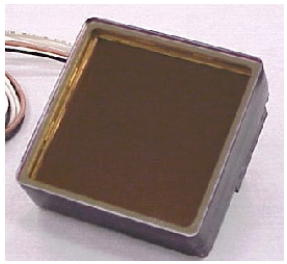
MCP is a thin glass plate with an array of holes (<10-100 μm diameter) - a continuous dynode structure



MCP gain depends on L/D ratio – typically 1000 for L/D=40



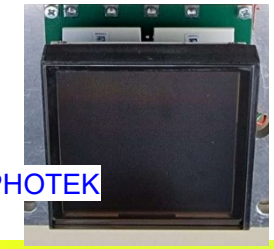
Anodes → can be segmented according to application needs



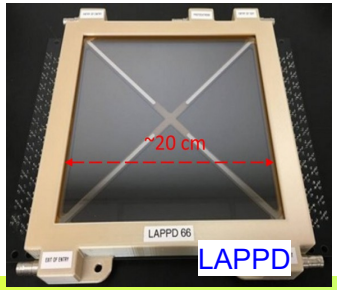
PHOTONIS



HAMAMATSU



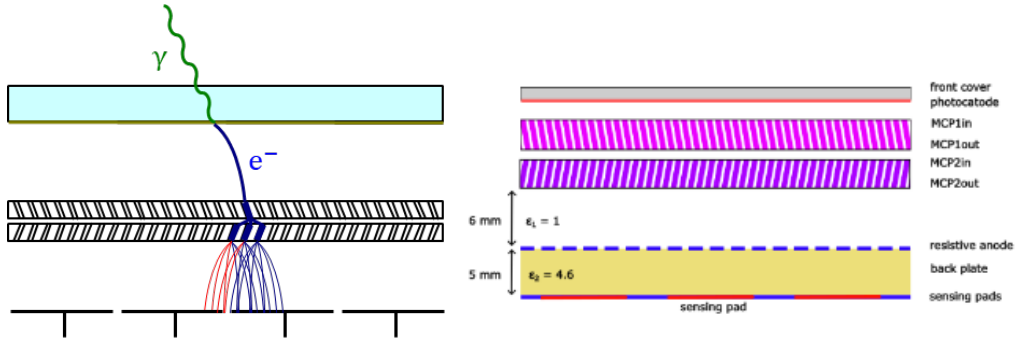
PHOTEK



LAPPD

LAPPD (large area picosecond photodetector) Gen II

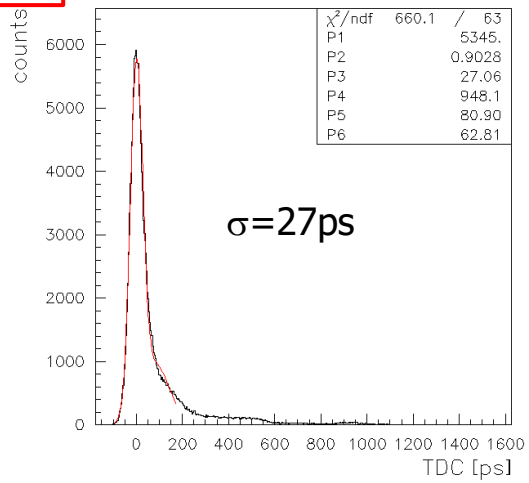
- MCPs with a novel, cheaper production method (ALD-coated glass)
- two parallel spacers (active fraction ≈ 97 %)
- gain ≈ $5 \cdot 10^6$ @ ROP (825 V/MCP, 100 V on photocathode)
- peak QE ≈ 25%
- internal anode pads or capacitively coupled readout electrode
- size 230 mm x 220 mm x 22 mm
- dark dount rate @ ROP: ~ 70 kHz/cm^2 with 8x10^5 gain
- half size version: HRPPD, ~ 10cm x 10cm



M.J. Minot et al. NIMA 787 (2015) 78

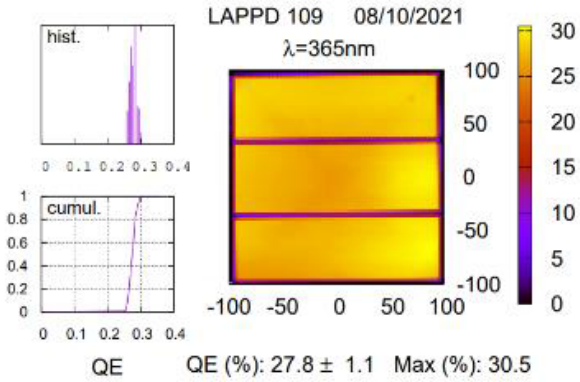
A. Kiselev et al, 10.1109/NSS/MIC44867.2021.9875860



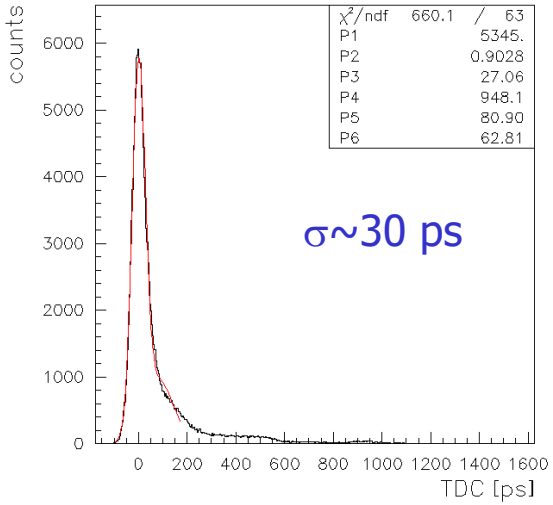


LAPPD – timing

LAPPD Q.E.

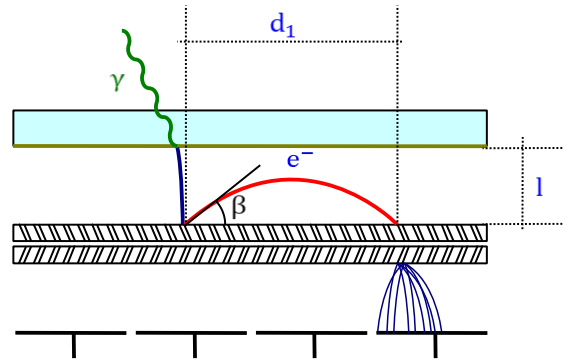


Understanding MC-PMTs: time spectrum for single photons

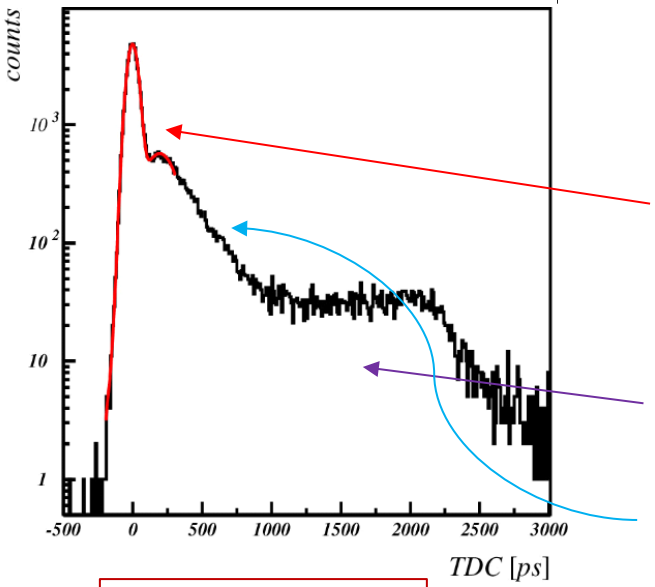


Time spectrum for single photons: photoelectron back-scattering produces a rather long tail in timing distribution and position resolution.

A simple model was developed to understand the features in the time spectrum for single photons.

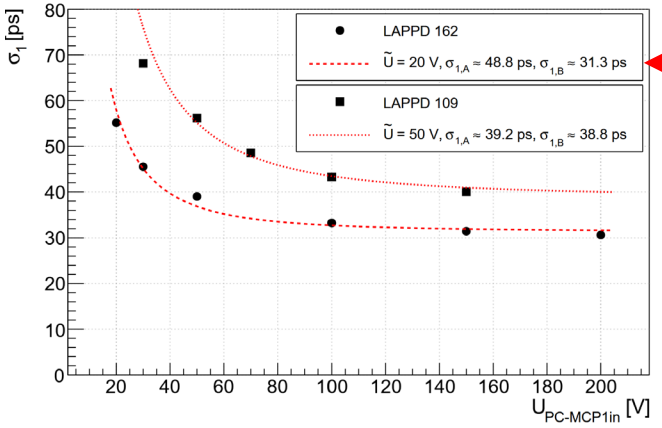


S. Korpar et al, NIMA 1088 (2026) 171466

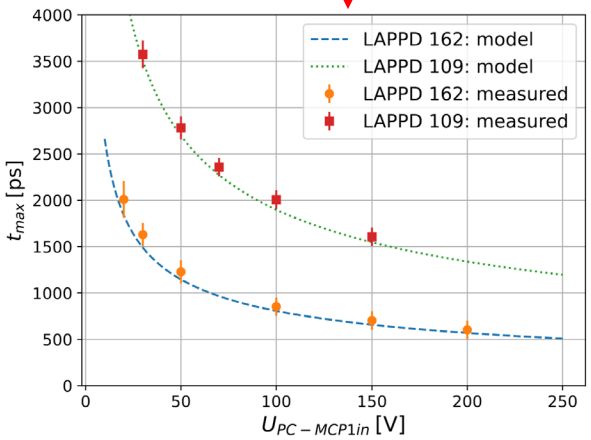


Typical single photon timing distribution with a narrow main peak (σ~30-40 ps) and contributions from photoelectron elastic back-scattering (flat distribution) and inelastic back-scattering.

S. Korpar et al, PD07



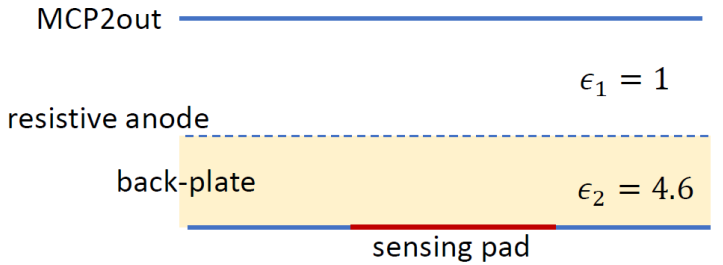
Main peak width and width of the flat tail vs PC-to-MCP1 HV.

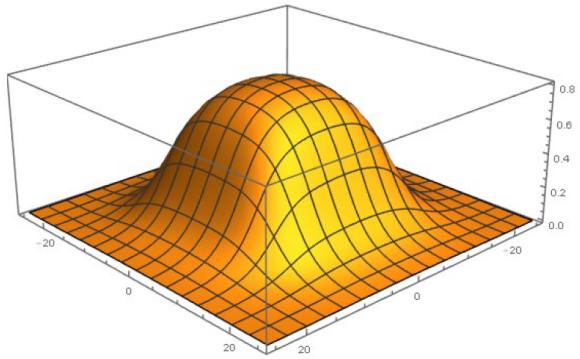


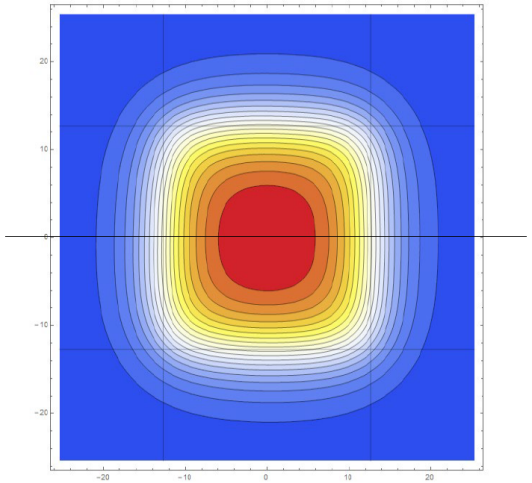
MCP PMT readout: capacitive coupling, modeling

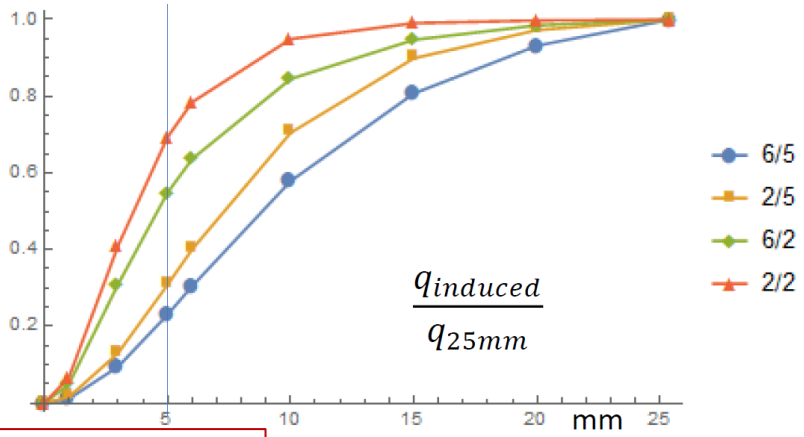
MCP-PMT charge sharing for capacitively coupled sensing pads: apply the Shockley-Ramo theorem

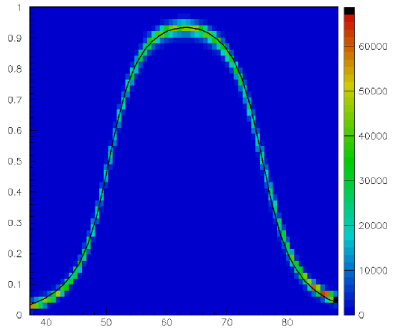
- calculation of charge sharing for different MCP2out-resistive andode/resistive anode-sensing electrode distances (6/5-measured, 2/5, 6/2, 2/2)
- fraction of the charge induced vs. square pad size when signal is produced in the centre of the pad

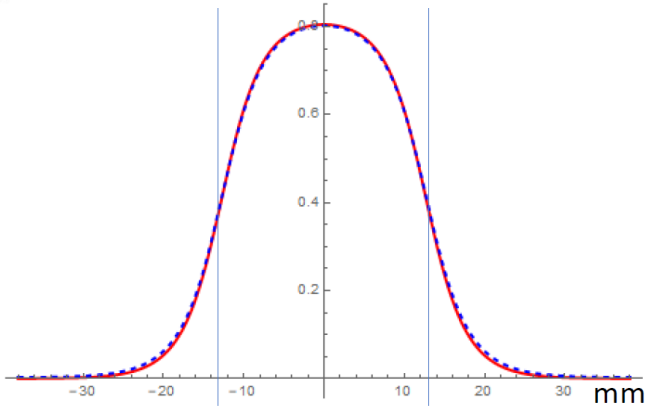












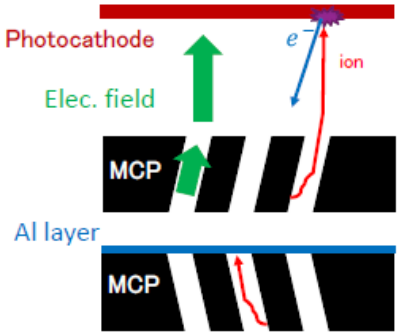
Capacitive coupling: due to charge spread on sensitive pads, the granularity cannot be reduced ad lib

S. Korpar et al, NIMA 1088 (2026) 171466

Charge sharing – capacitively coupled read-out electrodes; in coulour: measurement; black: model prediction

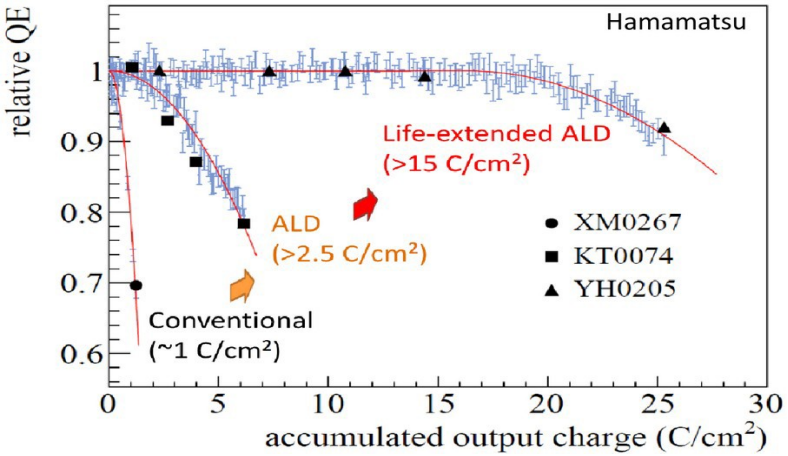
MCP PMT ageing and high rate operation

MCP PMTs: photo-cathode degradation due to ion feedback, main concern in high intensity experiments

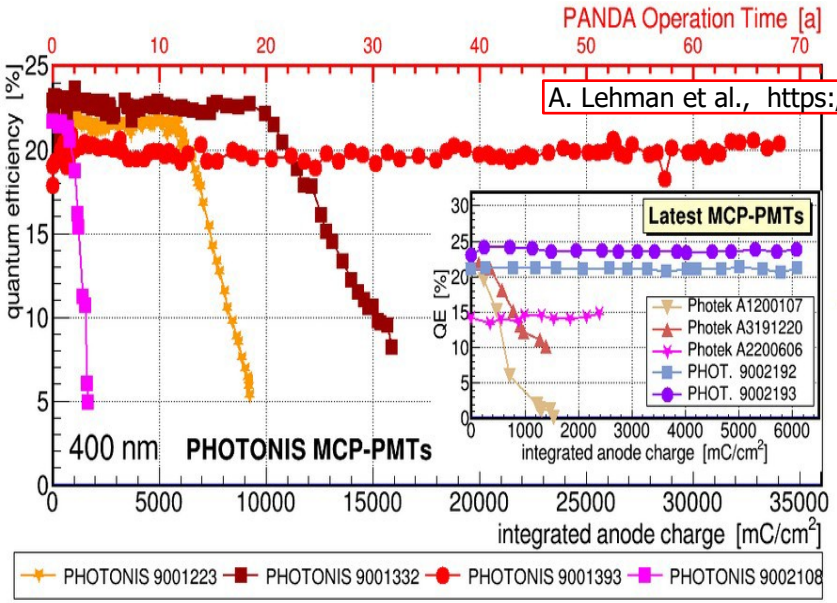


ALD (atomic layer deposition) coating of MCP pores → ~100x photo-cathode lifetime increase

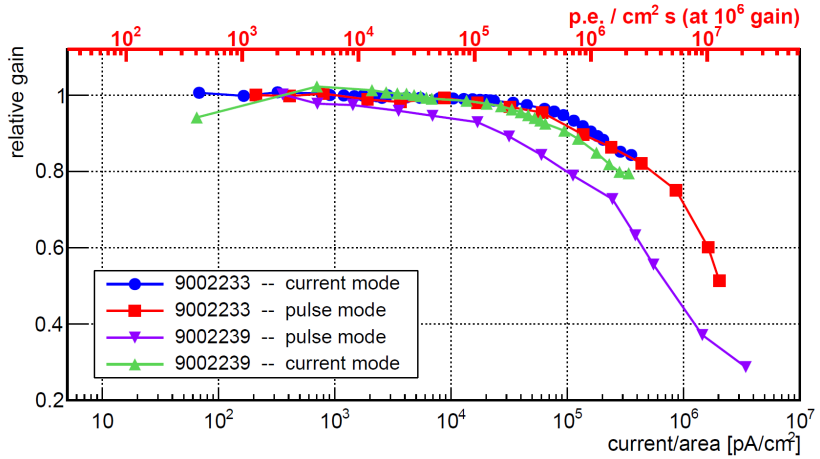
- Hamamatsu 1-inch YH0205 (>20 C/cm²) [K. Inami, 2021]
- No QE degradation for Photonis MCP-PMT (R2D2) to >34 C/cm²
- Little QE degradation in LAPPD 8-inch up to 5.6 C/cm² [V. A. Chirayath, CPAD2021]
- Extensive studies of MCP-PMTs for PANDA [A. Lehmann et al]



K. Inami, 2021, Talk at ECFA TF4 Symposium



A. Lehman et al., https://arxiv.org/abs/2403.13938



High rate performance studies

→ Gain degradation at fluxes of 10^7 photoelectrons /s /cm²

MCP-PMTs: New materials and read-out options

New materials, new coatings, longevity and rate capability study

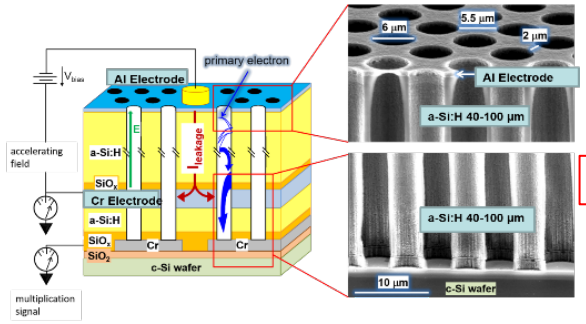
This concerns the R&D on new materials to produce VPD, new shapes and new coatings and their consequences on their longevity and rate capability

New photocathode materials, structure and high quantum efficiency

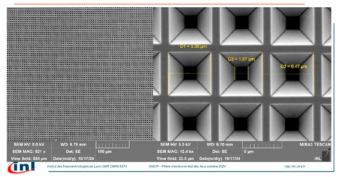
New photocathode materials, new structures and their impact on improving the quantum efficiency for different wavelengths

Time and spatial resolution performance

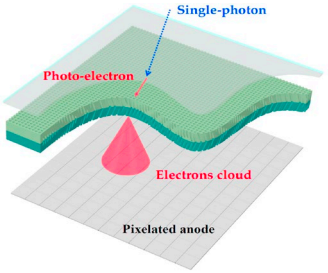
Study of VPD timing and spatial performance using appropriate readout electronics and appropriate anode structures

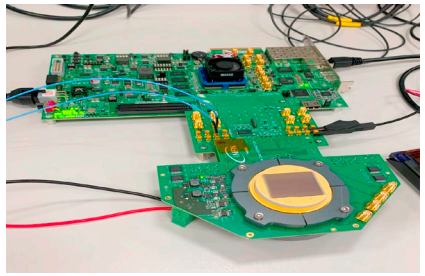


A. Franco et al. Sci. Rep. 1 (2014).

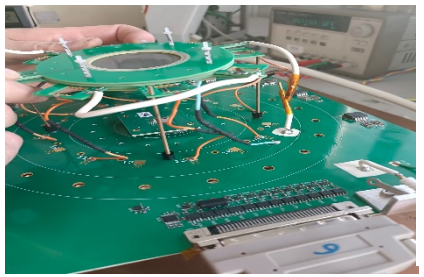


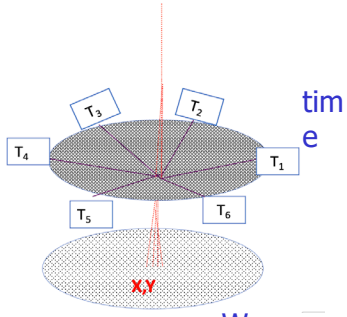
Si nanometric structure for reflective photocathode





MCP+Timepix4





time

Woven strips

MCP+PICMIC concept

Novel vacuum-based devices

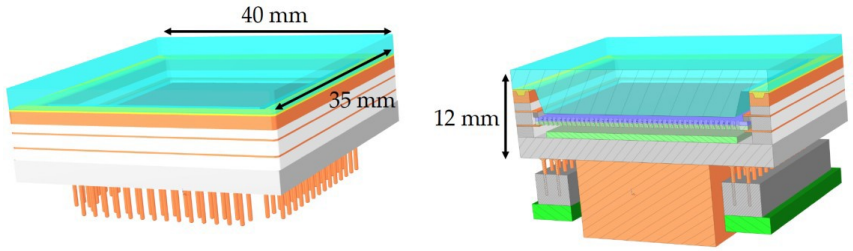
MCP-PMT with CMOS anode

Conceptual design for 4D detection of single photons

- Hybrid concept: MCP-PMT where the pixelated anode is an ASIC (CMOS) embedded inside the vacuum
- Prototype with Timepix4 ASIC as anode (array of 23k pixels)

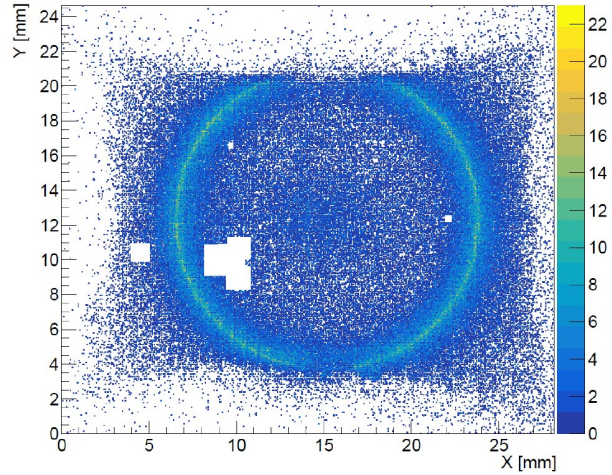
Envisaged performance

- <100 ps time resolution and 5-10 μm spatial resolution
- Rate capability of >100 MHz/cm² (<2.5 Ghits/s @ 7 cm² area)
- Low gain (~10^4) operation possible → x100 lifetime increase



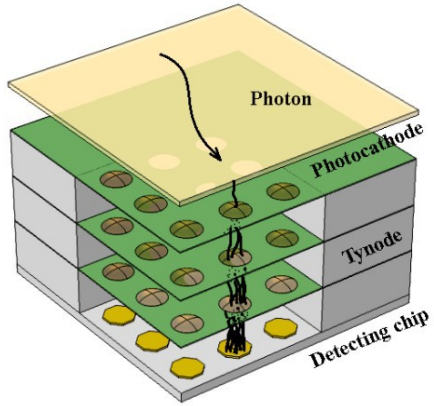
M. Fiorini et al, NIMA 1082 (2026) 170965

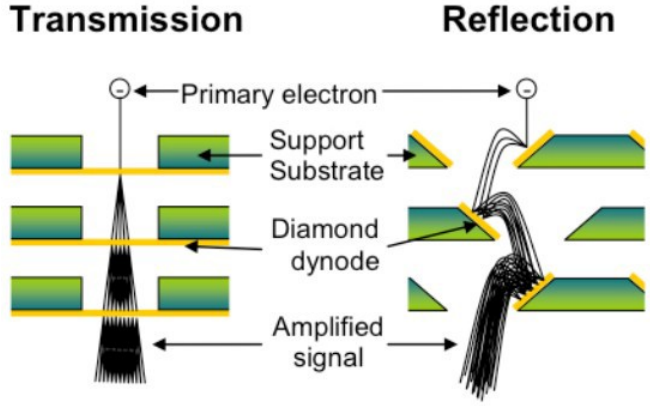
Beam test
Oct 2024



Tynodes (→ Time Photon Counter)

- Transmission mode dynode → tynode
- Fabrication of tynodes (MgO ALD, diamond) using MEMS technology
- "Anode" is a CMOS chip (e.g., TimePix)
- Very promising properties
  - Very compact; high B-field tolerance; very fast
  - Very low DCR; very good 2D spatial resolution





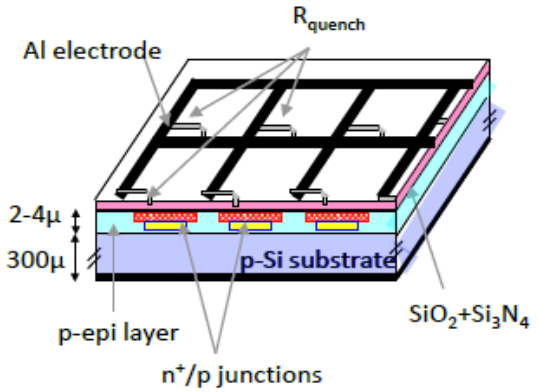
H. van der Graaf et al., NIM A847 (2017) 148

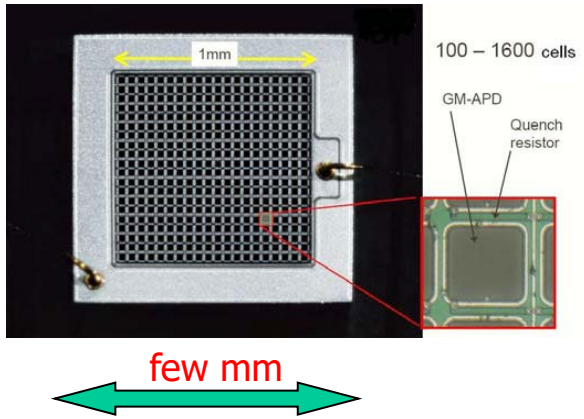
J.S. Lapington et al, 1092 (2026) 171792

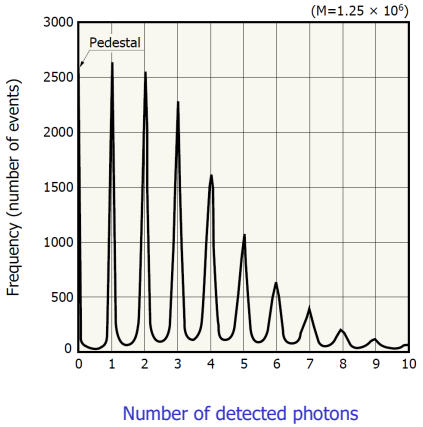
Solid-state low-light-level sensors: Silicon photomultipliers SiPM

An array of APDs operated in Geiger mode – above APD breakdown voltage (microcells or SPADs – single photon avalanche diodes)

Detection of photons:
- absorbed photon generates an electron-hole pair
- an avalanche is triggered by the carrier in the high field region → signal
- voltage drops below breakdown and avalanche is quenched (passive or active quenching)
- each triggered microcell contributes the same amount of charge to the signal







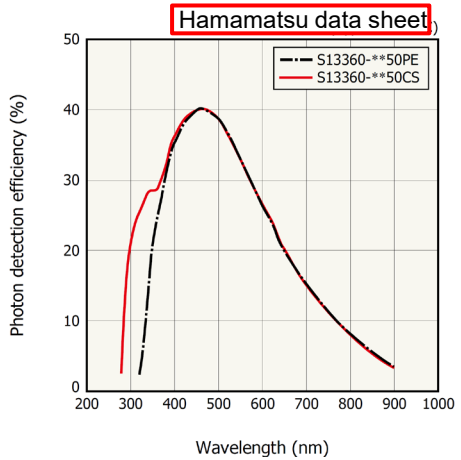
SiPMs as single photon detectors

Characteristics:

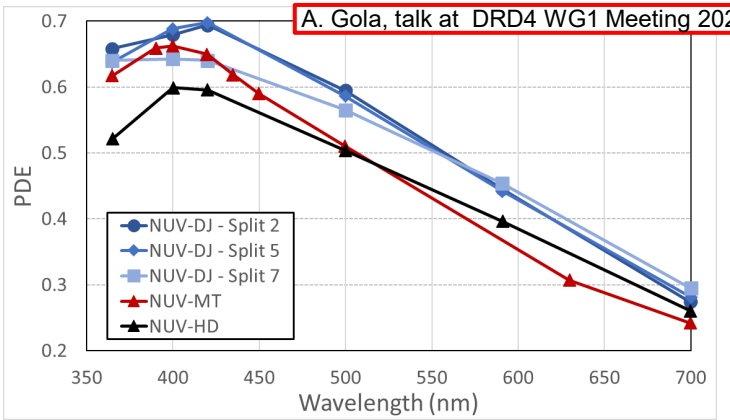
- low operation voltage ~ 10-100 V
- gain ~ 10^6
- peak photon detection efficiency
  PDE = QE x ε_{geiger} x ε_{geo}
  up to 65%(@400nm) (up to 3x PMT!)
  (ε_{geo} – due to dead space between the microcells)
- time resolution ~ 100 ps
- works in high magnetic field

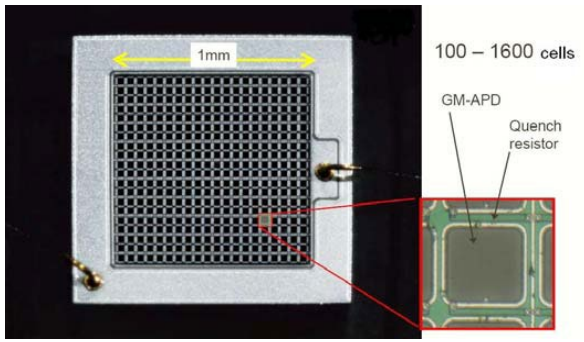
- dark counts ~ few 100 kHz/mm^2
- radiation damage (p,n)

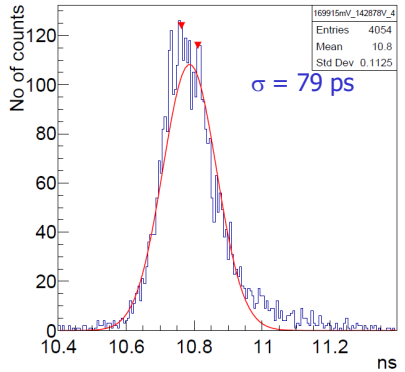
Hamamatsu data sheet



A. Gola, talk at DRD4 WG1 Meeting 2024

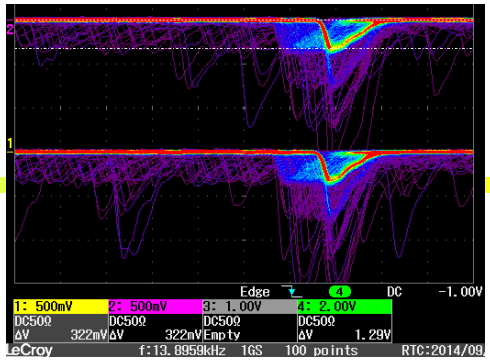




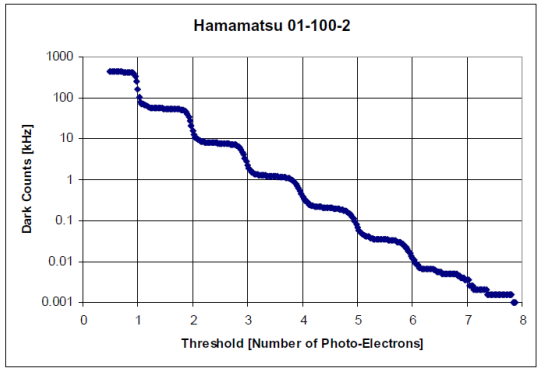


M.V. Nemallapudi et al 2016 JINST 11 P10016

SiPM: noise



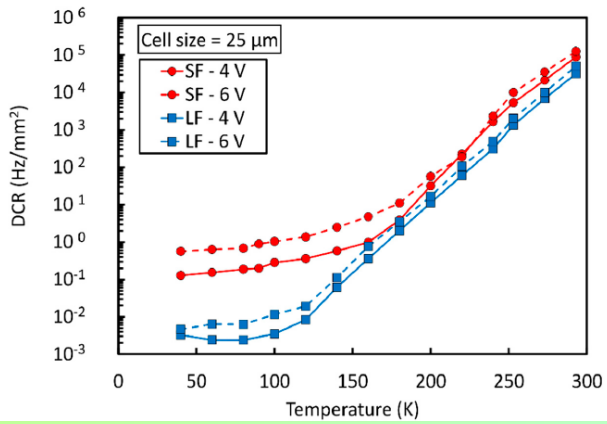
- dark counts are produced by thermal generation of carriers, trap assisted tunnelling or band gap tunnelling
- signal equal to single photon response
- typical rate dropped from $\approx 1\mathrm{MHz/mm^2}$ for early SiPM devices to below $100\mathrm{kHz/mm^2}$ for more recent devices
- gets roughly halved for every -$8^{o}\mathrm{C}$
- increases linearly with fluence



- optical cross-talk produced when photons emitted in avalanche initiate signal in neighbouring cell; reduced by screening – trenches

- after-pulses produced by trap-release of carriers or delayed arrival of optically induced carriers in the same cell

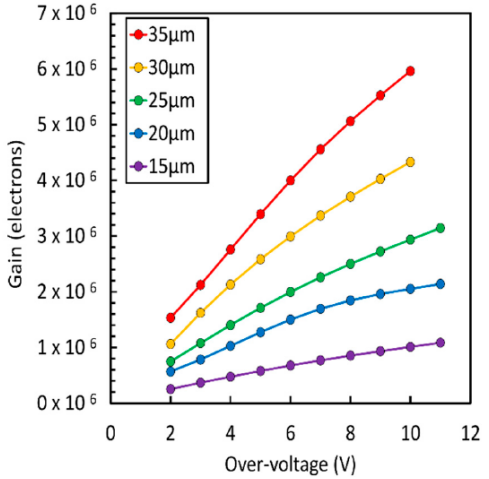
A. Gola et al. Sensors 19(2019)308

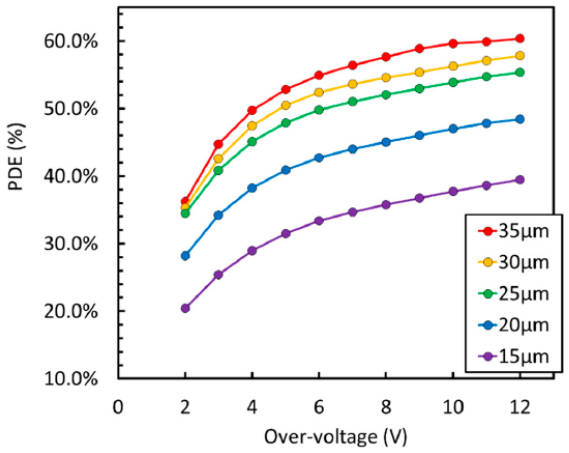


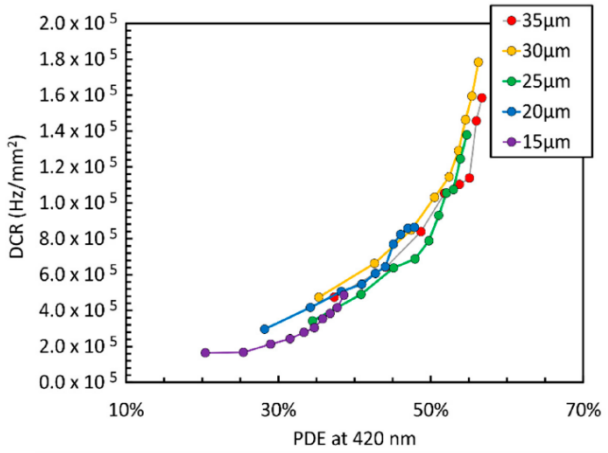
SiPM: parameter correlation

Higher overvoltage:

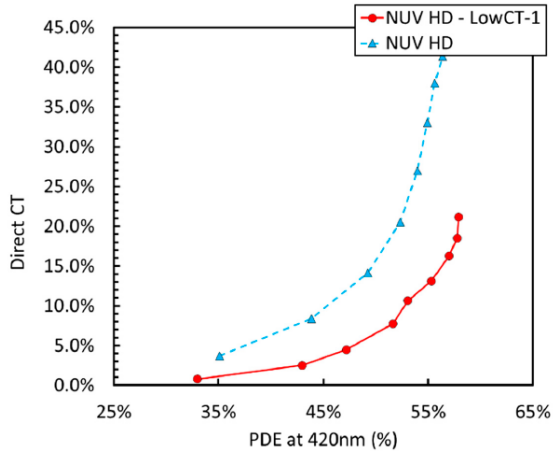
- higher field:
  - higher avalanche trigger probability → higher PDE
  - faster signal → better timing
- higher gain:
  - better signal to noise
  - more optical cross-talk → higher ENF, worse timing
  - more after-pulses







A. Gola et al. Sensors 19(2019)308

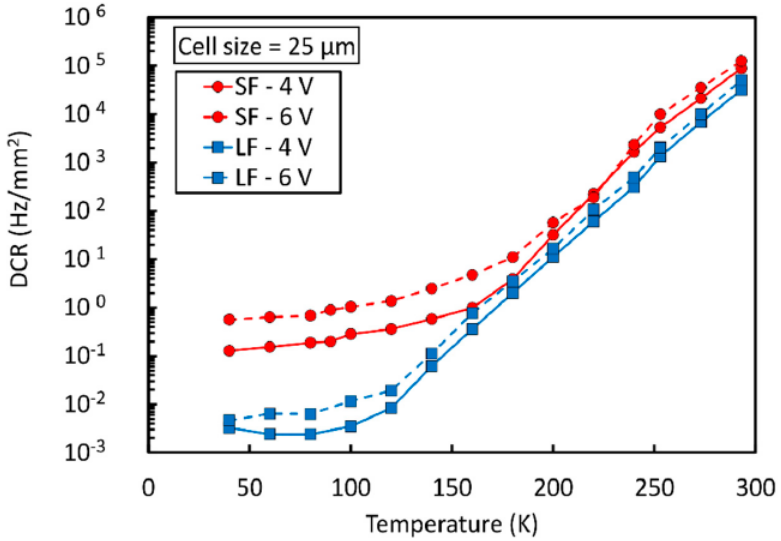


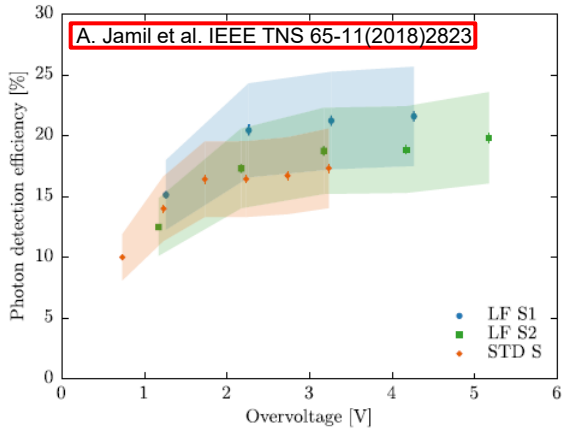
VUV SiPM for cryogenic applications

LAr, LXe applications:

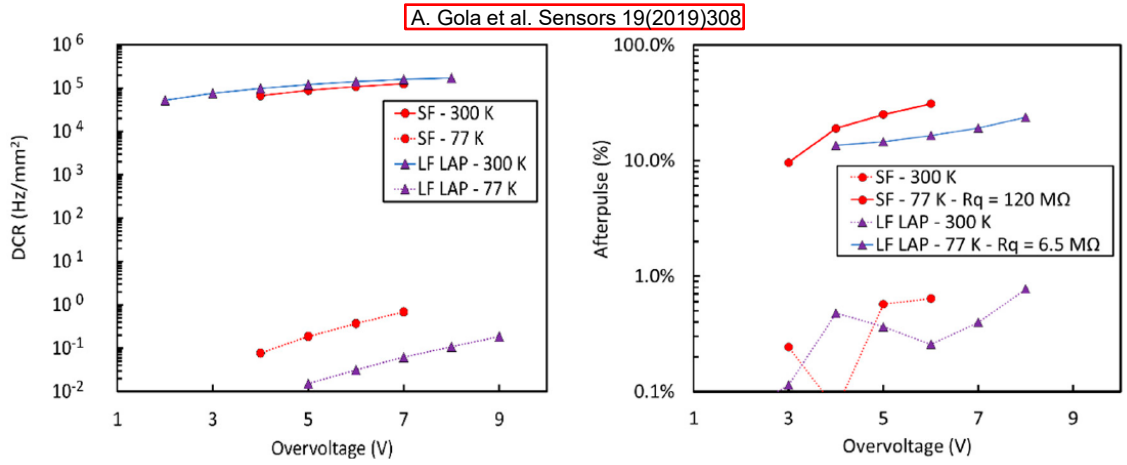
- VUV sensitivity required:
  - 128 nm (LAr), 178 nm (LXe)
  - optimization of anti-reflective coating ARC
  - PDE ≈ 20 %

- cryogenic temperatures:
  - low DCR ≈ $10\mathrm{mHz/mm^2}$ dominated by band-band tunnelling, reduced by low-field avalanche region
  - higher after-pulse rate ≈ 10%





A. Gola et al. Sensors 19(2019)308



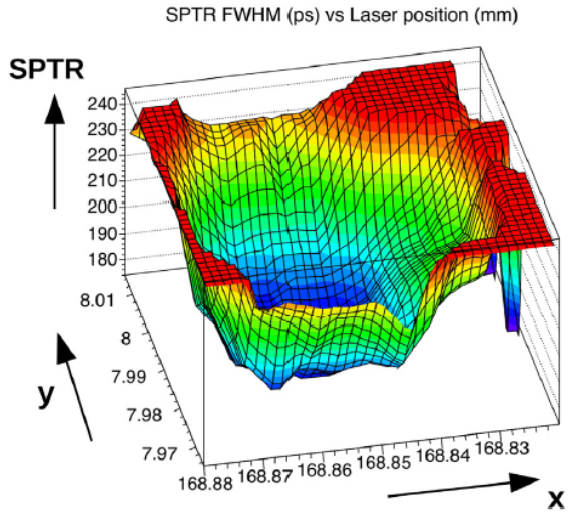
SiPM: single photon timing

Intrinsic TTS of SiPM microcells is extremely fast, < 20 ps for single microcells (SPAD), but timing deteriorates for larger devices. The main contributions:

- nonuniformity within microcell (edges)
- spread between microcells
- overall SiPM capacitance
- λ dependence - tails

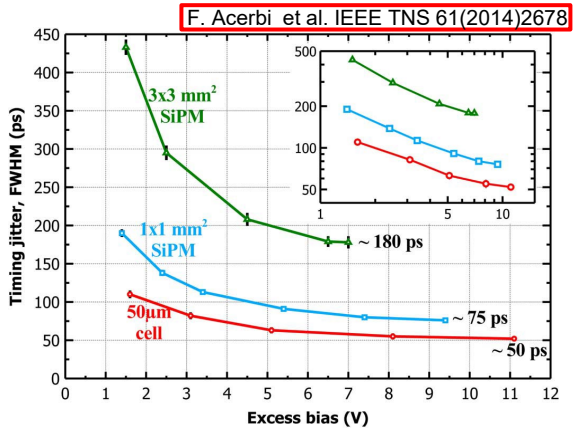
Comparison of timing properties for single $50\mu m$ SPAD, 1×1 mm^2 and 3×3 mm^2 SiPMs with the same SPAD for microcells:

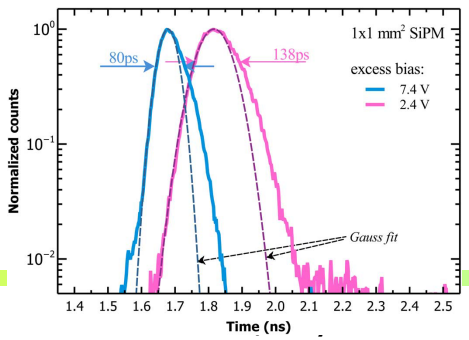
- timing improves with higher overvoltage – larger pulses, at the expense of increased SiPM noise
- best timing resolutions for single cell signals are $\sigma \approx 21$ ps, 32 ps and 77 ps
- TTS deterioration mainly due to a larger overall capacitance → reduced signal slope, $\sigma_t \approx \sigma_{el.}\left(\frac{dU}{dt}\right)^{-1}$



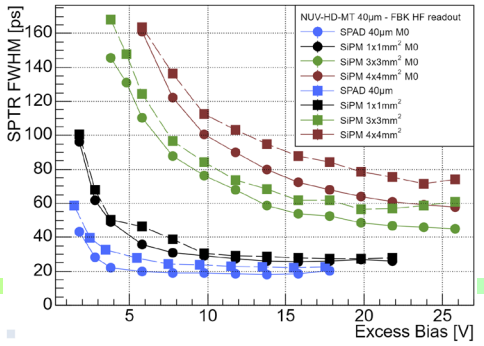
F. Acerbi et al. NIMA 926(2019)16

F. Acerbi et al. IEEE TNS 61(2014)2678





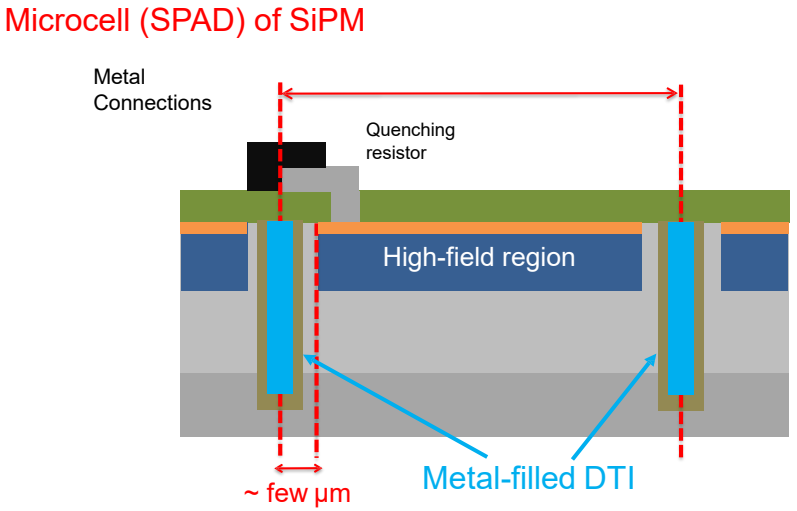
A. Gola, talk at DRD4 WG1 Meeting 2024



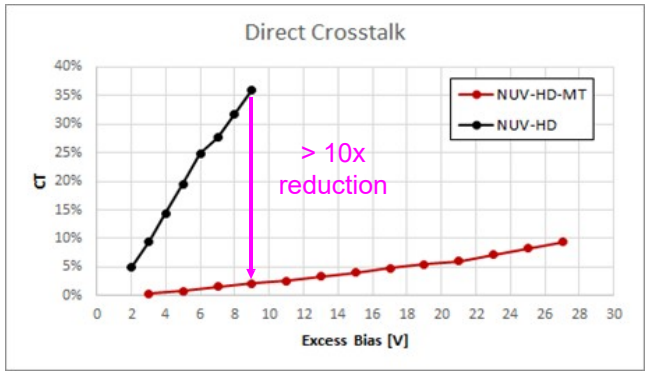
Reduction of optical crosstalk

Starting from the NUV-HD technology, FBK and Broadcom jointly developed the NUV-HD-MT technology, adding metal-filled deep trench isolation to strongly suppress optical crosstalk.

Other changes: low electric field variant, layout optimized for timing.



Conceptual drawing of the NUV-HD-MT, with the addition of metal-filled Deep Trench Isolation.



Reduction of optical crosstalk probability in NUV-HD-MT, compared to the "standard" NUV-HD. Measurement without encapsulation resin, i.e. only considering internal crosstalk probability.

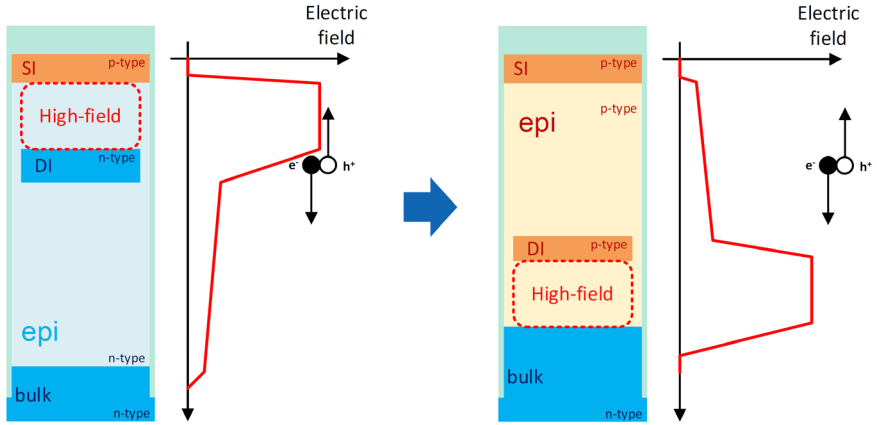
A. Gola, talk at RICH2022

SiPMs: structure optimization, example

By moving the high-field region towards the bottom of the epitaxial layer, the PDE is enhanced.

Avalanche is mostly triggered by electrons.

Conceptual drawing of the different NUV.MT (left) and NUV-DJ (right) → microcell structures

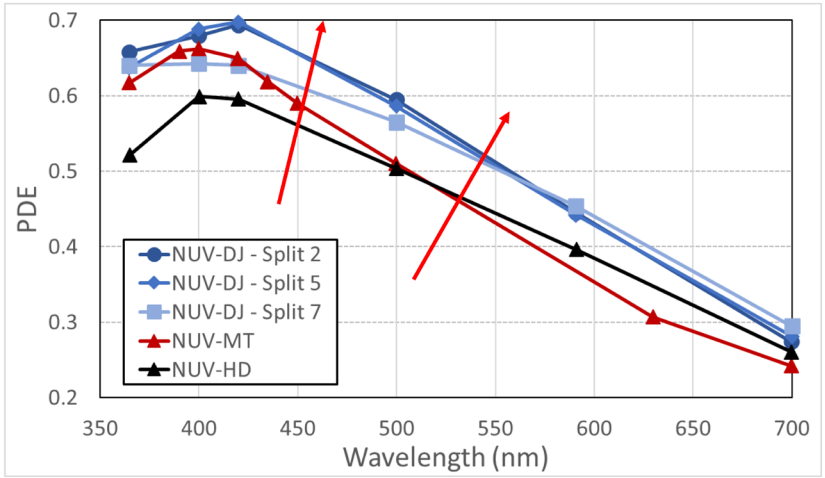


Conceptual drawing of the different NUV.MT and NUV-DJ microcell structures (cross-sections, not to scale)

PDE increase: from holes to electrons triggering the avalanche

PDE vs. wavelength measured on the 45 µm cell of the NUV-HD-MT technology (12 V) and on the 40 µmcell of the NUV-HD and of the newly introduced NUV-DJ SiPM technologies (9 V).

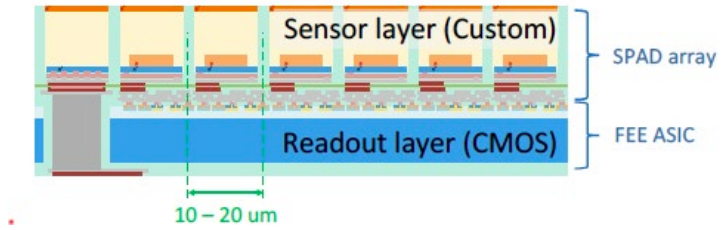
A. Gola, talk at DRD4 WG1 Meeting 2024

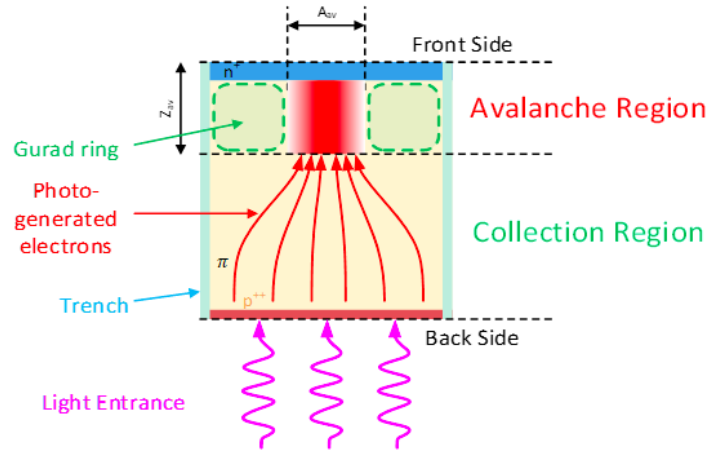


PDE vs. wavelength measured on the 45 µm cell of the NUV-HD-MT technology (12 V) and on the 40 µm cell of the NUV-HD and of the newly introduced NUV-DJ SiPM technologies (9 V).

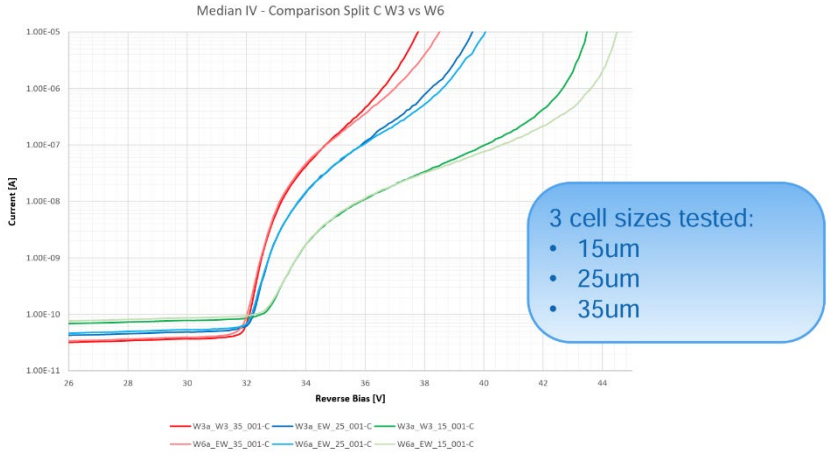
Backside illuminated SiPMs

Backside illuminated (BSI) SiPMs:
potential for an enhanced PDE and a better radiation tolerance.





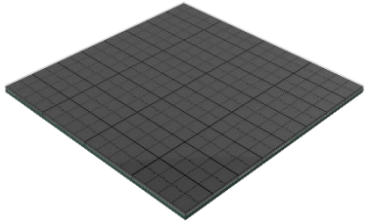
The first results of the
FBK IBIS Run samples



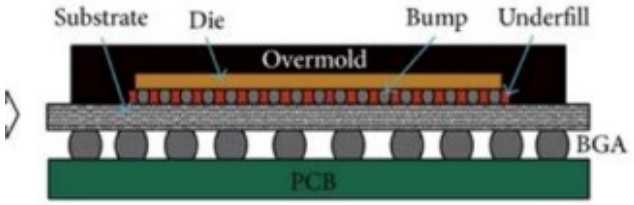
Radiation hardness:
Assuming the primary source of the dark count rate is field-enhanced generation (or tunneling)
→ The area sensitive to radiation damage is much smaller than the light-sensitive area

Ultragranular SiPMs with integrated electronics

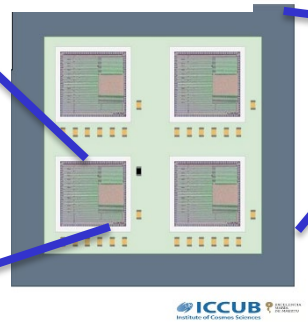
Timing of SSPD & Developing ultra-granular SiPM that integrates with the readout electronics

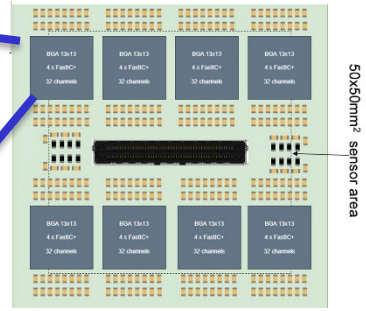


3x3 mm^2 SiPM array



FastIC+
(collab. CERN ICCUB)
Low power
Chip

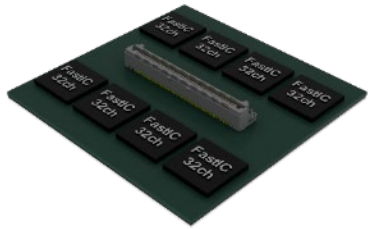


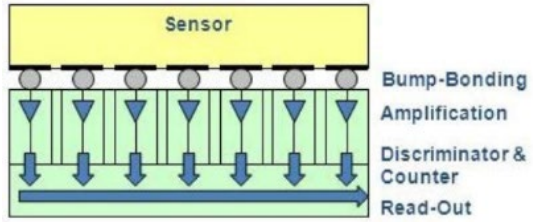


2024 Produced
and evaluated

design &
production 6.2025

256 Ch 5x5cm^2
Module proposal



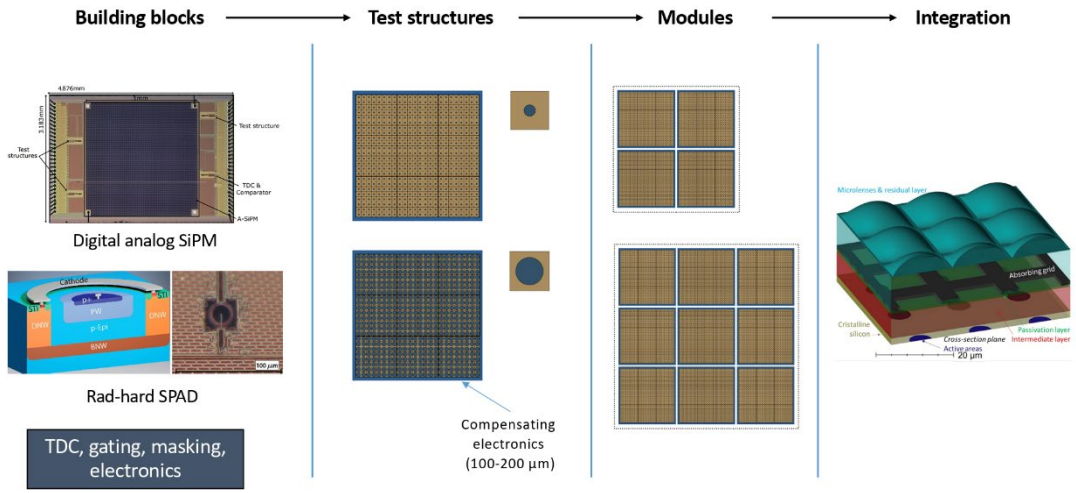


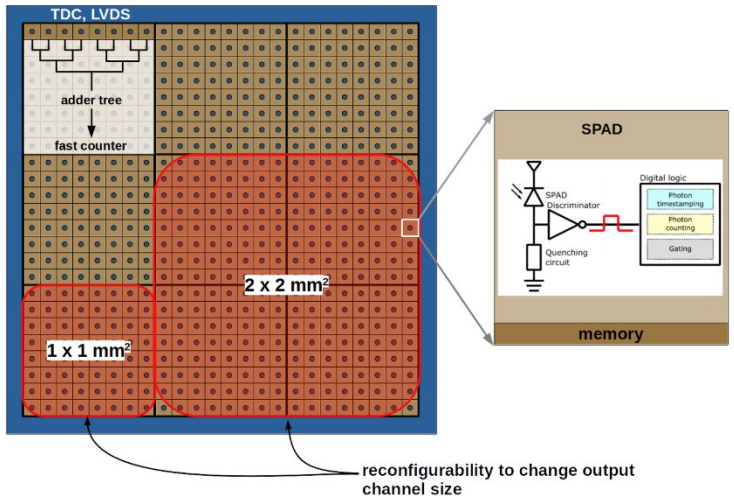
Ultra granular SiPMs

SiMs: SPAD with micro-lenses

CMOS-SPAD light sensors: co-integration of SPADs and electronics, digitised output signals

spadRICH - Radiation-hard digital analog silicon photomultipliers for future upgrades of RICH detectors





aqualab EPFL

Institut "Jožef Stefan" Ljubljana, Slovenija

Light concentrators

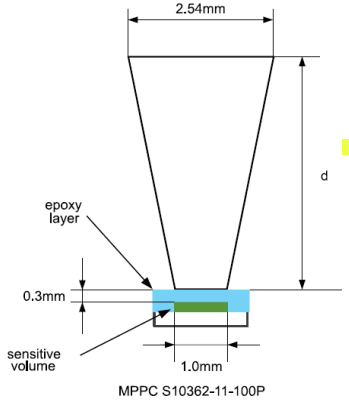
At the device level (lenses, Winston cones):
- For a given active area reduce sensor area – reduce dark count rate (tolerate higher fluences)
- use smaller faster devices

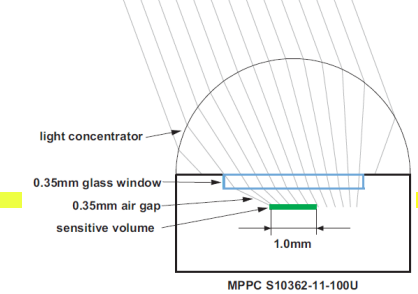
Higher concentration – narrower angular acceptance

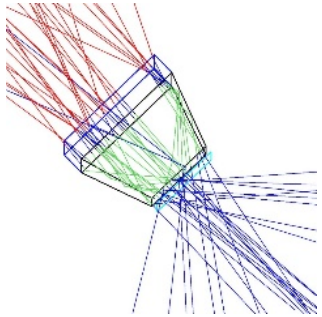
Imaging light concentrators:
- smaller photon impact angles on the sensor
- can be used with position-sensitive arrays

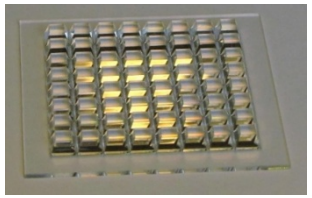
Non-imaging light concentrators:
- larger photon impact angles on the sensor – directly coupled to the sensor

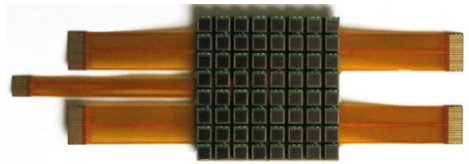
At the micro-cell level (micro-lenses, diffractive lenses, meta lenses):
- compensate for low fill factor – small cells, dSiPM
- concentrate light in cell centre – better timing

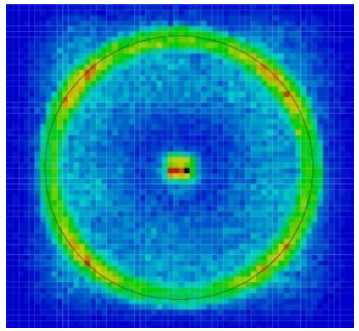


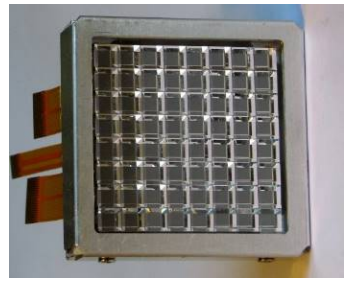












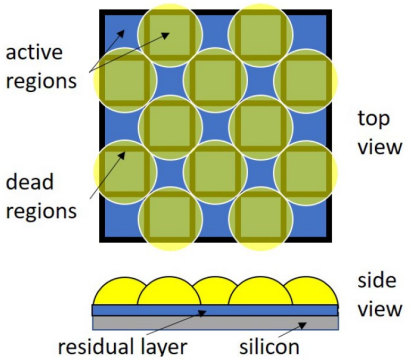
RICH with SiPMs + light concentrators

E. Tahirović et al., NIM A787 (2015) 203

Microlenses for light collection

Light concentration at the micro-cell level (micro-lenses, diffractive lenses, meta lenses):

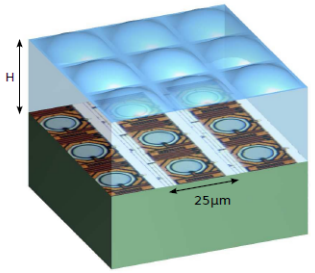
- compensate for low fill factor – small cells, dSiPM
- concentrate light in cell centre – better timing

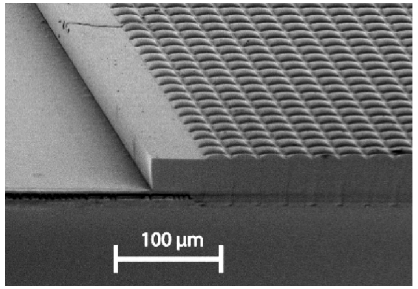


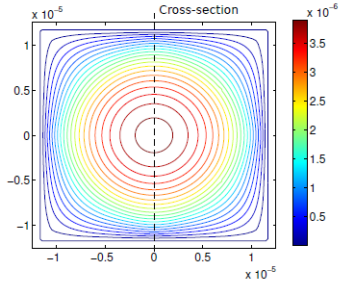
G. Haefeli et al., TNS,
DOI 10.1109/TNS.2025.3542597

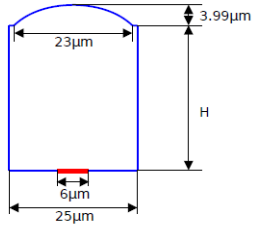
Micro-lens array coupled to SPAD array

- CMOS SPAD array, 128x128 $6\mu m$ diameter @$25\ \mu m$ pitch – 5% fill factor
- matching polymer plano-convex micro-lens array

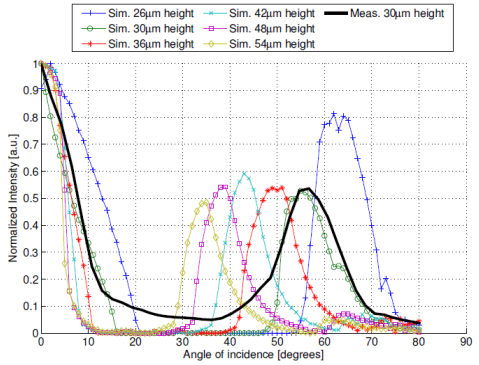


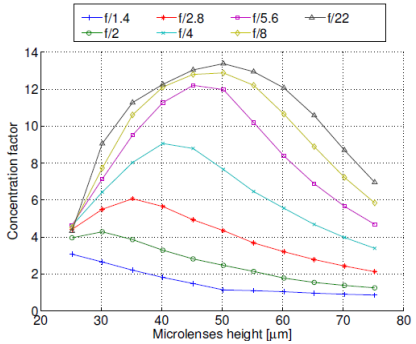




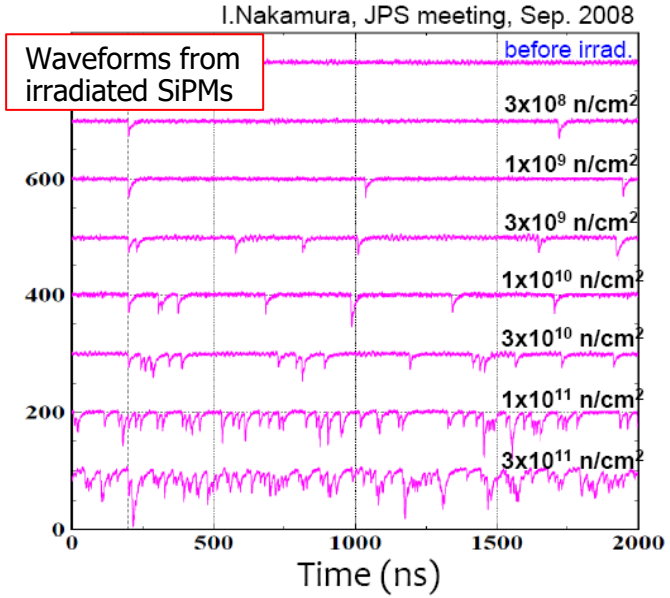


J.M. Pavia et al.
Opt.Exp. 22-4(2014)4202





SiPMs: Radiation damage



Show-stopper at fluences above ~10^{11} n cm^{-2} in case single (or few) photon sensitivity is required!

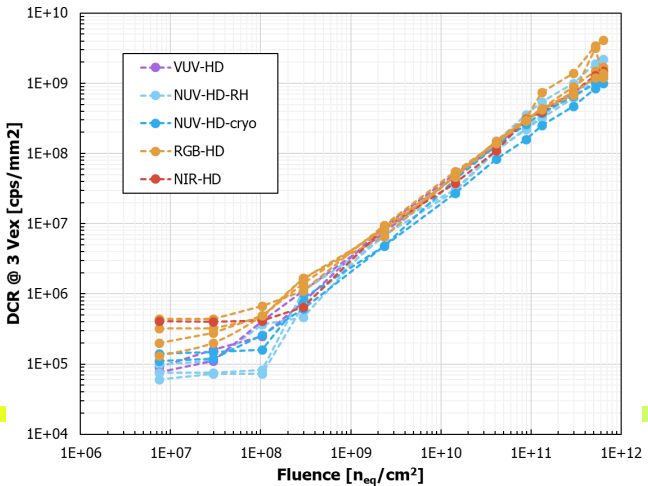
→ Use of wave-form sampling readout electronics

→ Operating the SiPMs at lower temperature

→ Annealing periodically (annealing at elevated temperature is preferred)

→ Reducing recovery time to lower cell occupancy

→ Radiation resistant SiPMs, other materials?



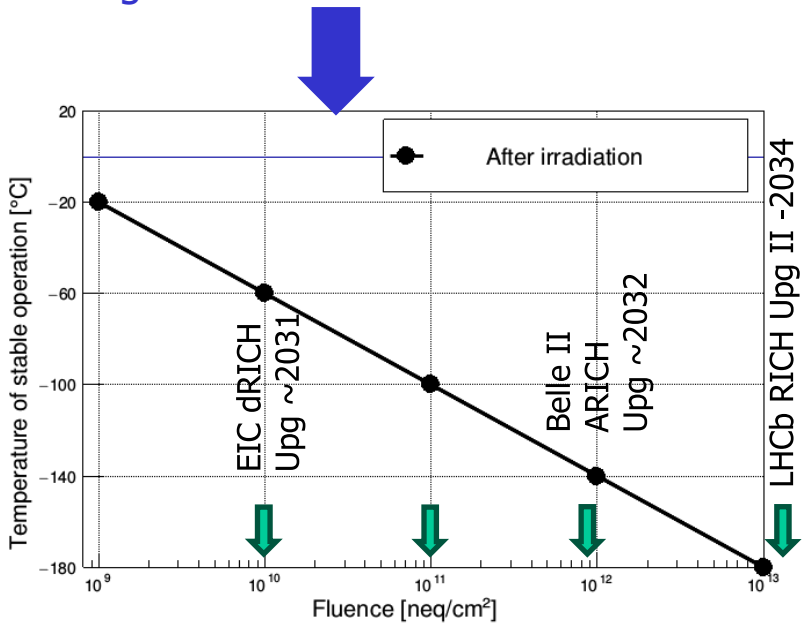
Beyond $10^7 \div 10^8$ n_{eq}/cm^2 little correlation between the DCR before and after irradiation:

- All technologies seem to "converge" toward similar values
- Independence of bulk damage from contaminants in the SiPM starting material?
- Room temperature annealing has little effect if shorter than ~1 day

SiPMs: radiation damage, mitigation

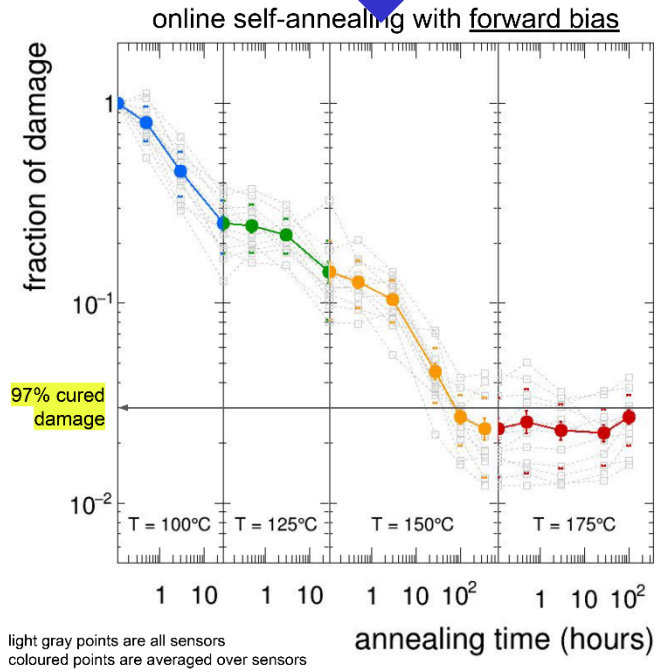
Operation of highly irradiated SiPMs for single photon detection –
cooling and annealing

Cooling: Temperature at which the SiPMs are ”usable” for single-photon detection, i.e. where the single photo electron peak @ 9V over-voltage is separated from the background.



D. Consuegra Rodrigez et al., Eur. Phys. J. C 84, 970 (2024)

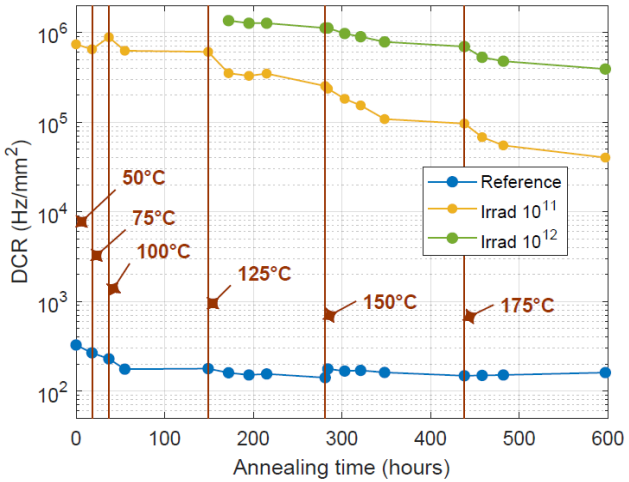
Annealing

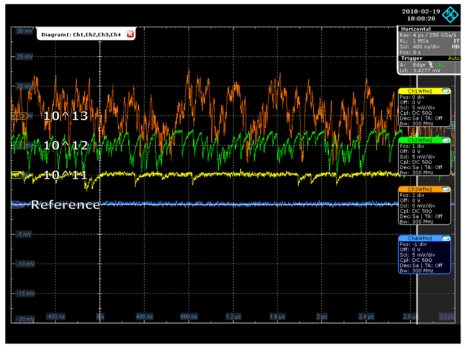


R. Preghenella, talk at PD24

SiPMs: Radiation damage, annealing at elevated temperatures

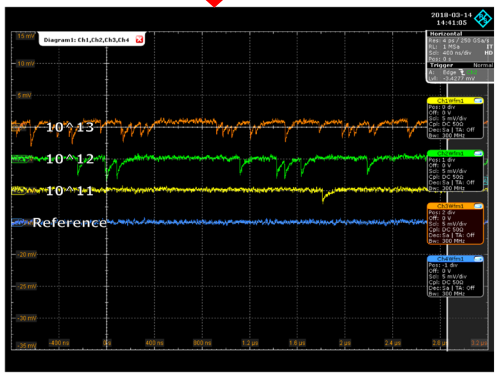
Dark counts at -30C of Hamamatsu S13360-1350CS SiPMs: non irradiated (blue) and irradiated up to 10^{11} (yellow), 10^{12} (green) and 10^{13} (orange) n_{eq}/cm^2

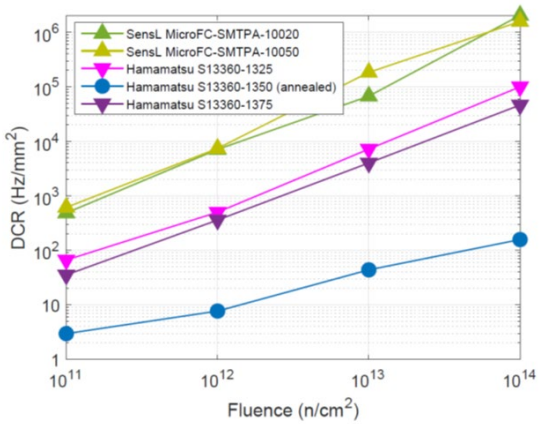




M. Calvi et al., NIMA 922 (2019) 243-249

annealing





DCR at 77 K versus neutron fluence
Blue circles: annealed sample
→ Annealing helps also if operating at 77 K

SiPMs: radiation damage, mitigation

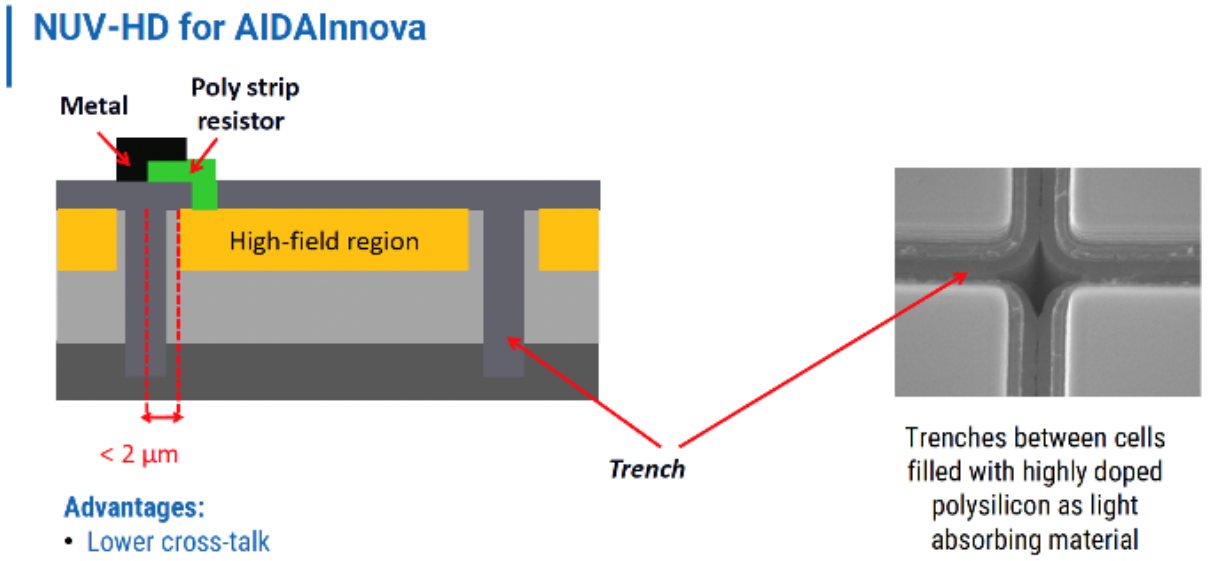
Fast & radiation hard SiPMs - enabling the use of SiPM in highly irradiated areas

Experimental structures, AidaInnova Run

Two different technologies:

- Low electric field
- Ultra Low electric field

Cell pitch: 15, 25, 40, 75um; SiPM sizes: $(0.25, 0.5,1,2,3)^2$ mm^2



Summary and outlook 1

Particle identification is an essential part of several experiments, and has contributed substantially to our present understanding of elementary particles and their interactions. It will continue to have an important impact in the next generation of experiments.

A large variety of techniques has been developed for different kinematic regions and different particles.

Precise timing has become an integral part of several PID methods.

Summary and outlook 2

Next generation of experiments in particle physics: photosensors with faster timing, wider spectral range and improved radiation tolerance.

Many new interesting developments are underway, in particular in SiPMs and MCP-PMTs – not all of them could be covered in this talk.

A detector R&D collaboration (DRD4) was set up early in 2024 to facilitate collaboration in this area of research, and proven to be of great help in coordination and information exchange in this field of instrumentation.

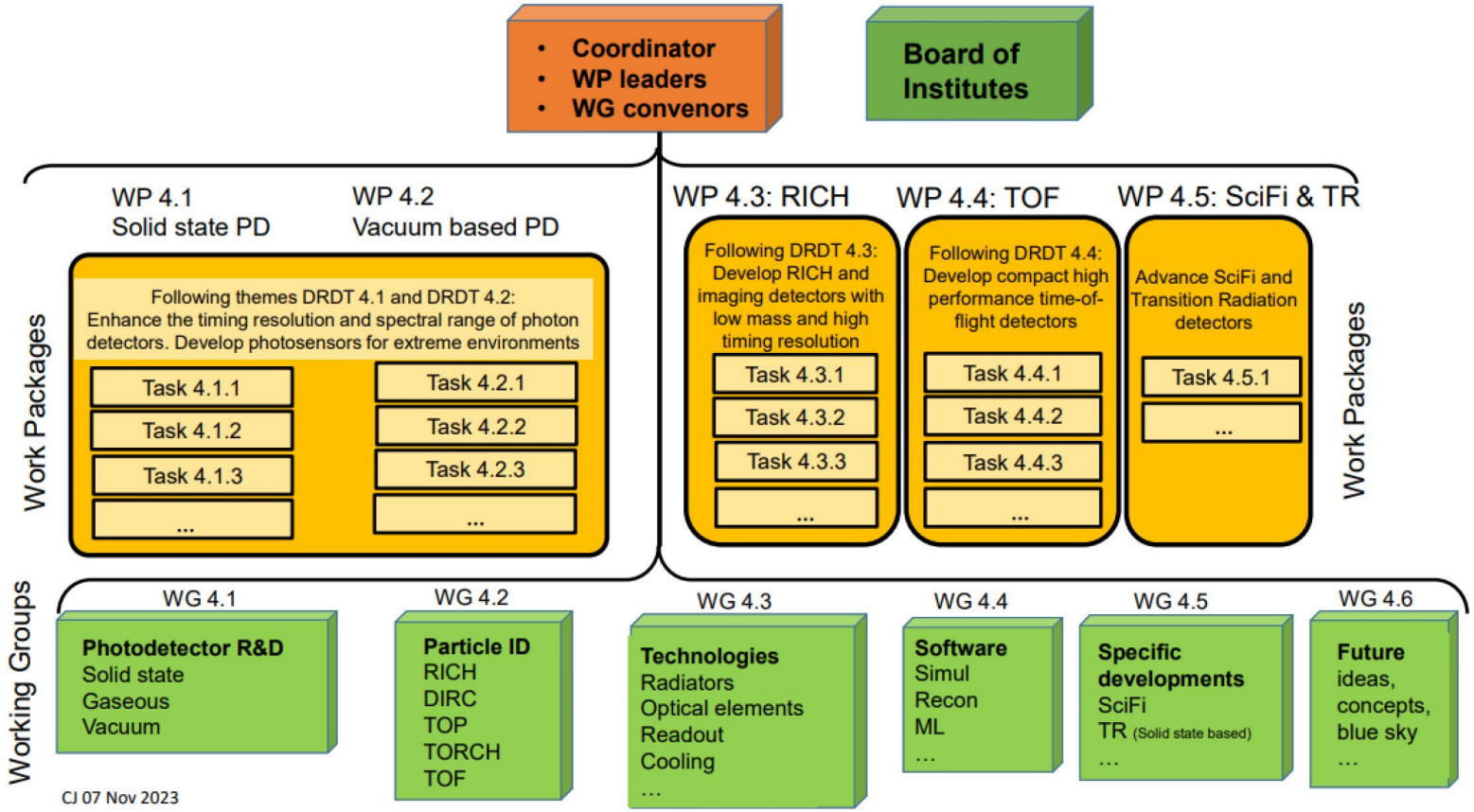
Detector R&D can be fun, also as a side project to an analysis ☺

More slides...

DRD4 : photon detectors and PID

Organization:

- Work packages: projects
- Working groups: discussion forums



DRD4:WP4.1 Solid-State Photodetecto

■ Task 1 -SSPD with new configurations and modes: Development of back-side illuminated SiPM (potential for better PDE and radiation tolerance); development of ultra-granular SiPM that integrates with the electronics by using 2.5D or 3D interconnection techniques; development of CMOS-SPAD light monolithic sensors for HEP; study of new materials for light detection

■ Task 2 -Fast radiation hard SiPMs: Standardize procedures for quantification of radiation effects; irradiated SiPMs characterization in wide temperatures range (down to -200 °C); study of annealing; study and quantify other measures enabling the use of SiPM in highly irradiated areas (e.g. smaller SiPMs, macro-and micro-light collectors)

■ Task 3 -Timing of SSPD, including readout electronics: Study and improve the timing of SiPMs; co-design of a multi-ch. readout ASIC exploiting the timing potential; integration and packaging with integrated cooling; vertical integration of SiPM arrays to FEE (better timing via reduction of interconnections' parasitic induct+capac)

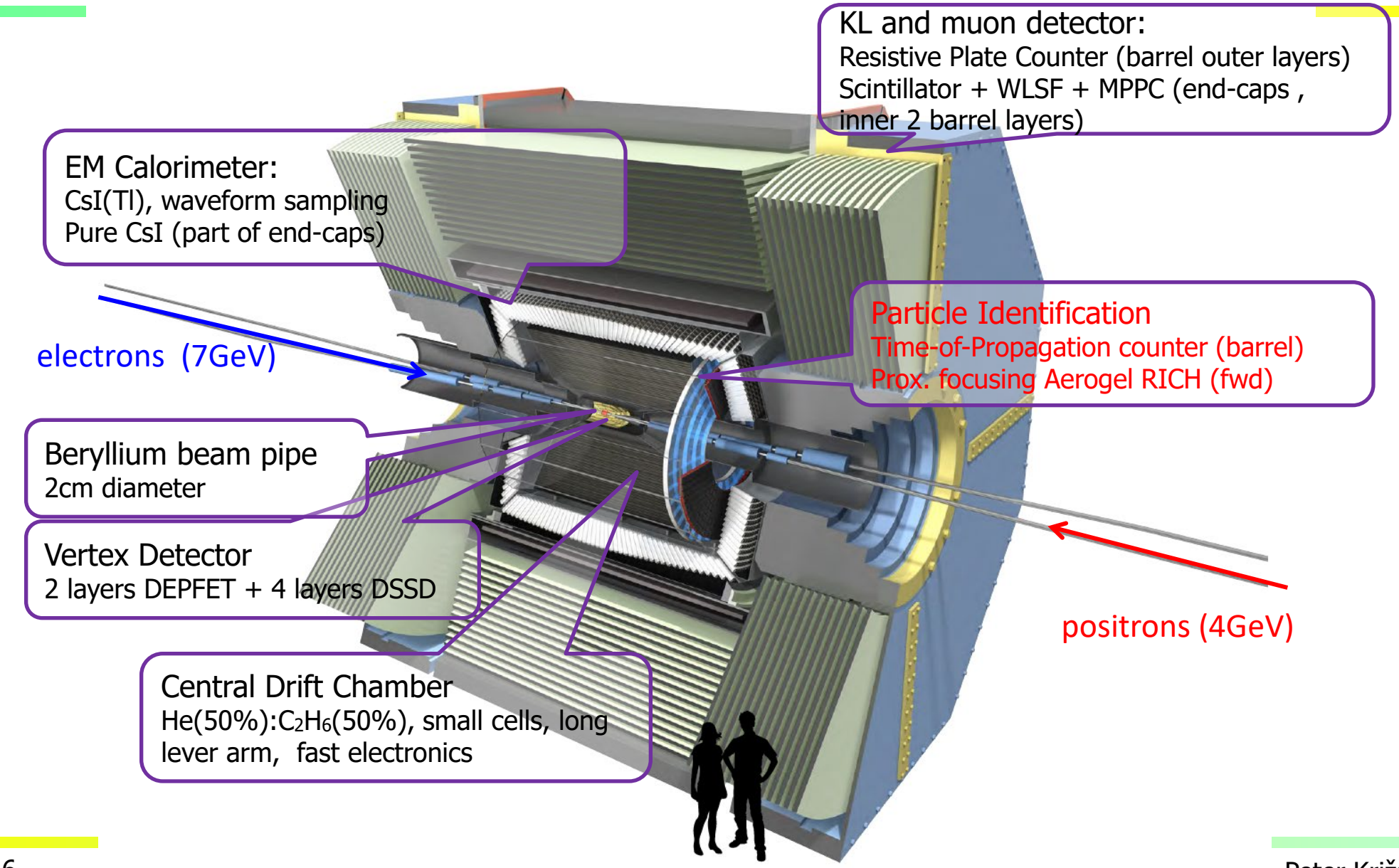
DRD4:WP4.2 Vacuum-based Photodetectors

■Task 1 -New materials, coatings, longevity and rate capability studies: Develop new materials and techniques to increase MCP-PMT tube lifetime and improve rate capabilities; use new techniques with new materials to achieve high aspect ratio with small diameter for better gain, time, and spatial resolution

■Task 2 -New photocathode materials, structure and high QE VPD: Search for new materials with the required characteristics to be used as photocathodes; develop photocathodes with new structures

■Task 3 -VPD time and spatial resolution performance: Development of large area MCP-based photodetector with combined excellent timing and position resolution, including electronics integration

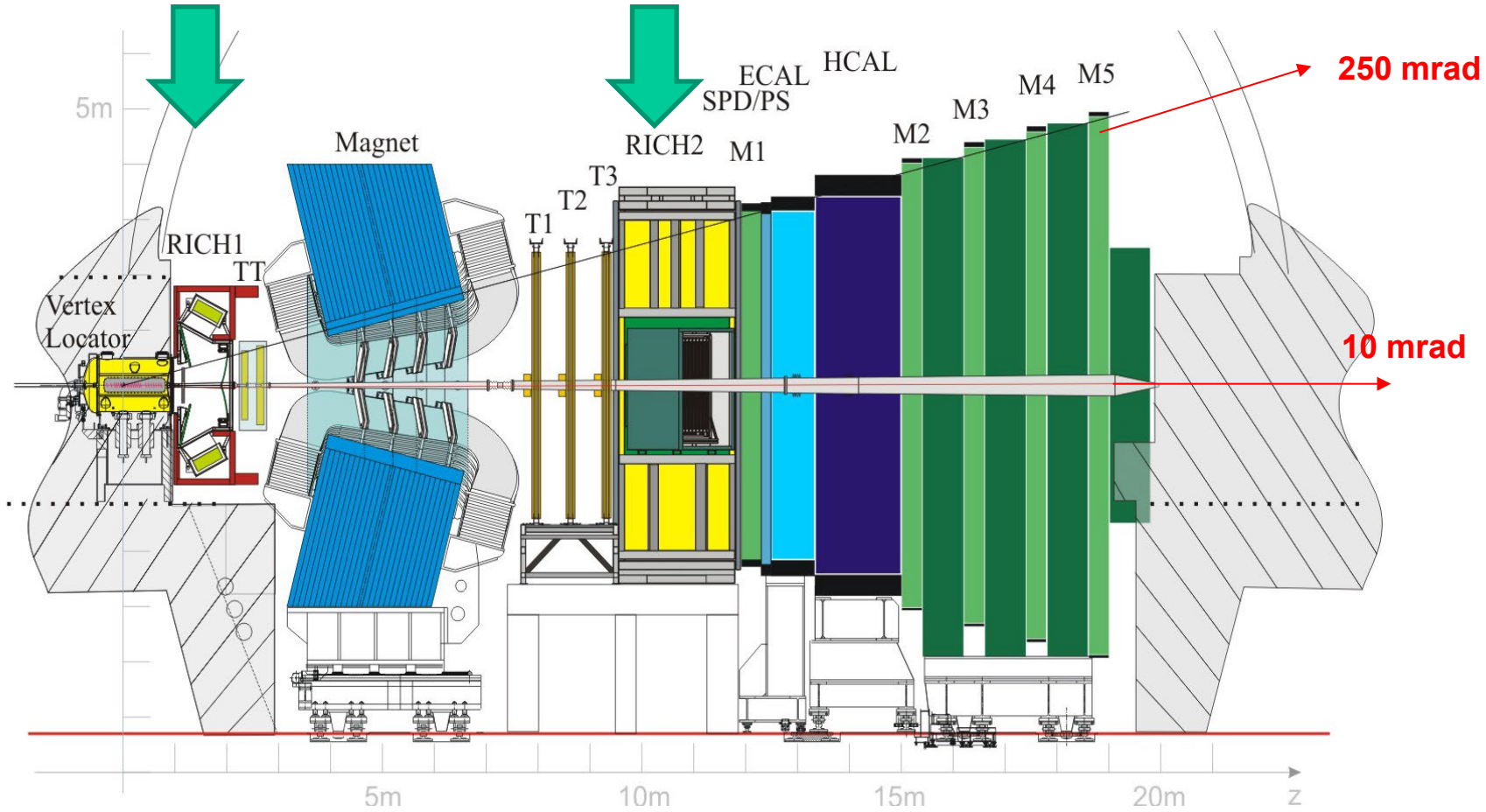
Hadron PID in the Belle II Detector



The LHCb RICH detectors

Large kinematic range: two RICH detectors

- RICH1 with C_4F_{10} gas (before the magnet)
- RICH2 with CF_4 gas



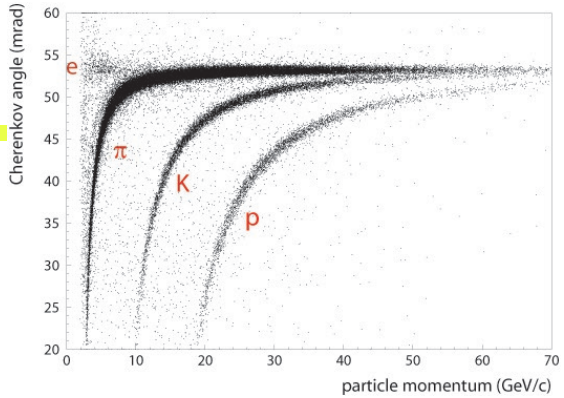
Vertex reconstruction:
VELO

Trigger:
Muon Chambers
Calorimeters
Tracker

PID:
RICHes
Calorimeters
Muon Chambers

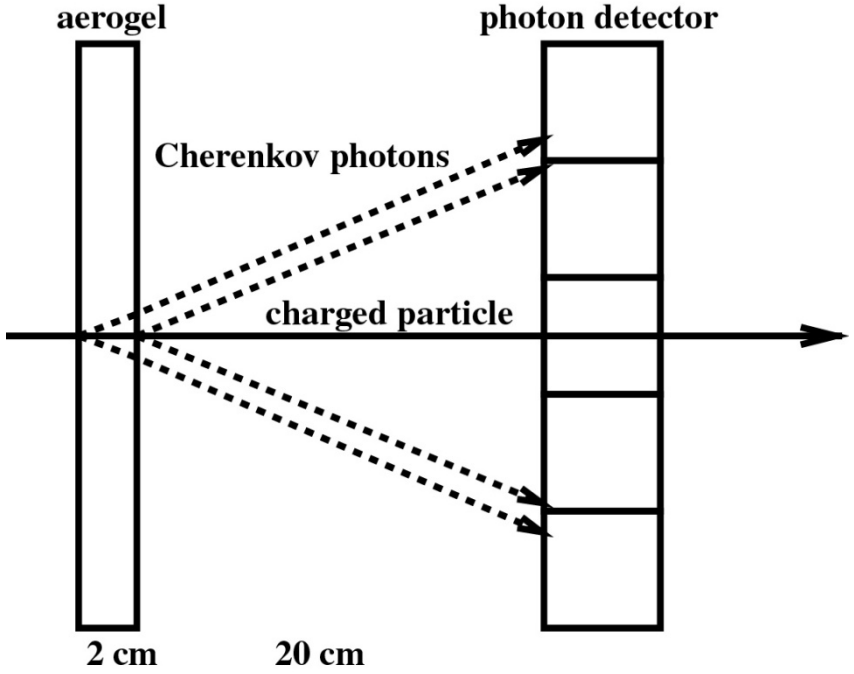
Kinematics:
Magnet
Tracker
Calorimeters

Resolution of a RICH counter



Determined by:

- Photon impact point resolution (~photon detector granularity)
- Emission point uncertainty (not in a focusing RICH)
- Dispersion: $1/\beta = n(\lambda)\cos\theta$
- Errors of the optical system
- Uncertainty in track parameters



Resolution per track:

$$\sigma_{track} = \frac{\sigma_0}{\sqrt{N_{pe}}}$$

single photon resolution

# of detected photons

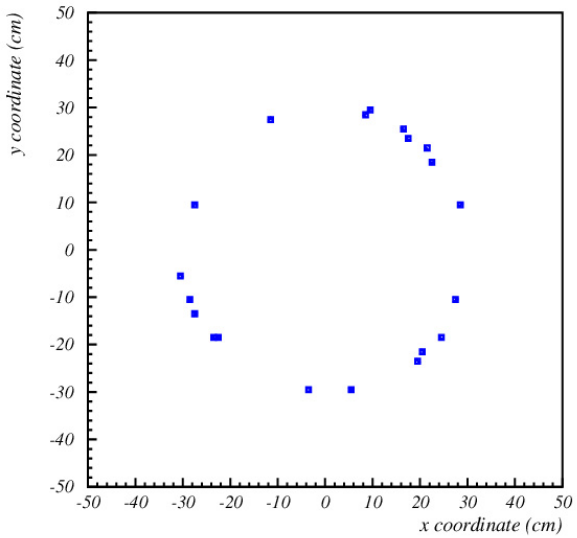
(in the case of low background)

Photon detection in RICH counters

RICH counter: measure photon impact point on the photon detector surface

→ detection of single photons with

- sufficient spatial resolution
- high efficiency and good signal-to-noise ratio (few photons!)
- over a large area (square meters)

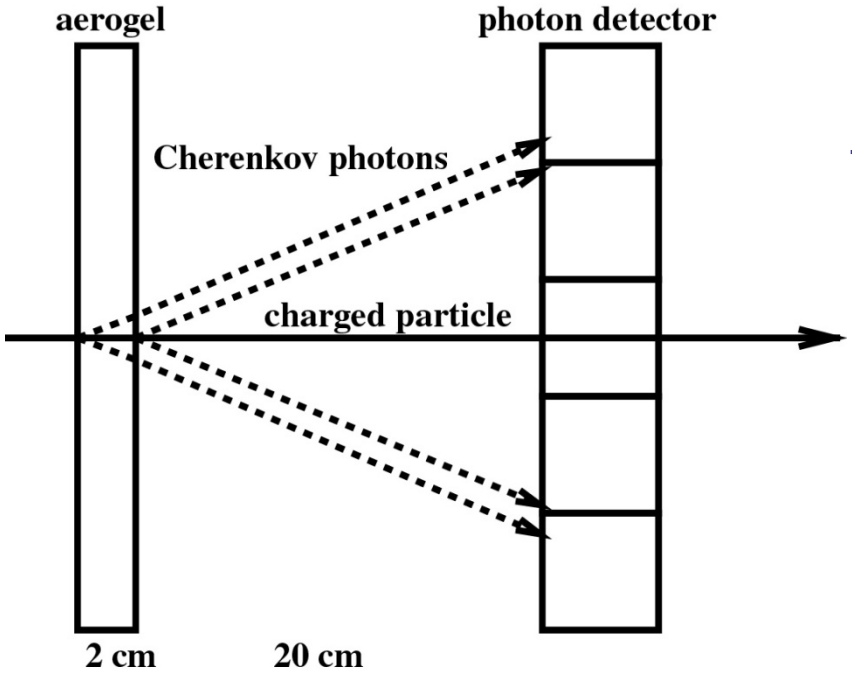


Special requirements:

- Operation in magnetic field
- High rate capability
- Very high spatial resolution
- Excellent timing (time-of-arrival information)

Photon detector is the most crucial element of a RICH counter

Endcap: Proximity focusing RICH



K/π separation at 4 GeV/c:

$\theta_c(\pi) \sim 308$ mrad (n = 1.05)

$\theta_c(\pi) - \theta_c(K) \sim 23$ mrad

For single photons: $\delta\theta_c(\text{meas.}) = \sigma_0 \sim 14$ mrad,

typical value for a 20mm thick radiator and 6mm PMT pad size

Per track:

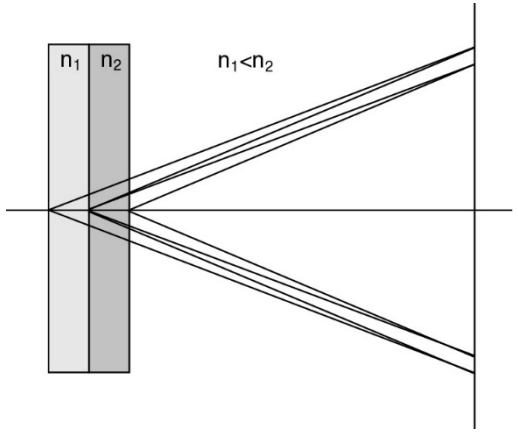
$$\sigma_{track} = \frac{\sigma_0}{\sqrt{N_{pe}}}$$

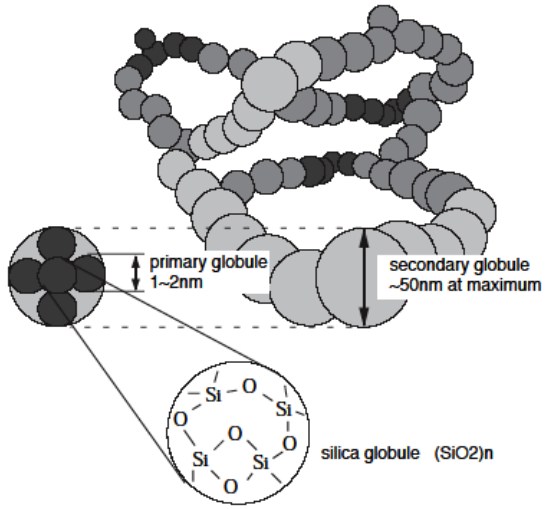
Separation: $[\theta_c(\pi) - \theta_c(K)]/\sigma_{track}$

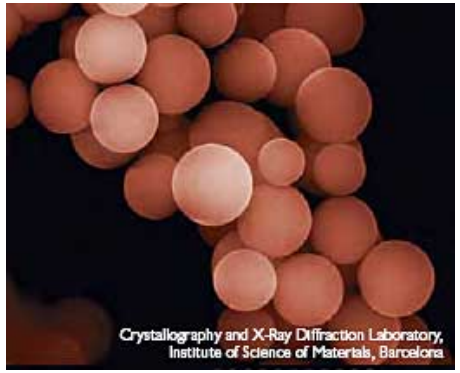
→ 5σ separation with $N_{pe} \sim 10$

Radiator with multiple refractive indices 2

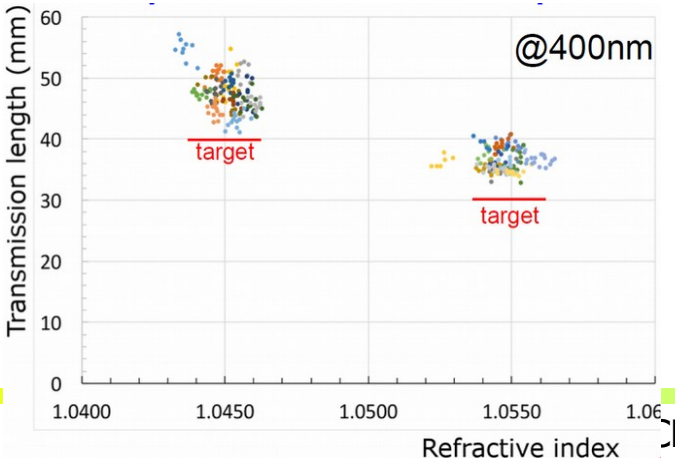
Such a configuration is only possible with aerogel (a form of Si_xO_y) – material with a tunable refractive index between 1.01 and 1.07.

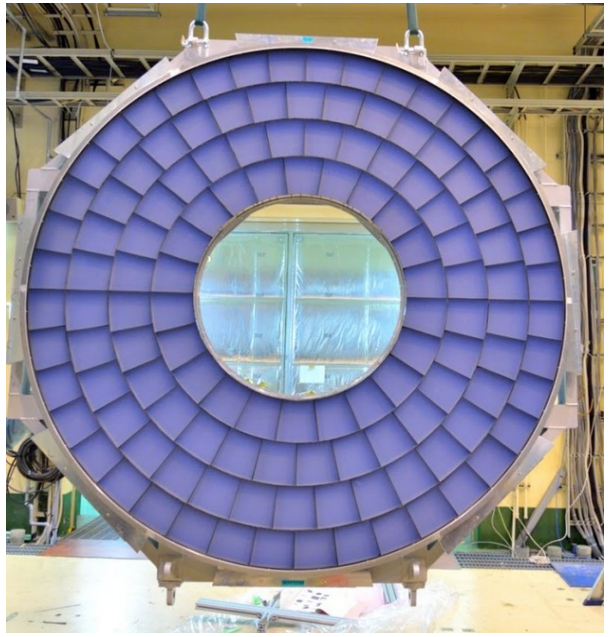






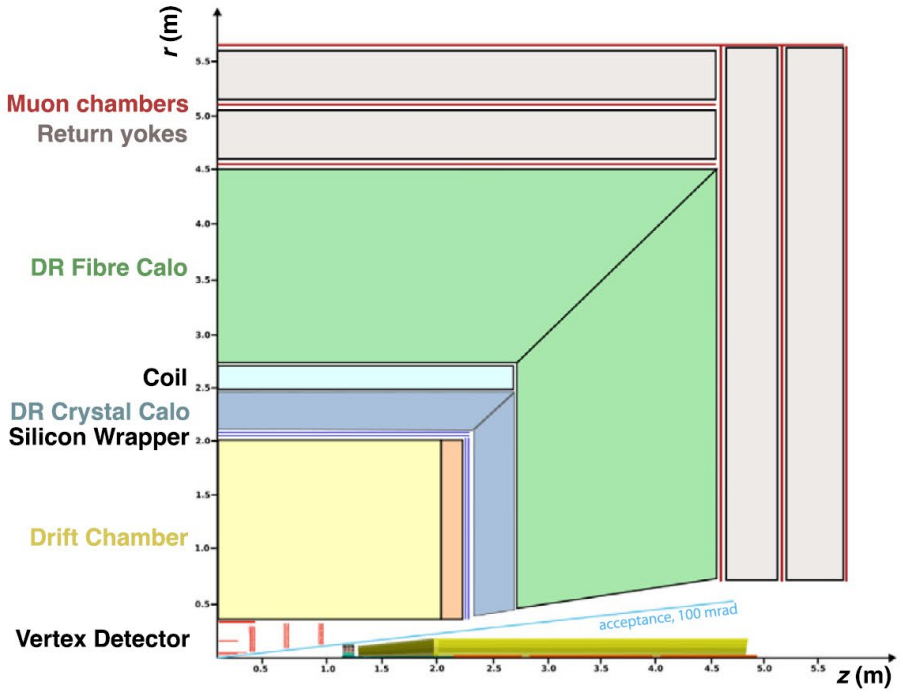
Requires aerogel with high transparency





Detector plane covered with 2 x 124 tiles water-jet cut tiles (~ 17x17cm)

FCC-ee detectors

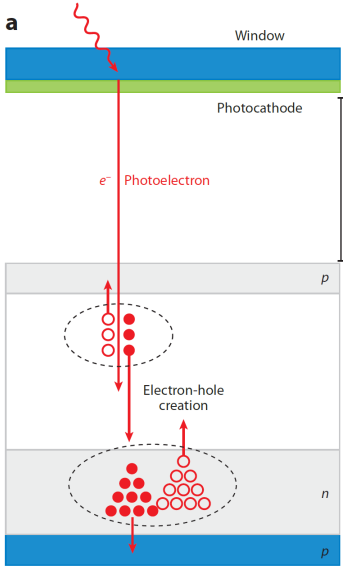


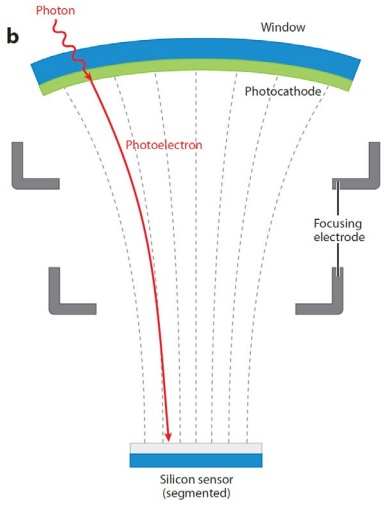
IDEA



Allegro

Hybrid photodetectors (HPD, HAPD)





Focusing and proximity focusing configurations

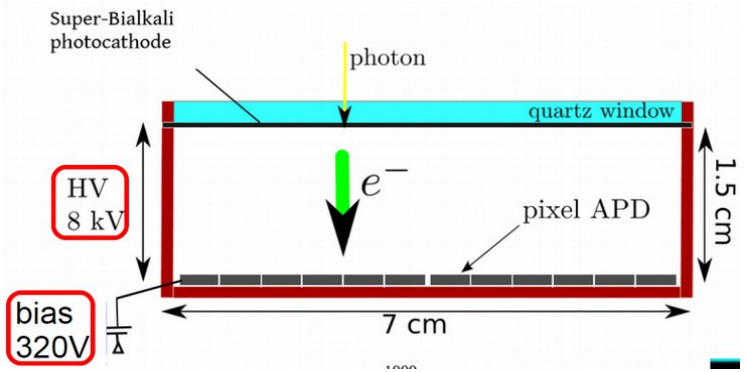


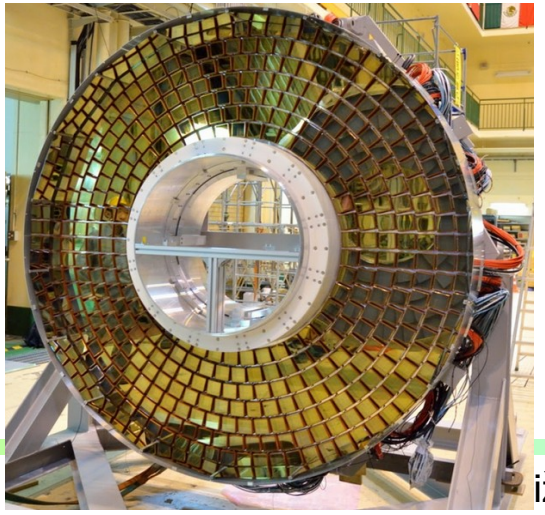
Photo-electron acceleration in a static electric field (8kV to 25 kV)

Photo-electron detection with

- Segmented PIN diode (HPD)
- Avalanche photo diode (HAPD)
- Silicon photomultiplier (VSiPMT)

Employed on a large scale:

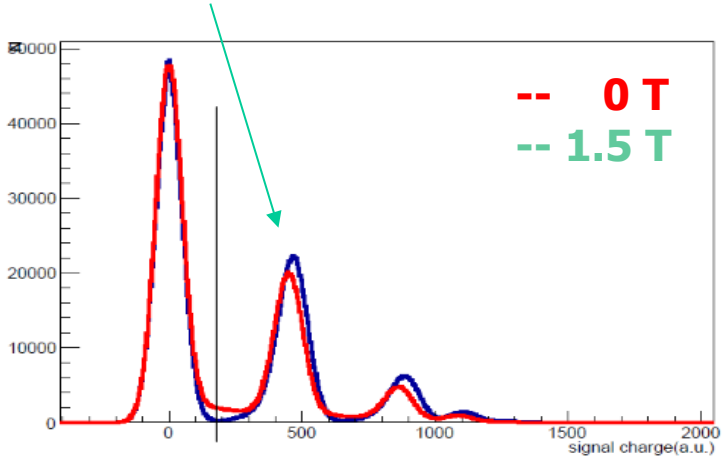
- HPD: RICH1+RICH2 of LHCb (Run 1+2), CMS HCAL
- HAPD: Aerogel RICH detector of Belle II

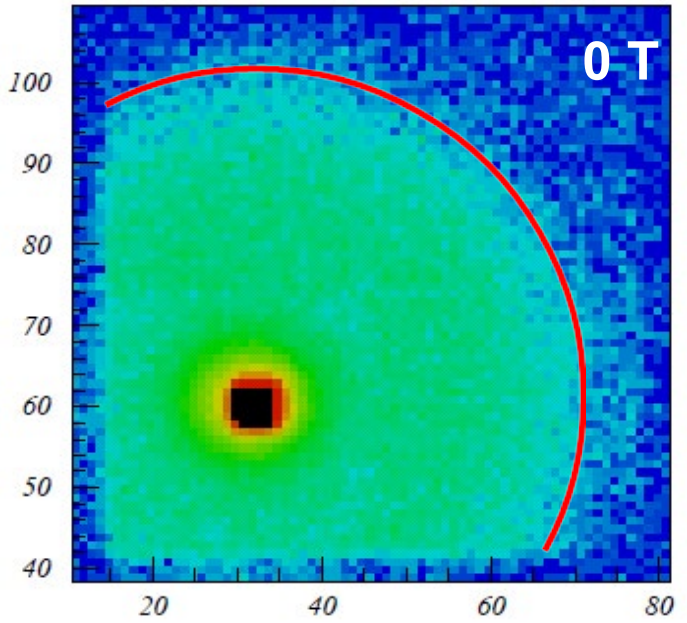


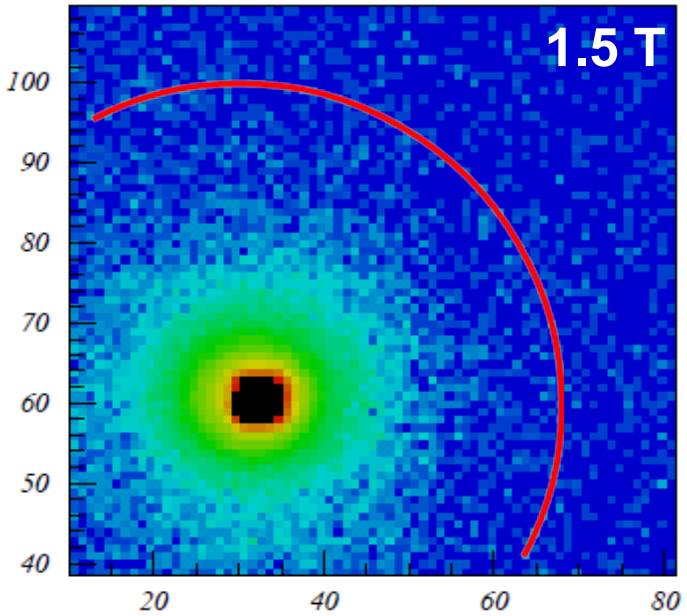
HAPD: photoelectron backscattering in magnetic field

- around 20% of photoelectrons back-scatter and the maximum range is twice the distance from photocathode to APD ~40mm

- in a strong magnetic field (perp. to the HAPD window) scattered photoelectrons follow magnetic field lines and fall back to the same pad
- photoelectron energy is deposited at the same pad



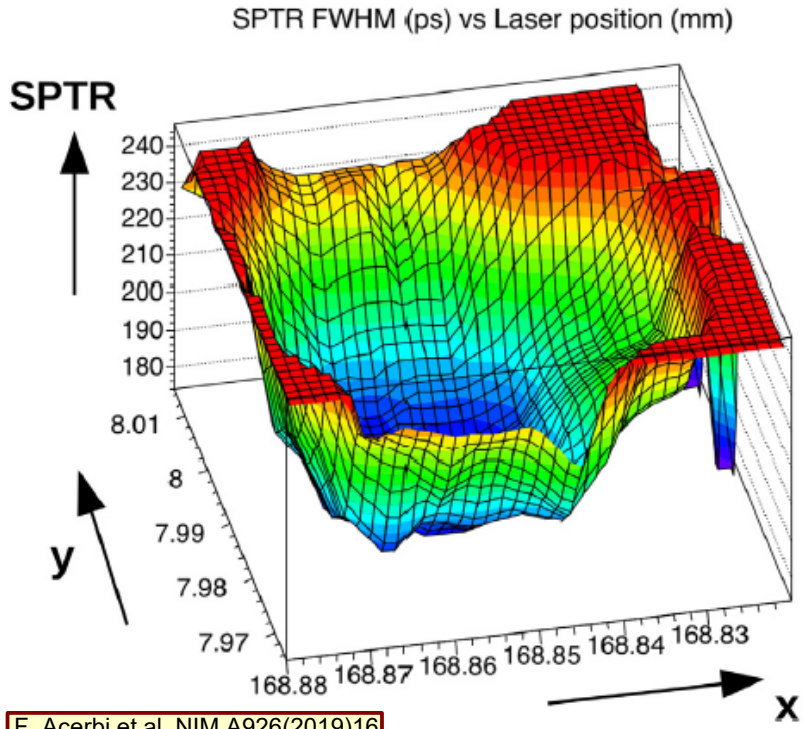




SiPM: timing variation

Variation of TTS over the device surface can contribute to overall time spread:

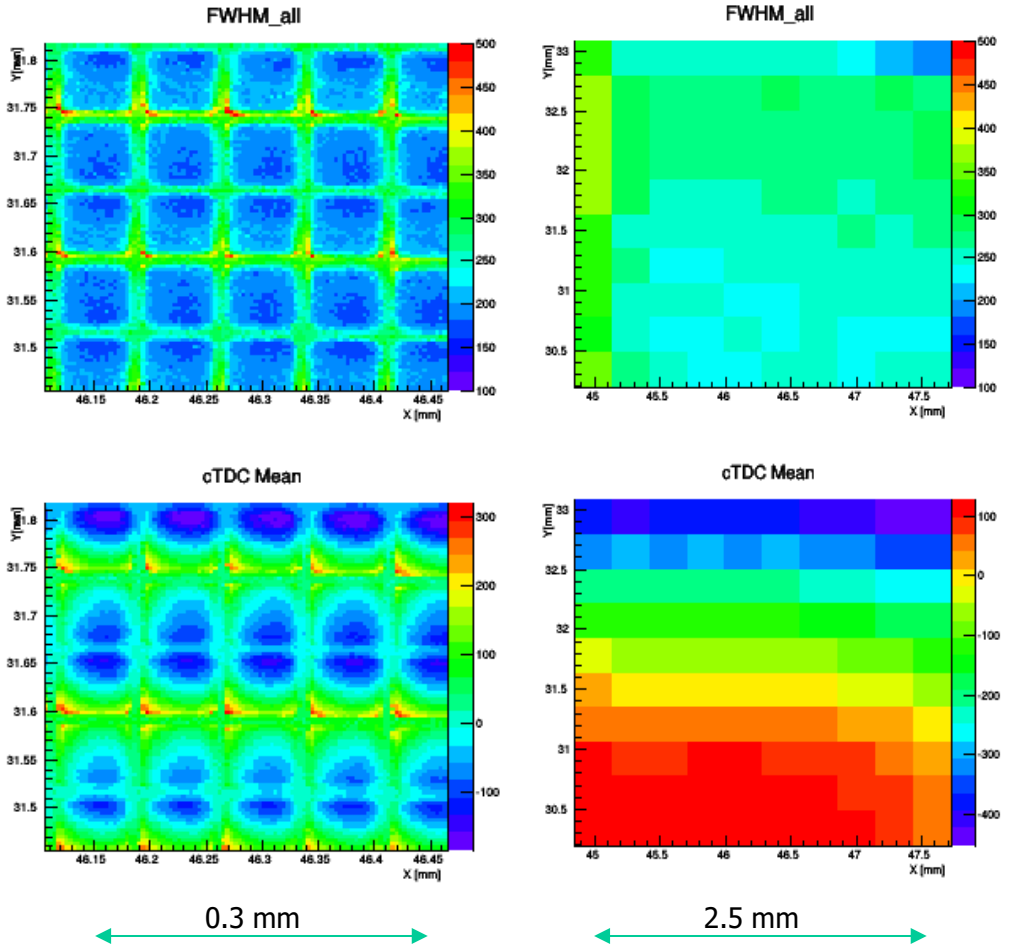
- variation within micro-cell
- variation for different micro-cells



F. Acerbi et al. NIM A926(2019)16

KETEK PM3375TS-SBO (early design)

S. Korpar et al. @IEEE 2015



FBK: Masking of outer regions of micro-cells: Improve signal peaking and mask areas of micro-cell with worse timing

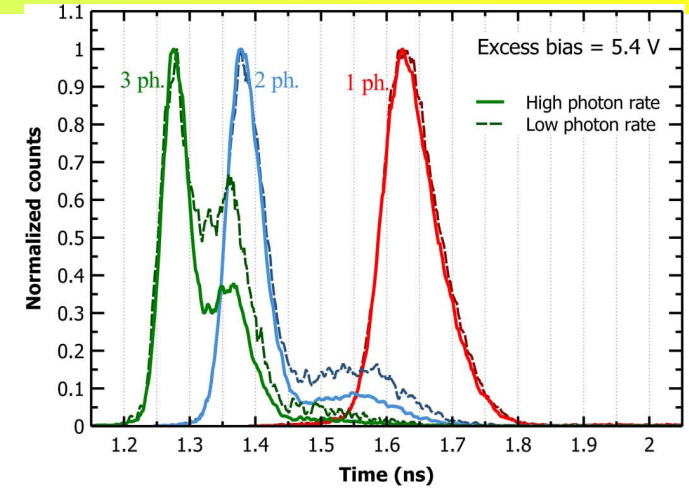
SiPM: timing for multi-cell signals

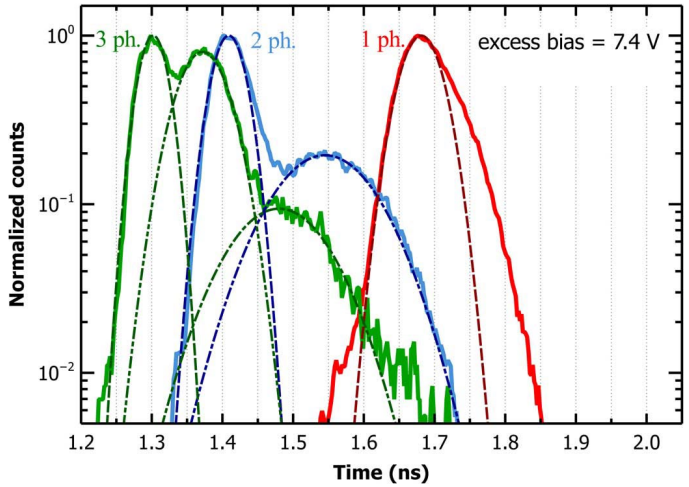
Optical cross-talk contribution to multi-cell signals spoils timing distribution – does not scale with $\frac{1}{N^{1/2}}$:

- two components for 2-micro-cell signals:
  - double photon events – proper scaling
  - single photon with cross-talk, timing somewhere between single and double micro-cell signals and resolution is worse
- ratio between contributions changes with light intensity

confirming optical cross-talk origin

- even more components for multi-micro-cell signals





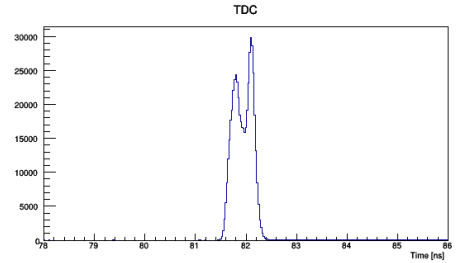
F. Acerbi et al. IEEE TNS 61(2014)2678

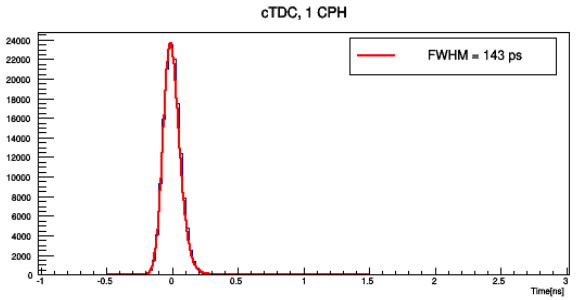
SiPM: timing test with pico-second laser

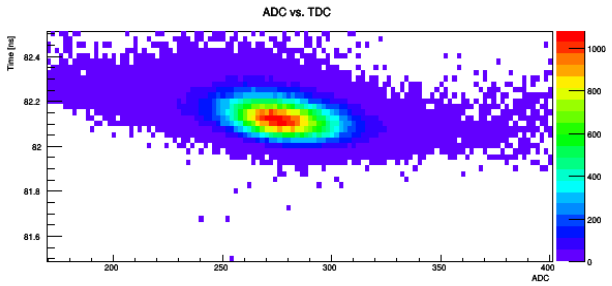
Optical cross-talk contribution to multi-cell signals spoils timing distribution - two components for 2-micro-cell signals:

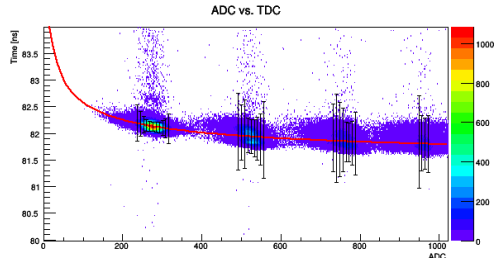
- double photon events – proper scaling
- single photon with cross-talk, timing somewhere between single and double micro-cell signals and resolution is worse

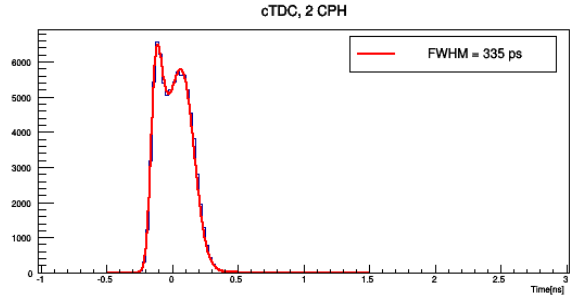
- AdvanSiD SiPM ASD-NUV3S-P-40
- OV=6V, T=-25°C, blue laser λ=408nm, ~35ps FWHM

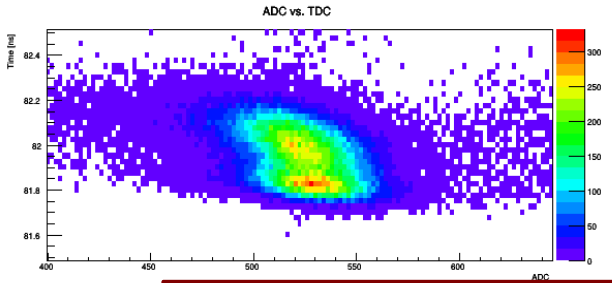


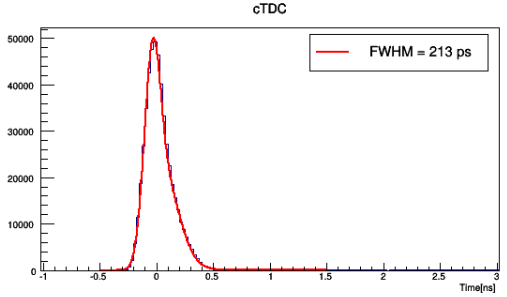








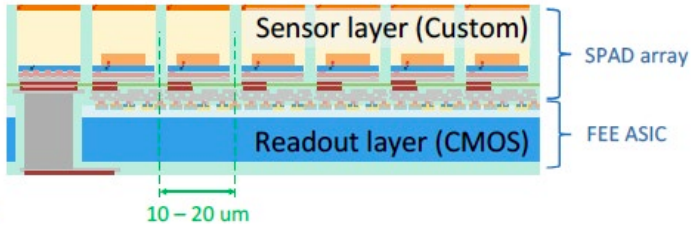




R. Dolenec et al. NIM A876(2017)257

Hybrid SiPMs

Separated sensing and readout layers, both in CMOS



Custom SiPM technology for sensing layer

- CMOS-compatible → transfer to large-volume foundries is possible
- ~10 lithographic masks - Lower cost per unit area compared to a full CMOS process (>40 masks)
- Customized fabrication process, no constraint form transistor fabrication → best electro optical performance possible, also after irradiation (e.g. DCR, DCR vs.T , PDE, correlated noise, etc)
- Cheap to iterate/adjust the design → Different sensing layers for different applications, room for subsequent upgrades without changing readout ASIC
- All the wafer area is sensitive to light → maximum detection efficiency (PDE)

CMOS technology for readout layer

- Free choice of CMOS node → optimal performance of readout.
- CMOS area can be smaller than sensing area (2.5D) → lower cost
- Independent design cycles of the sensing layer and readout layer → more efficient R&D phase

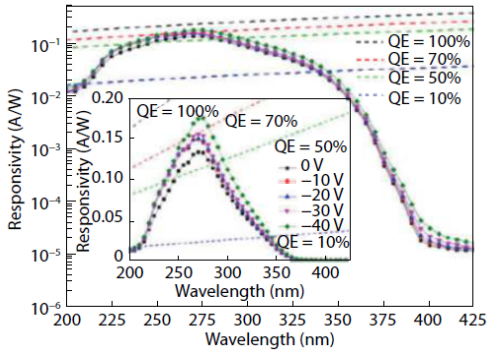
A. Gola, talk at DRD4 WG1 Meeting 2024

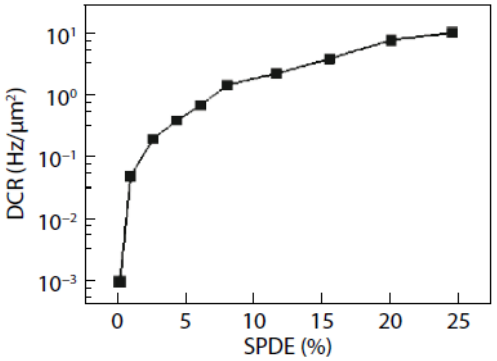
New materials

- new higher band gap materials - possibly lower DCR - higher radiation resistance, higher temperature
- (V)UV sensitive
- high dark count rate – dominated by trap assisted tunnelling

4H-SiC:

- $E_g = 3.26$ eV
- PDE $\approx 10\%$
- DCR $> 1\ \mathrm{MHz/mm^2}$
- nonuniform response





L. Su et al. J. Semicond. 40(2019)121802

